National Park Service
U.S. Department of the Interior

Science Report NPS/SR—2025/219
https://doi.org/10.36967/2307122

Landscape Phenology, Vegetation Condition, and Relations with Climate at Curecanti National Recreation Area, 2000–2019

The “blue marble” image is the most detailed true-color image of Earth to date. Much of the information contained in this image came from a single remote-sensing device: NASA’s Moderate Resolution Imaging Spectroradiometer, or MODIS. Flying more than 700 kilometers above Earth onboard the Terra satellite, MODIS provides an integrated tool for observing a variety of terrestrial, oceanic, and atmospheric features of the Earth.
NASA GODDARD SPACE FLIGHT CENTER

Landscape phenology, vegetation condition, and relations with climate at Curecanti National Recreation Area, 2000–2019

Science Report NPS/SR—2025/219

David Thoma

National Park Service
Northern Colorado Plateau Network
P.O. Box 848
Moab, UT 84532

Please cite this publication as:

Thoma, D. 2025. Landscape phenology, vegetation condition, and relations with climate at Curecanti National Recreation Area, 2000–2019. Science Report NPS/SR—2025/219. National Park Service, Fort Collins, Colorado. https://doi.org/10.36967/2307122

NPS 616/195564, January 2025

The National Park Service Science Report Series disseminates information, analysis, and results of scientific studies and related topics concerning resources and lands managed by the National Park Service. The series supports the advancement of science, informed decisions, and the achievement of the National Park Service mission.

All manuscripts in the series receive the appropriate level of peer review to ensure that the information is scientifically credible and technically accurate.

Views, statements, findings, conclusions, recommendations, and data in this report do not necessarily reflect views and policies of the National Park Service, US Department of the Interior. Mention of trade names or commercial products does not constitute endorsement or recommendation for use by the US Government.

The Department of the Interior protects and manages the nation's natural resources and cultural heritage; provides scientific and other information about those resources; and honors its special responsibilities to American Indians, Alaska Natives, and affiliated Island Communities.

This report is available in digital format from the National Park Service DataStore and the Natural Resource Publications Management website. If you have difficulty accessing information in this publication, particularly if using assistive technology, please email irma@nps.gov.

Contents

Contents (continued)

Contents (continued)

Figures

Page

Figures (continued)

Page

Figures (continued)

Page

Figures (continued)

Page

Figures (continued)

Page

Figures (continued)

Page

Figures (continued)

Page

Tables

Page

Abstract

Climate determines the vegetation composition in parks and climate change will affect vegetation condition and composition in the future. This study, which examined changes in climate, water availability, and vegetation from 2000 to 2019 in Curecanti National Recreation Area (NRA) in Colorado, USA, evaluates vegetation sensitivity to weather and climate for the purpose of understanding climate-vegetation relationships that can be used to understand what vegetation types may change. Specifically, it evaluates where change is likely in the NRA, when change may happen and why change may occur. This information is needed to help avoid surprises and can be used to help plan for inevitable change. Satellite images were analyzed with climate data to quantify vegetation sensitivity to climate and drought tolerance. Historic trends in vegetation production and phenology were evaluated and analysis with climate data identified which aspects of climate were most important to annual production and phenology for different vegetation types. Additionally, trends in climate and climate drivers of vegetation phenology were also identified. Study results suggest that annual trends in vegetation production increased in 98% of the area analyzed in and near Curecanti NRA between 2000 and 2019, and decreased in the other 2%. Further, from 2000 to 2019, the growing season shortened by 0.6 to 8 days for six vegetation alliance groups (Mesic Sagebrush, Dry Sagebrush, Quaking Aspen, Mixed Montane Shrubland, Disturbed, and Blue Spruce), but lengthened by 2 to 17 days for the other 10 alliance groups that are found in Curecanti NRA. Finally, the information generated in this study was placed in the context of a climate adaptation planning framework to demonstrate how it can be used for long-range management and planning.

Executive Summary

Quantitatively linking satellite observations of vegetation condition and climate data over time provides insight to climate influences on primary production, phenology (timing of growth), and sensitivity of vegetation to weather and the longer-term patterns of weather referred to as climate. This in turn provides a basis for understanding potential climate impacts to vegetation—and the potential to anticipate cascading ecological effects, such as impacts to forage, habitat, fire potential, and erosion—as climate changes in the future.

This report provides baseline information about vegetation production and condition over time at Curecanti National Recreation Area (NRA), as derived from satellite remote sensing. Its objective is to demonstrate methods of analysis, share findings, and document historic climate exposure and sensitivity of vegetation to weather and climate as drivers of vegetation change.

This report represents a quantitative foundation of vegetation–climate relationships on an annual timestep. The methods can be modified to finer temporal resolution and other spatial scales if further analyses are needed to inform NRA planning and management. The knowledge provided in this report can inform vulnerability assessments when planning for a changing climate. Patterns of pivot points and responses can serve as a guide to anticipate what, where, when, and why vegetation change may occur.

For this analysis, vegetation alliance groups were derived from vegetation-map polygons (Von Loh et al. 2007) by lumping vegetation types expected to respond similarly to climate. Relationships between vegetation production and phenology were evaluated for each alliance map unit larger than a satellite pixel (~300 × 300 m). We used a water-balance model to characterize the climate experienced by plants. Water balance translates temperature and precipitation into more biophysically relevant climate metrics, such as soil moisture and drought stress, that are often more strongly correlated with vegetation condition than temperature or precipitation. By accounting for the interactions between temperature, precipitation, and site characteristics, water balance helps make regional climate assessments relevant at local scales.

The results provide a foundation for interpreting weather and climate as drivers of changes in primary production over a 20-year period at the polygon and alliance-group scales. Additionally, they demonstrate how vegetation type and site characteristics, such as soil properties, slope, and aspect, interact with climate at local scales to determine trends in vegetation condition. This report quantitatively defines critical water needs of vegetation and identifies which alliance types, in which locations, may be most susceptible to climate-change impacts in the future. Finally, this report explains how findings can be used to plan for a changing climate by including scenario planning, to help manage park resources through transitions imposed by climate change.

Key findings:

- The patterns of pivot points and responses can serve as a guide to anticipate what, where, when, and why vegetation change may occur in the future.

- Multiple indicators suggest that, between 2000 and 2019, annual trends in vegetation production increased in 98% and decreased in 2% of the area analyzed in and near Curecanti National Recreation Area (*3.3 Trends in indicators of annual production*).
- Areas that decreased in both maximum and mean annual production occurred in small areas less than 100 ha and included Mixed Montane Shrubland, Riparian, Quaking Aspen, Douglas-Fir and Disturbed alliance groups. (*3.3 Trends in indicators of annual production*).
- Annual production was positively correlated with actual evapotranspiration in all alliance groups except for the Riparian, Water and Blue Spruce alliance groups (*3.5.2 Single-variable drivers of production*).
- Quaking Aspen, Douglas-fir, Mixed Montane Shrubland and a single polygon of Juniper were the least drought tolerant alliance groups, whereas Pinyon-Juniper, Riparian and a single polygon of Wet Meadow were the most drought tolerant (*3.6.1 Pivot points indicate drought tolerance*).
- Disturbed areas, Douglas-fir and Mixed Montane Shrubland were the alliance groups most sensitive to water deficit (*3.7.1 Vegetation response and climate sensitivity*).
- Three years of actual evapotranspiration was the best indicator of annual production at the park scale. This was also generally true at the alliance-group scale (*3.8 Multi-variable indicators of annual vegetation production*).
- By the end of the study period, the growing season was starting later for all vegetation alliance groups except Wet Meadow and Water, and ending later for all alliance groups except Blue Spruce (*3.9 Land-surface phenology trends at Curecanti National Recreation Area*).
- During the study period the growing season shortened by 0.6 to 8 days for Mesic and Dry Sagebrush, Quaking Aspen, Mixed Montane Shrubland, Disturbed, and Blue Spruce alliance groups. The growing season lengthened by 2 to 17 days for all other groups (*3.9 Land-surface phenology trends at Curecanti National Recreation Area*).
- Growing degree days, date of snowmelt and precipitation were the most important determinants of the start of growing season (*3.10.1 A priori model selection method*).

This report provides a foundation for interpreting weather and climate as drivers of changes in primary production over a 20-year period at the polygon, alliance-group and park scales. It can be used to determine what, when, where and why future climate change may impact vegetation. This is achieved by incorporating information in this report with Planning for a Changing Climate, which is intended to help plan management strategies that can facilitate desirable transitions imposed by climate change (see Section 4.4).

List of Acronyms

AET: actual evapotranspiration, mm

D: climatic water deficit, mm

EOS: end of growing season

GDD: growing degree days, °C

iSAVI: integrated growing season soil adjusted vegetation index

LOS: length of growing season

Meltd: day of complete snowmelt

MODIS: moderate resolution imaging spectrometer

NCPN: Northern Colorado Plateau Network of parks

NDVI: normalized difference vegetation index

NP: national park

NVC: National Vegetation Classification

NVCS: National Vegetation Classification Standard

P: precipitation, mm

PACK: water stored in snowpack, mm

PET: potential evapotranspiration, mm

POP: timing of peak growth

RAIN: rain, mm

SAVI: soil adjusted vegetation index

SNOW: snow water equivalent, mm

SOIL: soil moisture in top meter of soil, mm

SOS: start of growing season

SRAD: solar radiation, W m^{-2}

T: average temperature, °C

Tmax: maximum temperature, °C

Tmin: minimum temperature, °C

VP: vapor pressure, Pa

VPD: vapor-pressure deficit, Pa

W: water reaching the soil surface as snowmelt plus rain, mm

Acknowledgments

Thoughtful reviews from Danguole Bockus and Dustin Perkins improved this report.

1 Introduction

This report provides baseline information about vegetation production and condition over time as derived from satellite remote sensing at three scales: park, vegetation-alliance group, and vegetation-alliance polygon. The objective is to demonstrate the methods of analysis, share standardized findings, and document historical climate exposure and sensitivity to weather and climate as drivers of vegetation change at Curecanti National Recreation Area.

This study quantitatively defines the critical water needs of vegetation and demonstrates how vegetation type and site characteristics interact with climate at local scales to determine change in vegetation condition.

It provides a foundation for interpreting weather and climate as drivers of change in primary production over a 20-year period at local scales. It can be used to quantitatively determine which alliance types, in which locations, may be most susceptible to climate-change impacts in the future, providing a basis for vulnerability assessments in Planning for a Changing Climate (see Section 4).

1.1 The importance of primary production

Photosynthesis is the process in plants that converts sunlight, CO_2, water, and minerals into the chemical forms of energy (carbohydrates and sugars) essential to life. All terrestrial life depends on photosynthesis, also called "primary production," because it is the foundation of food webs. As the first step in creating food and habitat for wildlife, vegetation production is an important indicator, or "vital sign," of ecosystem health that can be tracked over time to assess conditions that support higher life forms in parks. The complex temporal and spatial patterns of primary production are influenced by many factors, including disturbances, such as wildfire and drought; differences in precipitation across space or over time; vegetation assemblages that differ in response to change; topography and soil properties; land use; and invasive species (Kariyeva and van Leeuwen 2011).

Sunlight provides the energy used to synthesize organic compounds from CO_2 and water. In semi-arid environments like the Colorado Plateau, sunlight and CO_2 are abundant and rarely limit production, but primary production is controlled by different environmental variables in different places. In tropical forests, primary production may be controlled by availability of sunlight (due to cloud cover and dense canopy) or soil nutrients. In deserts, primary production is mostly controlled by water availability. At the highest elevations on the Colorado Plateau, it may be controlled by cold temperatures and a short growing season. Changes in primary production may indicate changes in ecological structure (e.g., change in vegetation assemblage) or ecological function (e.g., loss of vegetation cover, resulting in erosion and loss of soil nutrients).

1.2 Satellite monitoring of primary production

Assessing the rate of photosynthesis and the condition of vegetation at broad landscape scales provides insight to the cycles of energy, nutrients, and water that sustain life in parks. Sunlight reflected from vegetation provides information about photosynthetic rates, leaf area, and biomass accumulation, as well as the habitat and forage conditions for animals. High-frequency satellite

remote sensing of vegetation condition provides a broad-scale view of spatial patterns in vegetation condition, production, and change in response to climate, disturbance, and management actions over time.

The Northern Colorado Plateau Network (NCPN) monitors landscape-scale vegetation condition and trends using satellite imagery collected more frequently than ground-based data (which are also collected). The high frequency of observations and complete spatial coverage of satellite images is ideal for assessing seasonal as well as annual conditions and trends. The imagery also provides insight on the response of vegetation to climate patterns and disturbances (e.g., fire and forest disease, often mediated by climate) that cannot be obtained at broad scales in any other cost-effective way.

Quantitatively linking satellite observations of vegetation condition and climate data over time provides insight to climate influences on primary production, phenology (timing of growth), and sensitivity of vegetation to weather and long-term weather patterns referred to as climate. This in turn provides a basis for understanding potential climate impacts to vegetation and the potential to anticipate cascading ecological effects, such as impacts to forage, habitat, fire potential, and erosion, as climate changes in the future.

Primary production assessed via satellite remote sensing does not indicate which species are present, or which species are performing well or poorly. It is also not a "good" or "bad" judgement (i.e., increased or decreased production is not inherently good or bad). Monitoring primary production is analogous to monitoring river flow. Flow monitoring measures the timing and abundance of water that provides habitat for animals and other essential ecological functions. It does not indicate which organisms are present, or how different species are faring.

1.3 Vegetation condition and vulnerability

Vegetation condition and trend are monitored as changes in vegetation production, or the cumulative green biomass of leaves that grow via photosynthesis. Green biomass is strongly correlated with near-infrared and red wavelengths of solar energy reflecting off vegetation measured by satellites (Thoma et al. 2002). The satellite imagery reveals repeating seasonal fluctuations in growth and senescence, as well as annual trends or abrupt changes due to disturbances. Although disturbances can be detected, it is beyond the scope of this analysis to do so because different methods are required than those used in this report.

Climate is a strong driver of vegetation distributions (Stephenson 1998). Variation in weather strongly affects vegetation condition through stress (e.g., drought) and disturbance (e.g., wildfire). Linking changes in vegetation production to climate provides important information about resistance to disturbance (resilient or susceptible) and recovery from disturbance (fast or slow).

Vegetation that is susceptible to disturbance and slow to recover is considered the most vulnerable to change (Kariyeva and van Leeuwen 2011). This kind of information can be used to assess vulnerability of vegetation assemblages to climate change.

1.4 Pivot points and responses

In semi-arid environments, vegetation persists when there is a positive balance between growth and resistance to drought (Noy-Meir 1973). Vegetation traits, such as rooting depth, xylem diameter, and stomatal density and resistance, interact with climate and site conditions to determine how vegetation responds to climate. Understanding these interactions provides insight to potential changes in vegetation condition and composition as the climate changes. When coupled with climate data, two important ecological characteristics, pivot points and responses, can be derived from measuring change in vegetation condition over time (Munson 2013).

A pivot point is the value of a climate variable at which annual vegetation production teeters between above- or below-average condition. For water variables, pivot points determine whether vegetation production increases or decreases given the water available for growth. A pivot point is analogous to the recommended eight glasses of water per day for adults: Except in extreme cases, more water is generally not bad—but less can have detrimental effects, even when unmet needs are slight. Semi-arid plants generally respond more positively than humans to water that exceeds minimum needs. But as with people, receiving less than the minimum can cause deterioration in condition. As such, the pivot point can be considered a critical water need as well as an indicator of drought tolerance. A species' basic water needs, and the rate of change when those needs are unmet or exceeded, are important ecological variables that determine how plants respond to weather and climate.

Plant traits determine how much water vegetation needs to maintain production. How much water is available depends on climate, weather, soil, and site properties. These interactions can cause variation in the magnitude of pivot points for the same climate variable across vegetation types. Some types may be more tolerant of drought conditions than others.

Vegetation response is the sensitivity of vegetation to a climate variable or, more specifically, the amount of change in vegetation production per unit change in a climate variable. This rate of change is a quantitative measure of vegetation sensitivity to climate. Cumulative annual vegetation production and phenology are indicators of vegetation response to a suite of environmental conditions. Some conditions are spatially variable but stable over time, such as slope, aspect, and soil properties. Others, such as climate, vary both temporally and spatially. The vegetation growing at any location reflects adaptations suited to the environment where it persists. If conditions change, either abruptly or gradually, plants respond. The change can be spatial, due to differences in soil type or elevation. It can also be temporal, as weather and climate change over time.

Differences in vegetation response rates, or sensitivity, to water availability reflect survival strategies for persisting through drought or responding rapidly when water is available, making species more competitive if their water needs are met. The survival strategies are a consequence of vegetation traits, including rooting depth, stomatal density, leaf area, and perennial versus annual growth forms that confer competitive advantages under different climate conditions. Generally, plant traits that favor one strategy preclude the other (Thoma et al. 2019; Noy-Meir 1973).

Individual plant responses to environmental conditions cumulatively scale up, resulting in spatial and temporal landscape patterns that can be detected in satellite imagery (Thoma et al. 2019). Because vegetation production and phenological responses are interrelated, it is useful to measure and report the two simultaneously. It is not always possible to know what caused a change noted in satellite imagery, but communication with park staff and ground-based monitoring can help interpret findings in this report.

1.5 Phenology

The annual cycle of vegetation growth and senescence, and reoccurring biological phenomena such as seasonal migrations, are collectively known as phenology. Commonly known measures of vegetation phenology include timing of bud burst, first leaf, and spring bloom, all observed from the ground (de Beurs and Henebry 2010). The high frequency observations from satellites make it possible to track vegetation phenology (Dunn and de Beurs 2011) at broad spatial scales that include an assemblage of different vegetation species, referred to as "land-surface phenology." Land-surface phenology is an indicator of ecosystem health because it regulates dependent ecological functions, such as pollination and onset of forage production (Dunn and de Beurs 2011). On the Colorado Plateau, springtime vegetation growth is preceded by warming temperatures and snowmelt. In drier regions, onset of springtime growth may be limited if there was insufficient accumulation of fall and winter soil moisture (Workie and Debella 2018).

Changes in land-surface phenology can provide an early indication of cascading climate-change impacts that may result in changing species assemblages and shifting range boundaries (Workie and Debella 2018). These may affect pollinators, as well as bird and mammal migrations. Determining the drivers of phenology, and changes in phenology over time, provides insights on the cascading effects on pollinators and migrating animals that depend on growth initiation, forage production, and the length of the growing season.

2 Methods

2.1 Overview

At a scoping meeting in May 2002, network and park staff delineated a project area consisting of Curecanti National Recreation Area (NRA) plus a strip approximately 1.6 kilometers (1 mile) wide around its boundary (Figure 1). The total project mapping area was 48,639 hectares (120,189 acres). Of this area, 17,068 hectares (42,176 acres) were within the NRA boundary and 31,571 ha (78,013 acres) were in the environs. The environs were delineated to provide data to support management coordination on adjacent private and federal lands (the latter managed by the National Park Service, the US Forest Service, and the Bureau of Land Management).

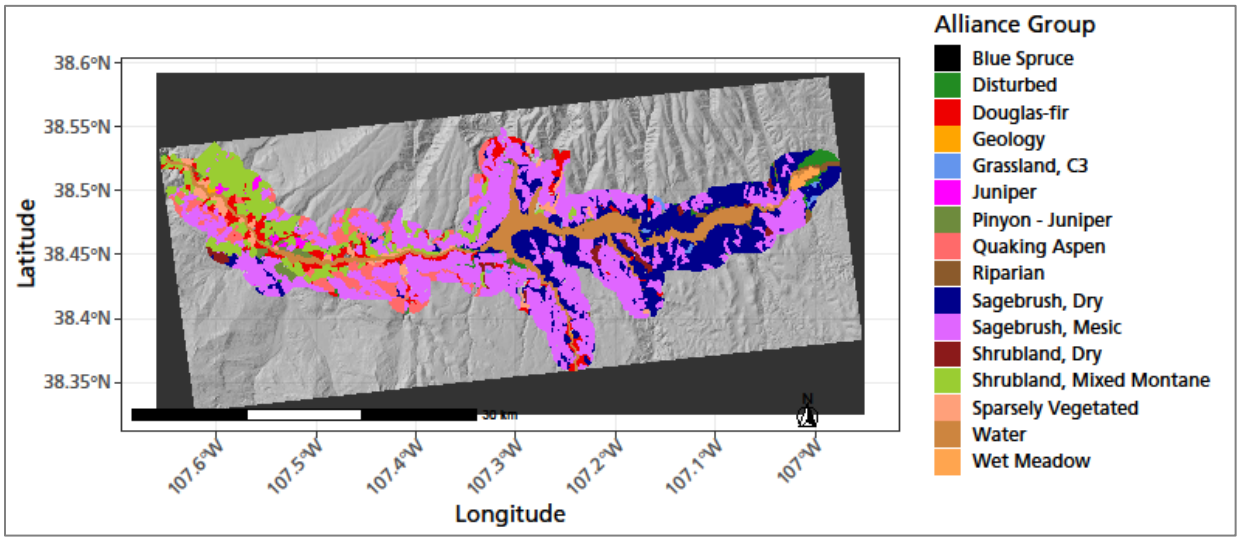

Figure 1. NCPN alliance groups analyzed for trends in production, phenology, and climate relations at Curecanti National Recreation Area. Colored areas represent the distribution of different vegetation alliance groups. Areas not colored within the study boundary are alliance polygons smaller than the minimum target area of 8.3 hectares. NPS / DAVID THOMA

This report was compiled by comparing climate data with variation in land-surface greenness over time, as measured in satellite imagery of the park's vegetation-mapping project area (Von Loh et al. 2007). A large archive of 838 remotely sensed satellite images was downloaded and processed in the statistical analysis software "R." A large amount of gridded climate data for the same area was downloaded and processed in Excel to estimate water-balance variables, such as soil moisture, evapotranspiration, and water deficit from temperature and precipitation (see Section 2.6). The imagery and water-balance/climate data were merged in R separately for each vegetation alliance polygon (see Section 2.2) and analyzed statistically for spatial patterns across park landscapes and over time for trends.

2.2 Remote-sensing targets

Three scales of analysis are presented in this report: vegetation-alliance polygon, vegetation-alliance group, and parkwide. Vegetation-alliance polygons were derived from vegetation-map polygons by

lumping together vegetation types expected to respond similarly to ecological disturbances, such as climate change (Jennings et al. 2009; Von Loh et al. 2007). The polygon scale features finer spatial resolution—but with higher resolution comes more complexity in interpretation. The group scale lumps similar alliances together for broader-scale interpretations, but is not always as accurate as the polygon scale, because lumping even slightly dissimilar objects introduces variation. The park-scale analysis is achieved by lumping all alliance polygons into a single analysis or by averaging analysis results across alliances to the park scale.

It is important to note that satellite-based proxies for primary production reflect production from all vegetation within a sampling unit, regardless of the alliance name (which identifies the dominant or diagnostic vegetation types). For example, a forested alliance type may include shrub or graminoid understory that influences the satellite signal. Untangling the proportional influence of the named alliance components from background components is beyond the scope of this report.

2.2.1 Alliance polygons

The National Vegetation Classification Standard (NVCS) identifies eight hierarchical levels of classification, ranging from Formation Class (Level 1, the broadest scale) to Association (Level 8, the finest scale). The finest scale used in this report was the vegetation Alliance (Level 7). The NVCS defines a vegetation alliance as "A characteristic range of species composition, habitat conditions, physiognomy, and diagnostic species, typically at least one of which is found in the uppermost or dominant stratum of the vegetation layer, and reflecting regional to subregional climate, substrates, hydrology, moisture/nutrient factors and disturbance regimes" (FGDC 2008).

Vegetation alliances are useful targets for tracking production and phenology because they are spatially repeating, relatively homogenous in type composition, and share similar affinities and responses to environmental conditions, such as climate. They are also mapped consistently across park units, making them an ideal classification level for cross-park analysis. Polygon boundaries for the alliances were obtained from park vegetation maps (Von Loh et al. 2007).

Analysis at the alliance level, rather than association level, resulted in larger and fewer polygon targets that contained a larger number of satellite pixels. This helped ensure that satellite-image pixels fell mostly within target polygons and improved the signal-to-noise ratio necessary for tracking change in response to climate. Improving the signal-to-noise ratio in remote sensing of sparsely vegetated environments is achieved by spatially averaging pixels within relatively homogenous areas (Thoma et al. 2017). For this reason, the analysis in this report relies primarily on aggregated pixel means across the spatial extent of each target polygon, rather than per-pixel analysis. More detail on pixel screening to exclude low-quality observations and outliers can be found in Sections 2.3 and 2.5.

2.2.2 NCPN alliance groups

For the purposes of this study, alliances that respond similarly to climate based on structure and life-history traits were further grouped by NCPN ecologist Dana Witwicki (personal comm.) to simplify interpretations and reporting. We created our own grouping system to simplify the alliance naming

conventions and reduce the large number of alliances, which were too numerous for meaningful reporting.

Beginning with 98 different National Vegetation Classification (NVC) alliances mapped consistently across NCPN park units, we created 32 alliance groups based on floristics, canopy structure, and local environmental conditions. Of those, 16 occurred in Curecanti NRA (Table 1, Figure 1). The alliance group names are shortened representations of the dominant alliance(s) in each group. Note that, because alliance groups represent an aggregation of multiple alliance types, not all polygons assigned to a given alliance group necessarily contain the species for which the group is named. Hereafter, we refer to the grouped alliance categories as "NCPN alliance groups" or "alliance groups," but it should be noted that these groups are similar to, but different than, Level 6 of the NVC.[1] A key that links each NCPN alliance group to vegetation-mapping units familiar to NCPN managers can be found in Table S-1 of Thoma (2024). The image-analysis targets were the ungrouped alliance polygons, so while results reported in the body of this report are for NCPN alliance groups, results are also available by polygon for ungrouped alliances in the supplemental tables (Thoma 2024).

Table 1. NCPN alliance groups and corresponding National Vegetation Classification alliances, Curecanti National Recreational Area.

NCPN alliance group	National Vegetation Classification alliance(s) [A]
Blue Spruce	Blue Spruce Southern Rocky Mountain Forest & Woodland Alliance
Disturbed	Non-natural
Douglas-fir	Douglas-fir Southern Rocky Mountain Forest & Woodland Alliance Douglas-fir Middle Rocky Mountain Dry-Mesic Forest & Woodland Alliance
Geology	Bare
Grassland, C3	Arizona Fescue - Mountain Muhly - Muttongrass Southern Rocky Mountain Montane Grassland Alliance
Juniper	Utah Juniper / Shrub Understory Woodland Alliance
Pinyon - Juniper	Two-needle Pinyon - Utah Juniper / Shrub Understory Colorado Plateau Woodland & Scrub Alliance
Quaking Aspen	Quaking Aspen Rocky Mountain Forest & Woodland Alliance

[A] The alliance names shown in this table do not match those found in Von Loh et al. (2007) because alliance names and codes in that report were subsequently updated to USNVC Version 2.01, released March 30, 2017. The names from 2007 were cross-walked to the current names displayed here. For information on nomenclature, see FGDC (2008).

[1] Although there is an NVC Group level (6), the "NCPN alliance groups" discussed in this report were developed independently from the NVC for the purposes of this study.

Table 1 (continued). NCPN alliance groups and corresponding National Vegetation Classification alliances, Curecanti National Recreational Area.

NCPN alliance group	National Vegetation Classification alliance(s) [A]
Riparian	Narrowleaf Cottonwood Riparian Forest Alliance Canadian Horseweed - Canada Thistle - Prickly Lettuce Ruderal Wet Meadow Alliance Box-elder - Cottonwood species - Spruce species Ruderal Riparian Forest Alliance
Sagebrush, Dry	Wyoming Big Sagebrush Dry Steppe & Shrubland Alliance
Sagebrush, Mesic	Spiked Big Sagebrush - Mountain Big Sagebrush Steppe & Shrubland Alliance Mountain Big Sagebrush - Mixed Steppe & Shrubland Alliance
Shrubland, Dry	Fourwing Saltbush Scrub Alliance Prairie Sagewort Dwarf-shrubland Alliance
Shrubland, Mixed Montane	Utah Serviceberry - Alderleaf Mountain-mahogany - Littleleaf Mountain-mahogany Shrubland Alliance Gambel Oak - Mountain Snowberry Shrubland Alliance
Sparsely Vegetated	Rocky Mountain Indian-parsley - Rockspirea - American Red Raspberry Cliff, Scree & Rock Alliance
Water	Water
Wet Meadow	Baltic Rush - Mexican Rush Wet Meadow Alliance

[A] The alliance names shown in this table do not match those found in Von Loh et al. (2007) because alliance names and codes in that report were subsequently updated to USNVC Version 2.01, released March 30, 2017. The names from 2007 were cross-walked to the current names displayed here. For information on nomenclature, see FGDC (2008).

2.3 Satellite imagery

Since early 2000, the moderate resolution imaging sensor (MODIS) on the Terra satellite, operated by NASA, has collected daily imagery of Earth at a spatial resolution of 250 meters (820 ft). Because cloud cover, cloud shadows, aerosols, smoke, and water vapor can interfere with clear views of Earth's surfaces, daily images are composited into a single image for 16-day windows of time (product MOD13Q1). The 16-day composite images are created from values obtained from the clearest view during the 16-day window, and are generally the best quality observations for every pixel during the 16-day window.

Even so, during extended periods of poor atmospheric viewing conditions, some pixel values are unreliable. For this reason, each pixel in the composite image is tagged with a quality rating that can be used to screen out unreliable values influenced by poor viewing conditions. Sophisticated algorithms are used to assess the quality of every pixel value based on measurements of atmospheric conditions made by the satellite during image acquisition (Didan et al. 2015).

There are 23 fixed, 16-day window periods in a year (with a few overlapping days at year's end to account for leap years). Thus, there were 457 viewing opportunities and 23 observations per year for every pixel in the NCPN during the period of record covered in this report. Observation completeness was calculated on an annual and seasonal (March–November) basis for the 20-year study period as the percentage of pixels in each polygon that were observed under high-quality

viewing conditions. In semi-arid environments, there are typically many high-quality observations during the growing season, but fewer in winter due to clouds and snow cover.

2.4 Soil Adjusted Vegetation Index

The Soil Adjusted Vegetation Index (SAVI) is a measure of primary production (Bunting et al. 2019; Qi et al. 1994) obtained from reflectance in red and near-infrared wavelengths, adjusted for soil backgrounds in semi-arid environments (Huete 1988). It is calculated as

$$SAVI = \frac{(1 + L)\,(NIR - Red)}{(NIR + Red + L)}$$

where L is the soil background adjustment factor ($L = 0.5$), NIR is reflectance in near infrared wavelengths, and Red is reflectance in red wavelengths.

These wavelengths were selected specifically because they are sensitive to the abundance of green vegetation and optimized for detecting spatial and temporal changes in vegetation. We use SAVI in this report, rather than the normalized difference vegetation index (NDVI), because of the thin vegetation cover and soil background reflectance in most NCPN parks. This combination of factors results in unfavorable signal-to-noise ratios that can make remote sensing of spatial and temporal changes difficult in semi-arid environments. However, in addition to working with a vegetation index specifically designed to reduce the background noise caused by soil variability (SAVI), there are many steps in the processing workflow that help further alleviate these issues.

2.5 Pixel timeseries extraction and smoothing

Despite precautions taken by the imagery providers to minimize noise and provide an analysis-ready product from the MODIS sensor, there were lingering issues that required attention prior to analysis (Thoma et al. 2017). Each polygon larger than 8.3 hectares (the area of a MODIS pixel at NCPN latitudes) was analyzed independently for trends in production and phenology and its relationship with multiple climate variables. Pixels extracted from target polygons above the 90th percentile or below the 10th percentile of average greenness were removed from analysis. This step served several purposes. First, it removed pixels that fell on alliance-group boundaries if the reflectance was very different across the boundary, such as riparian ribbons adjacent to dry uplands. Second, it eliminated areas that may have been classified incorrectly in the vegetation maps if the result of misclassification included an area of substantially different reflectance. It also eliminated inclusions of contrasting reflectance (if any occurred).

After outliers were removed, each pixel was weighted according to its proportional area that fell within the target (see Section 2.2). This step further minimized the effect of any remaining pixels that overlapped target boundaries. After computing an area-averaged value at each timestep for the pixels within a polygon target, missing polygon-average values were interpolated.

For each polygon timeseries , missing daily values were a consequence of the 16-day periodicity of observations and the quality screening that occurred in earlier steps. In order to fill these gaps, missing values were interpolated using a Savitzsky-Golay filter, resulting in a complete daily timeseries for each polygon. Finally, a smoothing filter was used to remove high frequency noise from the timeseries of each polygon. After smoothing across large gaps in winter, prominent dips in the timeseries (i.e., artificially low values that were an artifact of the smoothing) were truncated to a minimum winter value based on pixel values that were likely reflectance from bare soil or senesced vegetation (Wang et al. 2018). This process resulted in a smoothed and complete daily timeseries for each polygon.

2.6 Water-balance model

Vegetation responds to seasonal and interannual variations in temperature and water availability depending on adaptations and site conditions (Thoma et al. 2019; Munson et al. 2015). To understand climate drivers of vegetation condition and potential impacts across large environmental gradients (hot/dry to cold/wet), we used a water-balance model to determine how different aspects of climate and site characteristics affected vegetation production and phenology. The water-balance model quantitatively accounts for temperature, precipitation, and their interactions with local site conditions (such as soil water-holding capacity, slope, and aspect) that affect soil moisture, evapotranspiration, and drought stress (Thoma et al. 2020). To calculate the water-balance variables in the model, we used 1-kilometer, gridded, Daymet temperature and precipitation data (Thornton et al. 2018).

The model partitions precipitation (P, mm) into rain (RAIN, mm) or snow (SNOW, mm of water), which accumulates until warming temperature (T, °C) causes it to melt. Soil moisture (SOIL, mm) is stored in the top meter of soil, which was treated in the model as a single layer with a maximum storage defined by its water-holding capacity. Water holding capacity was obtained from soil surveys where data were available (NRCS 2015) but was fixed at 100 millimeters otherwise. This fixed value accommodated analyses where soil surveys have not yet been conducted and accounted for some water storage in geologic structures (cracks or porous, rocky material) that may be mapped as having no water-holding capacity but that support sparse vegetation detected by the satellite sensor. Water input that exceeds the storage capacity becomes runoff.

Potential evapotranspiration (PET, mm), calculated via the Oudin method, is the amount of water that could be evapotranspired from short grass with the available energy if water was unlimited. The Oudin method calculates PET using daily mean temperature, daylength, and solar radiation (Oudin et al. 2005). Actual evapotranspiration (AET, mm) is the loss of water from soil via evapotranspiration, limited by soil-water availability. Climatic water deficit (D, mm) is the unmet water need of vegetation, and is a measure of drought stress calculated as the difference between PET and AET (Stephenson 1998).

Water-availability variables include P, RAIN, SNOW, and SOIL. Variables that estimate water use include AET and PET; however, AET is limited by dry soil. Two aspects of heat that influence vegetation growth are average annual temperature (T) and growing degree days (GDD) (McMaster and Wilhem 1997).

This study also evaluated two variables that could influence vegetation production and phenology: vapor-pressure deficit (VPD, Pa) and solar radiation (SRAD, W m^{-2}), available from Daymet. Vapor-pressure deficit is the difference between the amount of water vapor air can hold and the amount of vapor in the air. Solar radiation is the energy plants receive from the sun that can be used for photosynthesis (Grossiord et al. 2020; Seager et al. 2015; Stephenson 1990).

In the following sections, state variables representing condition at a point in time (e.g., SOIL, T, VPD) are averaged (Table 2). Variables representing fluxes of water (water passing through the environment) are summed annually or seasonally—except for SOIL, which is presented as an average value because soil water-holding capacity has an upper limit that summation could exceed, which is physically impossible (Table 2).

Table 2. Climate and water-balance variables used to identify correlations with vegetation production and phenology.

Variable	Abbreviation	Units	Type	Temporal summary
Precipitation	P	mm	flux	Sum
Rain	RAIN	mm	flux	Sum
Snow	SNOW	mm	flux	Sum
Snowpack Water Equivalent	PACK	mm	flux	Sum
Water as Rain plus Snowmelt	W	mm	flux	Sum
Date of Complete Snowmelt	Meltd	day-of-year	state	Day
Actual Evapotranspiration	AET	mm	flux	Sum
Potential Evapotranspiration	PET	mm	flux	Sum
Climatic Water Deficit	D	mm	flux	Sum
Solar Radiation	SRAD	W m^{-2}	state	Mean
Temperature (Annual Average)	T	°C	state	Mean
Temperature (Maximum)	Tmax	°C	state	Maximum
Temperature (Minimum)	Tmin	°C	state	Minimum
Soil Moisture	SOIL	mm	flux	Mean
Vapor Pressure	VP	Pa	state	Mean
Vapor-pressure Deficit	VPD	Pa	state	Mean
Growing Degree Days	GDD	°C	state	Sum

The effects of summing or averaging have important implications for interpreting results. Whereas additional precipitation can substantially change the cumulative magnitude of annual precipitation, it takes a large amount of water input to change an annual average soil-moisture value even a small amount. For example, 10 millimeters of additional precipitation falling on dry soil on one day in one year would increase annual precipitation by 10 millimeters but increase average annual soil moisture by just 0.027 millimeters (10/365). Temperature and pressure variables are also summarized as means in this analysis. Units of measure are provided in Table 2.

Snowmelt date (Meltd) used in the phenology analysis was determined from the water-balance model variable, PACK. This term is the daily snow water equivalent (mm) stored in the snowpack that accumulated over winter. In spring, PACK declines rapidly with warming temperature. Determining the day of complete melt is somewhat subjective due to flashy spring snow events that may linger for one to a few days, even in late spring after the initiation of vegetation growth. The algorithm used to identify day of melt begins by searching backward from May 1 (user-specified date) for PACK values greater than four millimeters (user-specified depth) for a span of three days (also user-specified). In the water-balance model, the combination of depth and span are the minimum degree days necessary to yield the user-specified depth of snowmelt water. Visual inspection of snowmelt date plotted on the timeseries of daily PACK values confirmed this was a reasonable approach to differentiating between periods that were predominantly snow covered or snow-free.

2.7 Measures of vegetation production

Because net primary production is generated through photosynthesis and spectral indexes are responsive to abundance of photosynthetically active vegetation, vegetation indexes are good proxies for primary production (Paruelo et al. 2000). Characteristics of the annual repeating cycle of SAVI curves were used as proxies for production and phenology (Figure 2). We determined trends in three variables derived from the SAVI timeseries for each polygon: mean annual SAVI, maximum annual SAVI (maximum value regardless of month in which it occurred), and iSAVI (sum of the daily interpolated SAVI, the area under the curve during the growing season from February through October). Daily interpolation was made via linear regression with a maximum gap size of 16 days. Mean annual SAVI (sum of 16-day observations divided by 23, the number of observations per year) is a measure of average productivity across the calendar year. Maximum annual SAVI is an indication of peak instantaneous rate of vegetation production, or rate of maximum biomass accumulation. It is strongly correlated with both green cover and leaf-area index. The sum of SAVI (iSAVI) is a proxy for vegetation production during the growing season. It is most strongly correlated with biomass production and cumulative productivity (Johnson et al. 2018; Garroutte et al. 2016; Thoma et al. 2002).

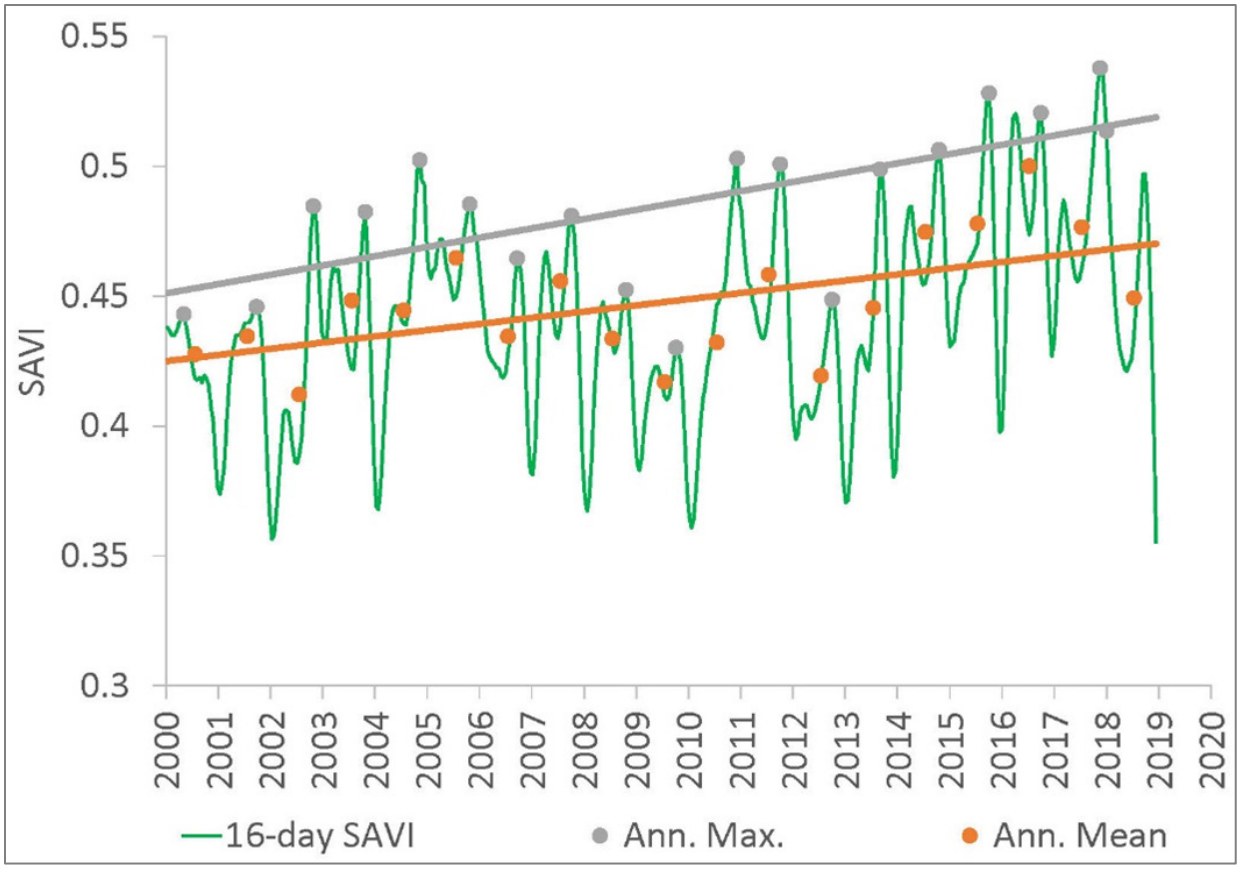

Figure 2. Measures of annual production from a timeseries of 16-day soil adjusted vegetation index (SAVI) values derived from MODIS imagery. Linear trends against time for annual maximum and annual mean values are shown as straight lines. NPS / DAVID THOMA

2.8 Calculating the measures

Trends in production were assessed by tracking changes in maximum and mean annual SAVI for 2000–2019 using the annual aggregated timeseries method (AAT) and Mann-Kendall trend test (Forkel et al. 2013) (see Figure 2). The rate of change (regression slope) was estimated via linear regression, and the significance of change was estimated by the Mann-Kendall trend test (Forkel et al. 2013). Trends in annual maximum values were more reliable than changes in mean annual values because the latter used full annual curves that included screened and gap-filled winter values. Trends in growing-season greenness were considered in the annual pivot-points analyses below.

Representing the sum of daily interpolated SAVI values during the growing season, iSAVI is a holistic measure of the cumulative production of actively photosynthesizing vegetation (Mendez-Barroso et al. 2009; Reed et al. 1994). This proxy for aboveground net primary production results from the intentional construction of spectral indexes, such as SAVI, that are strongly responsive to absorbed, photosynthetically active radiation used by plant canopies to capture and store carbon and energy during growth.

Trends in iSAVI timeseries were noted in some polygons, which confounds relationships with climate unless the trend in iSAVI is removed before analysis. For this reason, we used the first difference in iSAVI, which represents the change in growing-season production from one year to the next, as an indicator of response to weather on an annual basis. This helps guard against overfitting when a trend exists in a timeseries. The annual change in iSAVI was calculated as

$$\Delta iSAVI = \frac{iSAVIt_2 - iSAVIt_1}{t_2 - t_1}$$

where t_1 is the first year of growth, t_2 is the second year of growth, $iSAVIt_1$ is the sum of growing-season SAVI for year t_1, and $iSAVIt_2$ is the sum of growing-season SAVI for year t_2. Positive values of ΔiSAVI indicate increasing growth from one year to the next, while negative values indicate decreasing growth. This framing of the response variable makes an increase or decrease in growth contingent on conditions in the previous year, allowing change to be linked to variation in weather from one year to the next. This is essentially equivalent ($r^2 \sim 0.99$) to the specific-growth concept used in plot-based studies of vegetation response to climate over long periods of time (Munson 2013).

2.9 Climate correlates with annual production

Two types of analysis were used to explore climate relations with annual production (iSAVI).

2.9.1 Single-variable analysis

First, simple linear-regression models compared a single climate variable to the annual increase or decrease in production relative to the prior year. The adjusted r^2 measured the strength of the relationships between the climate variable and vegetation production in a range between 0 and 1, with stronger relationships closer to one. This revealed the proportion of variation in ΔiSAVI explained by variation in climate.

Simple linear regression was used to determine pivot points and production responses (Figure 3; see Section 1.4). Every polygon was tested against every climate and water-balance variable. After screening out relationships that were not significant (p-value > 0.05), the adjusted r^2 terms were averaged across polygons from the same alliance group to see if any one climate variable outperformed the others as a predictor of vegetation production.

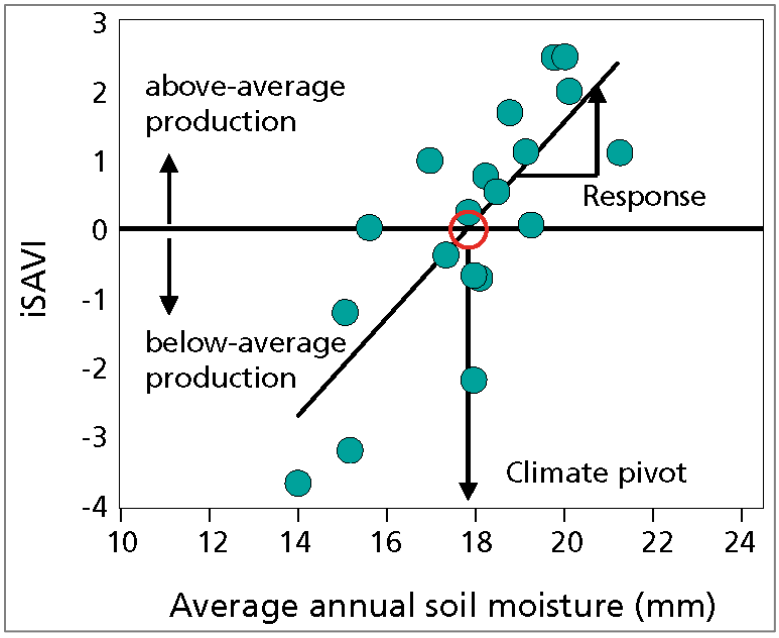

Figure 3. Conceptual diagram of soil-moisture pivot point and response of a single vegetation-alliance map unit to variation in annual average soil moisture. Vegetation production transitions from below- to above-average condition at the soil-moisture pivot point. The response is the rate of change in iSAVI per millimeter of change in average annual soil moisture. Pivot-point figures like this can be constructed for other climate variables. Although not shown graphically, the standard error of pivot points is available for every polygon and variable that had a statistically significant relationship (see Table S-2 in Thoma 2024). NPS / DAVID THOMA

2.9.2 Multiple-variable analysis

Second, multiple-regression models compared multiple climate variables simultaneously with production. These included lagged climate effects characterizing climate conditions 1–2 years prior to an observation. This modeling framework helps account for legacy effects, or conditions in prior years that set limits on production in a current year (Sala et al. 2012). By accounting for legacy effects, the longer-term cumulative effects of drought or good growing conditions in prior years can be considered.

Additionally, this approach can help determine if climate variables interact in important ways to influence production. Whereas the linear-regression framework used to determine pivot points only considers the influence of a single variable, such as AET, on production, multiple regression can determine interactions of AET and D, or other interactions and lags that include effects from prior years.

To account for multiple interacting factors that collectively influence vegetation production on an annual basis, we established a suite of a priori candidate models (Table 3) based on expected vegetation responses to climate variables and lags from our earlier experience working in semi-arid landscapes. In those studies (Thoma et al. 2019; Witwicki et al. 2016), we found water-balance variables to be better predictors of vegetation response than temperature and precipitation. In addition, lag effects were apparent as much as two years prior to a given satellite observation.

Table 3. A priori models of climate influence on vegetation production competed via multiple linear regression modeling to identify best correlates with production.

Model [A]	Climate variable [B]											
	AET	AET (lag1)	AET (lag2)	D	D (lag1)	D (lag2)	SOIL	SOIL (lag1)	SOIL (lag2)	P	P (lag1)	P (lag2)
AET1	X	–	–	–	–	–	–	–	–	–	–	–
AET12	X	X	–	–	–	–	–	–	–	–	–	–
AET123	X	X	X	–	–	–	–	–	–	–	–	–
AET123_D1	X	X	X	X	–	–	–	–	–	–	–	–
AET123_D12	X	X	X	X	X	–	–	–	–	–	–	–
AET123_D123	X	X	X	X	X	X	–	–	–	–	–	–
SOIL1	–	–	–	–	–	–	X	–	–	–	–	–
SOIL12	–	–	–	–	–	–	X	X	–	–	–	–
SOIL123	–	–	–	–	–	–	X	X	X	–	–	–
AET1_D1	X	–	–	X	–	–	–	–	–	–	–	–
AET12_D12	X	X	–	X	X	–	–	–	–	–	–	–
D1_SOIL1	–	–	–	X	–	–	X	–	–	–	–	–
D1_SOIL2	–	–	–	X	–	–	–	X	–	–	–	–
D1_SOIL12	–	–	–	X	–	–	X	X	–	–	–	–
P1	–	–	–	–	–	–	–	–	–	X	–	–
P12	–	–	–	–	–	–	–	–	–	X	X	–
P123	–	–	–	–	–	–	–	–	–	X	X	X

[A] See Table 2 for acronyms.

[B] "X" = variable used in model; "–" = variable not used in model. Lags refer to models that include the water balance term for the preceding one (lag1) or two (lag2) years.

We then competed the models against each other using multiple regression models and identified competitive models based on delta AICc values < 4 to determine the combination of climate variables acting over one or more years that have the most influence on growing-season production. Models that did not compete well (delta AICc > 4) were excluded. Several models could be competitive in any given polygon because every a priori model was evaluated for every polygon. We first looked for a global best model of primary production at the park level by aggregating results from all polygons in the park. Then, we tabulated how frequently the top model occurred by NCPN alliance group to determine the best climate correlates and lags (or the cumulative duration of effect) on production at the alliance-group level.

2.10 Conceptual basis of climate pivot points and responses

Using the pivot-point framework, annual change (ΔiSAVI) was regressed (linear regression) with climate data to determine the degree to which annual variation in weather affected production (Munson 2013). In this analysis, a pivot point is the critical magnitude of a climate or water balance variable where vegetation "teeters" between above- and below-average condition. Generally, water

pivot points are important in water-limited environments. Temperature pivot points are important at higher elevations, where cold temperature limits growth (Thoma et al. 2020).

Vegetation response, or sensitivity to climate or water balance, is the rate of change in condition per unit change in water or temperature. In this analysis, vegetation response is the slope of the regression line when interannual change in iSAVI is related to the corresponding change in climate or water balance for the same period (see Figure 3).

Pivot points and responses are depicted graphically (see Figure 3) as the x-axis value where each linear-regression line crosses the horizontal line, indicating no change from one year to the next. Production values plotting above the x-axis indicate that vegetation production increased from the previous year. Points below the line indicate vegetation production decreased from the previous year. If a deficit pivot point was exceeded during the growing season, vegetation production was likely below average, because vegetation has an inverse (or negative) relationship with water deficit, a measure of drought stress. If an AET pivot point was exceeded during the growing season, vegetation production was likely above average, because production is positively related to AET. Thus, the interpretation of exceeding a pivot point depends on the influence of the climate variable on vegetation (negative for water deficit, positive for water-availability variables).

When the x-axis variable is a water-availability metric, polygons that cross the horizontal line further to the left are considered more dry-tolerant. That is, their performance is above average at lower water availability than that of a polygon that crosses the horizontal line further to the right. For example, a vegetation assemblage with a precipitation pivot point of 250 millimeters is more dry-tolerant than a vegetation assemblage with a pivot point of 300 millimeters. The opposite is true if the x-axis variable is deficit. In that case, polygons that cross the horizontal line further to the left are less dry-tolerant; that is, their production declines to below-average condition when drought stress is relatively low.

The slope of the regression line quantifies the expected change in iSAVI per millimeter of water or degree of temperature. Polygons with steeper regression slopes are more sensitive to a change in water availability. For each unit change in a climate or water-balance variable, a more sensitive vegetation type will have a larger change in growing season iSAVI.

Together, pivot points and responses determined from historical observations of vegetation condition and weather are two important ecological indicators of the critical water amounts (in arid environments) or heat (in alpine environments) needed for growth, and how growth changes per unit change in the climate variable. For this reason, pivot points and responses are indicators of expected change in vegetation production as the climate changes in the future (Munson et al. 2011). When linked with projections of future climate, these two important ecological variables can be used in quantitative vulnerability assessments as part of the Climate Smart planning framework (Stein et al. 2014), which helps managers set long-range goals achieved by near-term tactical actions (see Section 4).

2.10.1 Operational use of pivot points for "now-casts"

This report provides information for estimating vegetation condition using climate data. By tracking the climate variable with the strongest relationship to production in real time relative to its corresponding pivot point, we can determine if weather conditions are below, near, or above predetermined pivot points, and by what amount. In this way, we can use climate data to provide real-time "now-casts" indicating when weather conditions suggest production is likely to be above or below that of the previous year.

The interpretation of climate conditions against a pivot-point value requires consideration of pivot-point precision determined by the standard error around the regression line where it crosses the horizontal axis. The range is larger in polygons where the relationship between climate and vegetation growth is more variable. At the alliance group level, pivot-point range is caused by variability in plant assemblages in different polygons of the same alliance, as well as variations in soil and site properties. Additional variation is caused by noise in the MODIS sensor when it operates near its sensitivity limits in sparsely vegetated environments, errors in the gridded climate data, and vegetation legacy effects that cause plants to respond differently to the same weather, depending on what happened in the recent past. All these factors contribute to the observed standard error of a pivot point that brackets weather conditions that determine if vegetation is likely performing above or below average.[2]

Vegetation performance when weather conditions are within the standard error of the pivot point is best described as "near average." When weather conditions exceed the standard error of the pivot point (either above or below the pivot point), there is higher confidence that vegetation production is above or below average.

2.10.2 Lapse-rate adjustment of station data for operational use with pivot points

Operationally, vegetation condition can be reported in real time using weather-station data to calculate daily water balance (see The Climate Analyzer). These data can be compared to a pivot point. The relationships between climate and vegetation in this report used Daymet (a gridded climate dataset). For this reason, before operational reporting commences using weather-station data, a relationship needs to be established between the Daymet climate dataset at a location of interest and the weather station, typically located at park headquarters. Specifically, station temperature and precipitation data should be lapse-rate adjusted for the location of interest if there is more than 500 meters' difference in elevation between the weather station and the site of interest. This is because temperature and precipitation change with elevation.

2.11 Phenology metrics and climate drivers

Phenology metrics were determined using the derivative method in the greenbrown R package (Forkel and Wutzler 2015) after smoothing and interpolation to daily values. The derivative method identifies growing-season phenology by recognizing inflections in the annual curves where growth

[2] Although not shown graphically, the standard error of pivot points is available for every polygon in Table S-2 in Thoma (2024).

rate accelerates (start), peaks (maximum) and decelerates (end) (Figure 4). Length of season (LOS) is the span of time between start-of-season (SOS) and end-of-season (EOS). These values were determined for every polygon-year combination where possible. In some cases, phenology metrics could not be determined because the amplitude of annual variation was small, which made it impossible to find inflection points. The LOS metric was dropped if either SOS or EOS could not be determined. SOS, EOS, and LOS metrics were also dropped if SOS occurred in winter (between November 1 and April 1) due to vegetation shadows that confound satellite-based phenology assessments (Norris and Walker 2020).

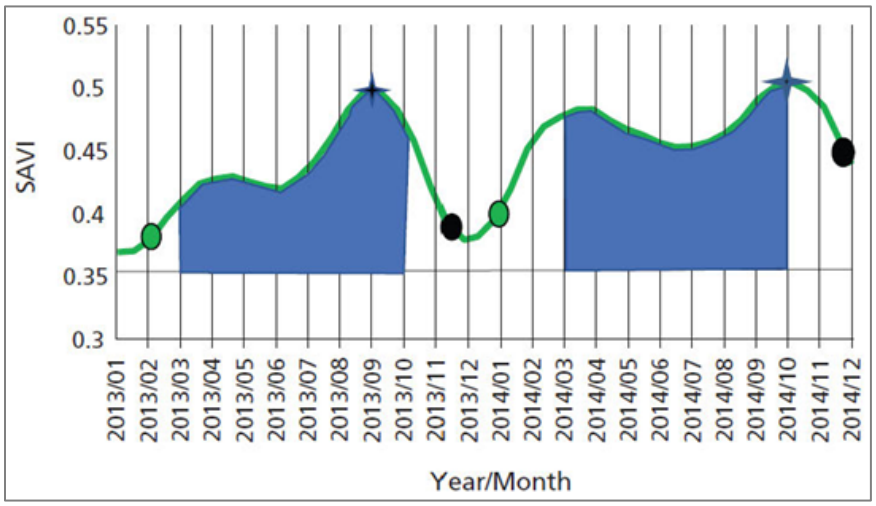

Figure 4. Integrated area under the growing-season curve (shaded area) for one polygon over two calendar years. The months used to calculate growing season production are fixed and include March through October (excepting polygons with winter peaks which are screened from phenology analysis). Phenology metrics are derived using a process that determines inflection points on the annual curves using the derivative (rate of change in growth rate) method. In some years, phenology cannot be determined in semi-arid environments due to weak or noisy signals. The fixed growing-season duration used for calculating iSAVI and the start and end of growing season determined from phenology analysis may not always agree. The start of growing season (green point), peak (star), and end of growing season (black point) indicate important annual milestones in vegetation growth over two consecutive years. NPS / DAVID THOMA

Polygon-level phenology metrics were summarized across alliance groups. The summary involved averaging linear regression slopes (days of change per year) across polygons within an alliance type, then multiplying the slope by the number of years (20) in the study to determine the average days of change in each phenology metric over the course of the study. Due to variation in the regression relationships, and the use of the regression slope to convert to days of change in each metric, the change in LOS in the summary tables is similar to, but not equal to, the length of time between SOS and EOS.

Climate drivers of phenology were identified by focusing on SOS because plant growth in spring is most sensitive to climate (Fu et al. 2014). A suite of climate variables was reduced by dropping variables highly correlated with day-of-year ($r^2 > 0.7$) and determining pairwise correlations between

the remaining explanatory variables. In the case of correlated variable pairs, the more integrative variable was retained.

The timing of SOS, peak greenness and its magnitude, senescence, and LOS were derived from the full annual curves for each polygon, with winter-period minimums truncated to 60% of the winter maximum during the period of record. The cutoff value of 60% was determined via trial and error that both minimized lengths of winter gaps and included growing-season SAVI in every year. This prevented long periods of snow or winter cloud cover from having undue influence on the timing of phenology. The truncation of winter minimum values described above was a simplified version of published methods (Wang et al. 2018).

Some vegetation types (primarily conifer and shrublands) in the western US exhibit a peak satellite-observed greenness (measured using the normalized difference vegetation index, or NDVI) in winter months that is an artifact of shadows when the angle between reflected sunlight and the satellite is large (Norris and Walker 2020). It is unknown how this issue affects SAVI. The bands used to calculate SAVI are the same as those used to calculate NDVI, but a soil-correction factor is applied in SAVI to account for variable background reflectance. There is currently no known solution for resolving this shadowing effect. Thus, polygon-year combinations that exhibit winter peaks cannot be used in phenology analysis. These polygon-years were removed by determining if their annual peak of greenness occurred during winter months, defined as the period between November 1 and April 1. If any winter peaks in SAVI occurred during any year of the study period, the polygon was removed from analysis for that year. This allowed retention of polygon-year combinations that did not result in spurious satellite observations, rather than entirely removing a polygon from analysis if only a few years failed the screening rules.

Two statistical methods were used to identify climate drivers of SOS, or green-up. This helped identify multiple lines of evidence for drivers if both methods yielded similar results. The first method relied on preconceived notions of phenology drivers. The second method, a machine-learning approach, let the data tell the story. In the first method, a priori models thought to be important in western rangelands were identified (Table 4) (St. Peter 2015). These models were competed against one another to determine the top models of SOS.

Table 4. A priori models of climate influence on the start of the growing season competed via multiple linear regression modeling to identify the best correlates with production.

	Climate variable [B]											
Model [A]	**AET**	**GDD**	**P**	**RAIN**	**D**	**VPD**	**SRAD**	**Tmax**	**Tmin**	**VP**	**SOIL**	**Meltd**
AET	X	–	–	–	–	–	–	–	–	–	–	–
GDD	–	X	–	–	–	–	–	–	–	–	–	–
P	–	–	X	–	–	–	–	–	–	–	–	–
RAIN	–	–	–	X	–	–	–	–	–	–	–	–
D	–	–	–	–	X	–	–	–	–	–	–	–
VPD	–	–	–	–	–	X	–	–	–	–	–	–
SRAD	–	–	–	–	–	–	X	–	–	–	–	–
Tmax	–	–	–	–	–	–	–	X	–	–	–	–
Tmin	–	–	–	–	–	–	–	–	X	–	–	–
VP	–	–	–	–	–	–	–	–	–	X	–	–
GDD_P	–	X	X	–	–	–	–	–	–	–	–	–
GDD_RAIN	–	X	–	X	–	–	–	–	–	–	–	–
GDD_SOIL	–	X	–	–	–	–	–	–	–	–	X	–
GDD_AET	X	X	–	–	–	–	–	–	–	–	–	–
SRAD_AET	X	–	–	–	–	–	X	–	–	–	–	–
SRAD_P	–	–	X	–	–	–	X	–	–	–	–	–
Meltd	–	–	–	–	–	–	–	–	–	–	–	X
Meltd_SRAD	–	–	–	–	–	–	X	–	–	–	–	X
Meltd_P	–	–	X	–	–	–	–	–	–	–	–	X

[A] Models were competed via generalized linear mixed-effects modeling to identify the best correlates with green-up (SOS). All climate variables were summed or averaged from January 1 to the day of year when green-up began. See Table 2 for acronyms.

[B] "X" = variable used in model; "–" = variable not used in model.

In the second method, the random forests machine learning technique was used to determine important drivers of phenology and provide predictive models of SOS (Breiman 2001). Random forests is a machine learning method for regression that constructs a multitude of decision trees until the optimum combination of factors describing a result is obtained. In this case, a priori candidate models were not specified beforehand. Rather, the random forests algorithm used climate and water balance variables to identify a top model using a training subset consisting of 70% of the data, which was randomly selected. The random forests algorithm generated 2,000 decision trees with a maximum of four variables randomly chosen per split, which is the recommended number for a model testing the utility of 12 predictors. Sampling was done with replacement, which is the default setting.

The top model was validated against a holdout (validation) dataset consisting of the remaining 30% of observations. Variable-importance plots were used to identify which variables had the most

predictive power. They consisted of percent increase in mean square error (%IncMSE), which is a measure of model improvement when adding each variable to the model, and increase in node purity (IncNodePurity), which is the difference in residual sum-of-squares in regression with or without each variable.

After model fitting with the training data, SOS predictions were made using the validation dataset, where SOS predictions could be compared against observations in the validation dataset. The accuracy of predictions for SOS were characterized by the mean absolute error (MAE), which is the mean value of the difference between predicted and observed SOS in units of days. The MAE is the average magnitude of error in days without specifying the direction of the error, thus specifying the average plus or minus error rate of predictions.

3 Results and Discussion

3.1 Completeness of satellite observations

The completeness of growing-season observations was 87% across all targets for the 20-year period of analysis. Clouds, aerosols, and snow cover reduced the average completeness of high-quality observations to 66% of potential observations on an annual basis across all polygon targets. The minimum completeness for any single polygon on an annual or seasonal basis was 45% and 59%, respectively.

Before analyzing satellite observations with climate and water balance, gaps were linearly interpolated to a daily time step prior to smoothing. This removed high-frequency noise in the timeseries that could not be removed via quality screening. There were no missing climate or water-balance data.

3.2 Timeseries

At Curecanti NRA, SAVI observations reflected differences in vegetation response to climate that were apparent when observations were organized by NCPN alliance group (Figure 5). Some polygons were generally greener than others (indicating higher productivity and biomass accumulation), but within alliance groups there was considerable variation. That variation can be due to species assemblages within the alliance and site properties that modify the local effects of climate. Some outlier polygons within alliance groups might need to be considered separately in future analyses if interest is in the central tendency of an alliance group. Although the Water alliance group can be ignored in this analysis, it is included because it may demonstrate useful information about vegetation growing along shorelines or in riparian areas adjacent to areas classified as Water, such as the streams that flow into and out of the reservoirs.

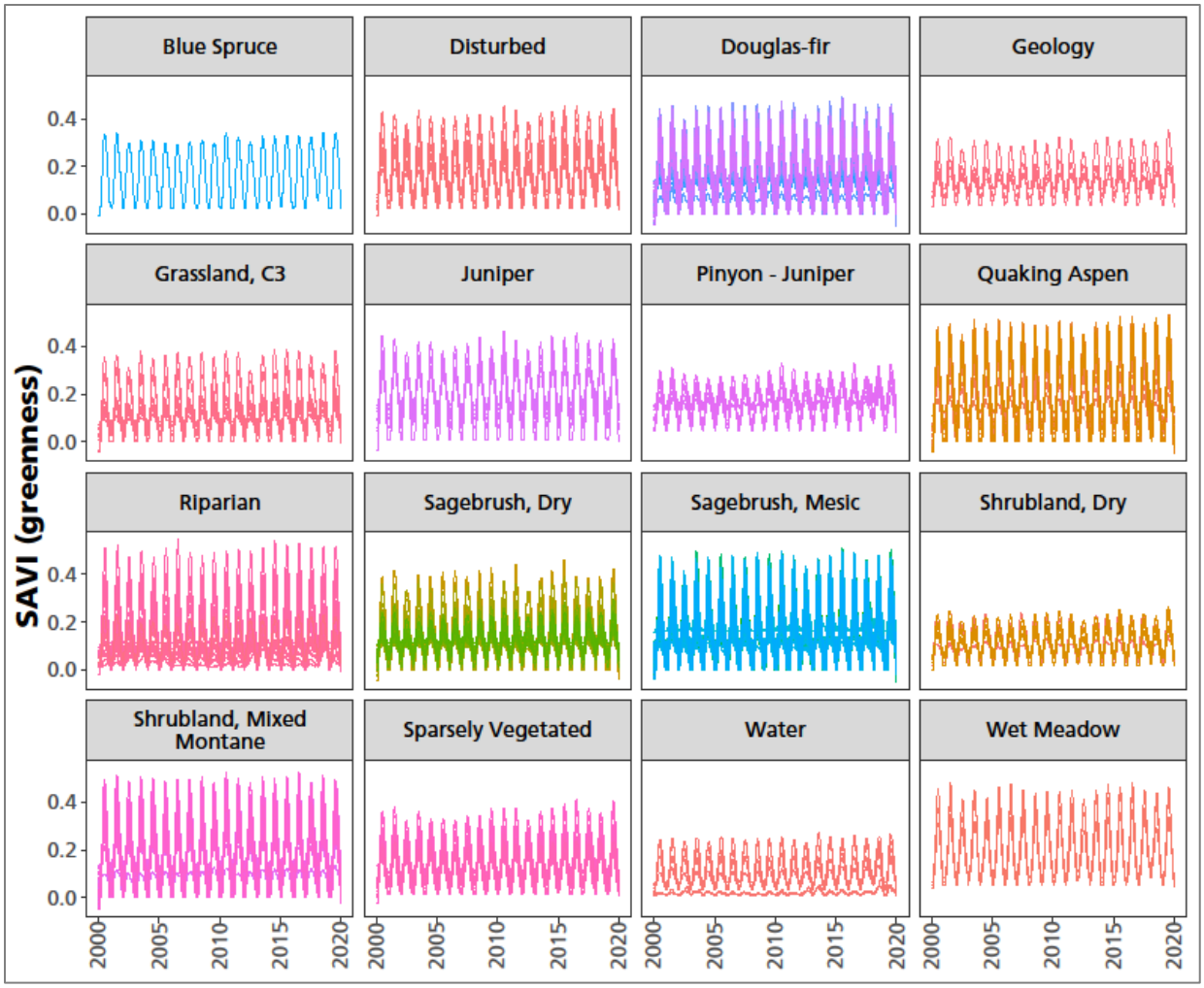

Figure 5. Soil-adjusted vegetation index (SAVI) timeseries by alliance group for 838 polygons analyzed for 2000–2019. Colors help differentiate individual polygon timeseries traces. Each polygon timeseries was filtered to include only high-quality pixel values, with minimum values truncated to winter minimum, gap-filled, and then smoothed with a Savitsky-Golay moving-window filter to remove high-frequency noise. Analysis was limited to polygons of > 8.3 hectares. A single-line trace indicates either all polygon units have similar seasonality and interannual variation, or only one polygon of the alliance group was sampled. NPS / DAVID THOMA

Gap-filled and smoothed timeseries illustrated a broadly similar upward trend in all alliance groups during the study period (Figure 5). However, the alliance groups showed a high degree of variability in the amplitude and timing of peak values. It was typical for some polygons in an alliance group to exhibit "outlying character," indicating they were not a good fit with other polygons in the group. This issue was most notable in the Douglas-fir, Riparian, Mixed Montane Shrubland, and Water alliance groups. Despite filtering out outlying polygons that had an annual average value greater than the 90th or less than the 10th percentile, this could happen for several reasons. Grouping vegetation types into alliance groups forces some dissimilarity among group members; misclassification in the vegetation-mapping process; or, less commonly, disturbance since mapping was completed that

resulted in a different vegetation response signal than what is characteristic of other polygons in the alliance group.

It is important to evaluate "outlier" polygons carefully, with consideration given to potential effects of land use or disturbance. For instance, timeseries in the Water alliance group were surprising because, based on the alliance-group name, little if any vegetation should have been present. However, Water polygon boundaries obtained from the vegetation map are static and do not reflect changing reservoir levels. Strong seasonality and relatively high-amplitude SAVI in some Water polygons suggested that (1) there was some vegetation growing in areas mapped as Water in some years, (2) there was some pixel overlap of polygon boundaries picking up vegetation signals that could not be removed despite the rigorous screening criteria, or (3) algal blooms in the reservoirs were detected as changes in SAVI. Without further investigation, it is not possible to know which of these issues, or what combination of issues, was in play.

3.3 Trends in indicators of annual production

Significant upward trends ($p < 0.05$) in maximum and mean annual SAVI occurred across 98% and 99% of the study area, respectively. Only 1.6% and 0.7% of the study area decreased in maximum or mean annual SAVI, respectively. Decreases were noted in many alliance groups but the largest area of decrease occurred in the Quaking Aspen (310 ha) and Douglas-fir (206 ha) alliance groups. The greatest area of mean annual and maximum annual SAVI increase occurred in the Mesic and Dry Sagebrush alliance groups representing 55% of the study area analyzed in and near Curecanti NRA (Table 5; Appendix A, Figure 31). The few areas showing downward trends in production may be due to natural disturbance, management actions, disease, fire or drought, any of which could likely be verified by site visits.

Table 5. Amount of park area with increasing (pos) or decreasing (neg) trends in mean annual or maximum annual SAVI by alliance group. Since there are two variables that can trend in the same or opposite directions there can be more than one row of information for each alliance group.

Alliance group	Annual trend		Park area (hectares)	# of polygons	% of analysis area
	Maximum	Mean			
Blue Spruce	pos	pos	9.7	1	0.02
Disturbed	pos	pos	1,300.6	8	3.34
Disturbed	neg	neg	38.3	1	0.1
Disturbed	neg	pos	33.5	1	0.09
Douglas-fir	pos	pos	3,437.4	119	8.82
Douglas-fir	neg	pos	149.7	7	0.38
Douglas-fir	neg	neg	44.1	2	0.11
Douglas-fir	pos	neg	12.7	1	0.03
Geology	pos	pos	71.8	5	0.18
Grassland, C3	pos	pos	400.0	14	1.03
Juniper	pos	pos	350.8	12	0.9

Table 5 (continued). Amount of park area with increasing (pos) or decreasing (neg) trends in mean annual or maximum annual SAVI by alliance group. Since there are two variables that can trend in the same or opposite directions there can be more than one row of information for each alliance group.

Alliance group	Annual trend		Park area (hectares)	# of polygons	% of analysis area
	Maximum	Mean			
Pinyon - Juniper	pos	pos	360.7	10	0.93
Quaking Aspen	pos	pos	2,707.5	53	6.95
Quaking Aspen	neg	pos	199.3	5	0.51
Quaking Aspen	neg	neg	90.5	5	0.23
Quaking Aspen	pos	neg	20.1	1	0.05
Riparian	pos	pos	1,093.1	36	2.81
Riparian	neg	neg	15.5	1	0.04
Sagebrush, Dry	pos	pos	9,533.9	156	24.47
Sagebrush, Dry	pos	neg	13.9	1	0.04
Sagebrush, Mesic	pos	pos	12,073.7	278	30.99
Sagebrush, Mesic	neg	pos	26.0	1	0.07
Sagebrush, Mesic	pos	neg	15.1	1	0.04
Shrubland, Dry	pos	pos	233.8	13	0.6
Shrubland, Mixed Montane	pos	pos	2,648.5	61	6.8
Shrubland, Mixed Montane	neg	neg	34.4	2	0.09
Shrubland, Mixed Montane	neg	pos	0.2	1	0.02
Sparsely Vegetated	pos	pos	535.1	32	1.37
Water	pos	pos	3,366.4	7	8.64
Wet Meadow	pos	pos	138.3	3	0.35

Results by polygon for significant trends in maximum and mean annual SAVI are in Table S-3 in Thoma (2024). Significant upward trends in growing-season iSAVI, determined via simple linear regression, were found at the alliance group level for all alliance groups (Figure 6). The upward trend in the Water alliance group could result from increases in stream- or reservoir-adjacent riparian vegetation or increases in algal blooms in the reservoirs over time.

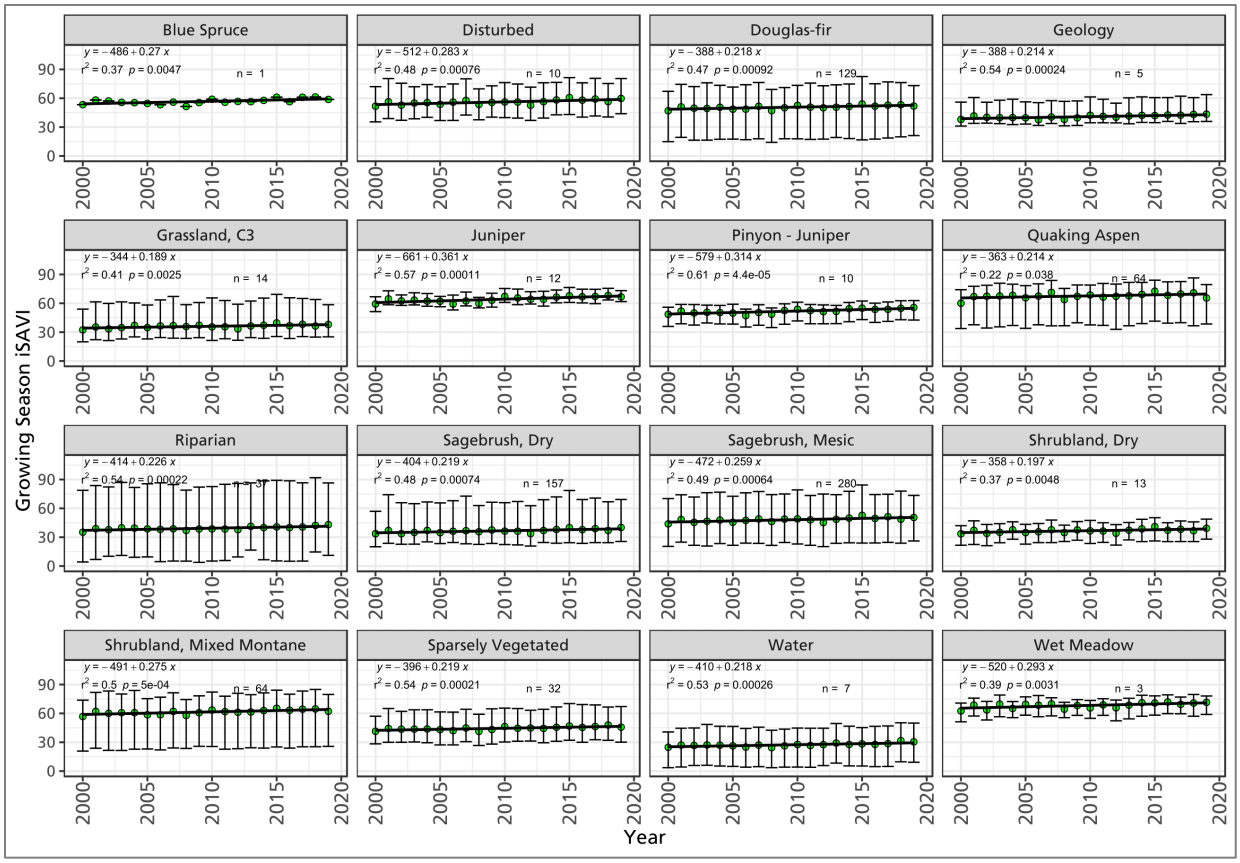

Figure 6. Trends in mean growing-season iSAVI by alliance group, determined via simple linear regression. Bars are the standard error among polygons within each alliance group. n = number of polygons analyzed in each alliance group, r^2 = coefficient of determination, p = p-value, y = growing season iSAVI, x = year. NPS / DAVID THOMA

3.4 Trends in indicators of growing season production

As a subset of the annual period, the growing-season iSAVI focused on the March through October period, revealing climate-driven temporal patterns in all alliance groups. The study began in 2000, which was a low production year. Other low production years include 2002, 2008, and 2012, which corresponded with dry periods. Most dry periods were followed by a recovery, with peaks in iSAVI from 2005–2007. A pronounced downward trend occurred from 2016–2018. By the end of the study above-average levels of production were observed in most alliance groups (Figure 7), demonstrating the resilience of Curecanti NRA vegetation production to short term drought stress during the study.[3]

[3] This finding does not imply vegetation composition was not affected or did not change. Composition change cannot be determined from this analysis.

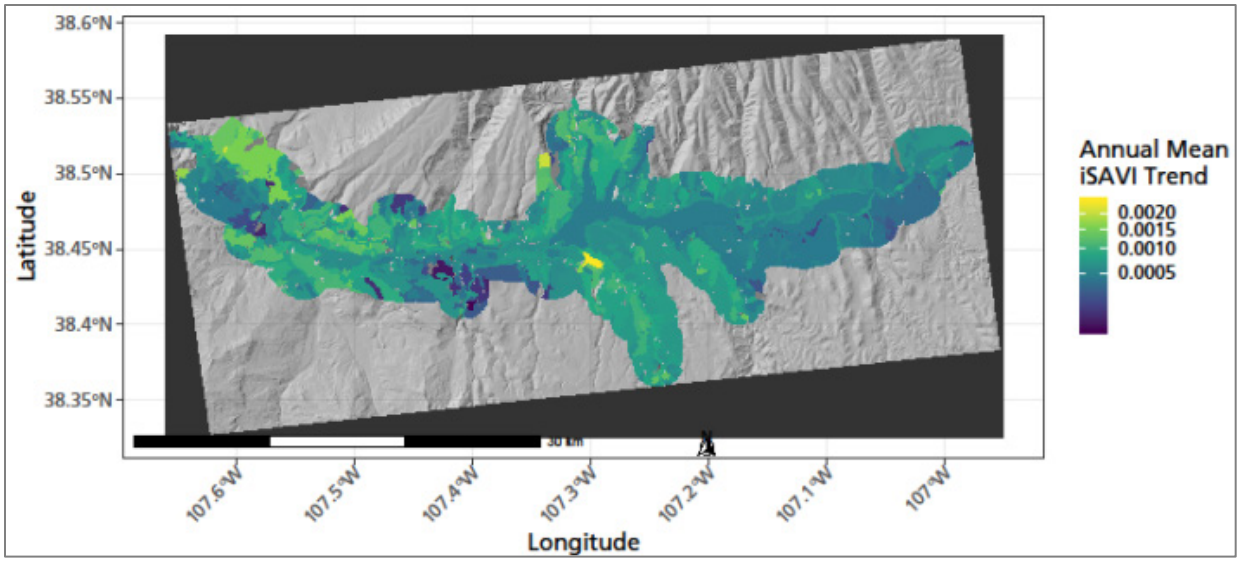

Figure 7. Spatial pattern of trends in mean annual iSAVI. Trend is average change in iSAVI per year from 2000–2019. NPS / DAVID THOMA

Evaluation of simple linear-regression slopes shows that Juniper and Pinyon-Juniper increased in greenness at faster rates than other alliance groups during the 20-year period of observations, while C3 Grassland and Dry Shrubland alliance groups increased at the slowest rates. Upward trends in growing-season production were observed in all alliance groups in the park (Figure 8; see Figure 6 for slopes).

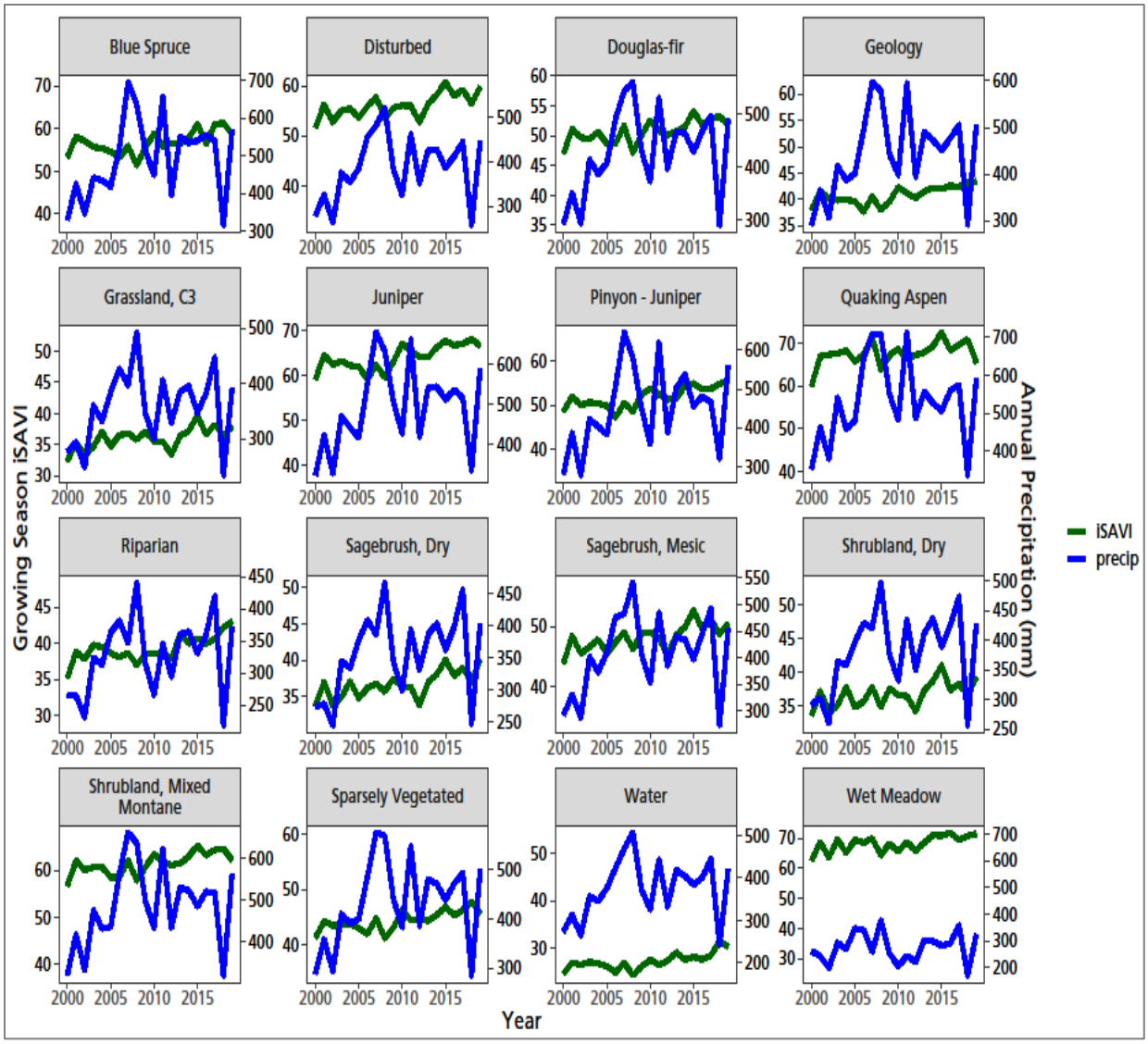

Figure 8. Co-variation in growing-season production, estimated as the iSAVI between March and October, and water-year cumulative precipitation averaged within alliance groups, demonstrating the link between climate and vegetation production in the park at the annual scale. The timeseries shown here is intended to illustrate precipitation as a master climate driver of production in semi-arid environments. Statistical analyses of the relation of production to precipitation and all other climate variables are the subject of following sections. NPS / DAVID THOMA

The mostly upward production trends for the woody-plant alliance groups in Curecanti NRA were consistent with other research findings on the Colorado Plateau, which showed shrubs as dominant where winter soil moisture was high and seasonal temperature variable, and grasses as dominant where summer moisture was available (Gremer et al. 2018). That study pointed out that rising temperature and increasing temperature variability, both associated with climate change, will result in conditions more favorable to shrubs because the change in temperature is expected to overwhelm the role of available soil moisture by late century. It also noted that shrubs are better adapted to larger temperature fluctuations than grasses. A review of woody-plant proliferation (Barger et al. 2011)

found that the seasonality of precipitation, land use, and atmospheric CO_2 concentrations were all important drivers of woody-plant expansion in semi-arid regions.

3.5 Climate relations

3.5.1 Qualitative patterns in annual precipitation and production

In most semiarid environments water is a growth limiting factor. For that reason it is instructive to qualitatively evaluate timeseries of annual precipitation and production to determine if vegetation responds strongly to variation in annual precipitation. Like annual trends in production, growing-season production in Curecanti NRA vegetation alliance groups also increased between 2000 and 2019 (Figure 8). However, no significant trends were noted for any of the water balance variables (p-value > 0.05 in all alliance groups; Appendix A, Figures 84 to 93). Improved water-use efficiency due to the fertilization effect of rising atmospheric CO_2 concentrations may explain some of the increase in production, and above average precipitation during the growing season may have also contributed to increases in growing-season production (Sorokin et al. 2017). Plotting the iSAVI difference from long-term average iSAVI with precipitation shows a weak temporal correspondence of interannual variation in annual precipitation and production (Figure 8), whereas CO_2 concentrations increased monotonically on an annual basis during the study period (see the NOAA Global Monitoring Laboratory). The link with precipitation is weak (Figure 8), so other drivers of annual and growing season production should be considered, including temperature. As will be shown later, most alliance groups at Curecanti have positive growth relationships with temperature. This provides qualitative evidence that vegetation production is co-limited by temperature and water availability in some alliance groups.

While peaks and valleys in the timeseries coincided in some years and some alliance groups, there were differences in the magnitude of vegetation response to precipitation, and evidence of a response delay that varied by alliance group. Production may respond to precipitation in some years and temperature in others, depending on whether heat or water limits growth in each year. Lags in vegetation response can be caused by legacy effects of vegetation condition in prior years that carry over to subsequent years. The combined effect of temperature suitable for growth and water availability is explored in Section 3.7.

Such legacy effects have been noted in semi-arid vegetation response to precipitation where prior conditions set the stage for current-year production. For example, a wet year following a drought may not be as productive as a wet year following an average precipitation year due to legacies in tillers, stems, root density, and seed production, which are limited in a drought (Thoma et al. 2016; Noy-Meir 1973). Because of prior conditions, the largest peaks in annual production do not always coincide with the largest peaks in annual precipitation.

In addition, the timing and magnitude of vegetation response to precipitation are affected by the structural and physiological traits of plants, including rooting depths, stomatal control of gas exchange, leaf morphology, and annual or perennial life cycle, and the site conditions where they grow (Munson et al. 2015). Plant physiology may explain why peaks and valleys in annual production are more pronounced in grasslands and shrublands but muted in woodland alliance

groups. Grasslands are generally more responsive to interannual weather variation, while woodlands with deeper rooting systems can be buffered from short-term droughts. Additionally, evergreens that retain leaves for multiple years have lower-amplitude seasonal cycles (Yang et al. 2019). Also, variation in the magnitude of vegetation response to variation in precipitation could be due to higher runoff in high precipitation years if a large proportion of precipitation fell in a few storm events.

Collectively, the response of vegetation to interannual variation in weather is complex. The study of these interactions across space and time is greatly aided by the high frequency of satellite observations coupled with continuous daily climate observations over the same period. Organizing the remotely-sensed observations by management-relevant vegetation types provides insights that may be useful in climate adaptation planning.

3.5.2 Single-variable drivers of production

At the park level, relationships between growth and climate variables were generally weak due to the highly variable response relationships with climate across vegetation types (not shown). However, when examined by alliance groups, better relationships emerged (Figure 9).

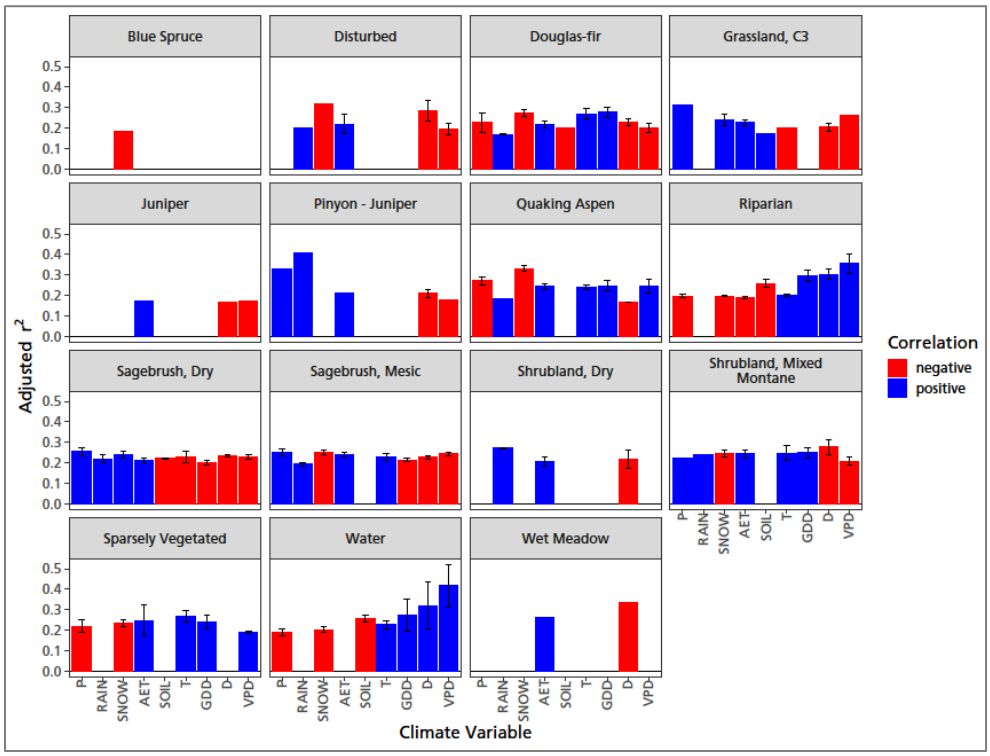

Figure 9. Significant (p-value < 0.05) relationships between water-year climate variables and first difference of growing season iSAVI, 2000–2019. Bar height is the mean variation in iSAVI explained by variation in climate or water-balance variable on the x-axis. Blue bar color indicates positive correlation, red bar color indicates negative correlation, and error bars are standard error. P = precipitation (mm), RAIN = precipitation as rain (mm), SNOW = precipitation as snow (mm of water), AET = actual evapotranspiration (mm), SOIL = average soil moisture (mm), T = average temperature (°C), GDD = growing degree days (°C), D = water deficit (mm), VPD = vapor-pressure deficit (Pa). NPS / DAVID THOMA

Vegetation production in all alliance groups was correlated with multiple aspects of climate. C3 Grassland, Dry Sagebrush, and Dry Shrubland were positively correlated with water abundance variables and negatively correlated with measures of heat, indicative of the water-limited conditions where these alliance groups occur. Riparian and Water alliance groups showed the opposite pattern, indicative of temperature-limited environments, which makes sense in places such as these alliance groups where water is abundant. Other alliance groups, including Disturbed, Douglas-fir, Quaking Aspen, Mesic Sagebrush, and Mixed Montane Shrubland, had more complicated responses to temperature and water variables. These complex responses may be related to the length of the growing season and magnitude of water availability during the growing season. For example, Douglas-fir is negatively related to both snow and annual precipitation (much of which falls in winter as snow), likely because high snow years with snow cover that persists longer leads to a shortened growing season. However, this same alliance group is positively related to rain and actual evapotranspiration, which represent additions of water during the growing season and growing season water use. Within alliance groups with multiple polygons, there was variation in relationship strength among polygons, indicated by error bars in Figure 9 (also see Table S-2 in Thoma 2024). This can be caused by variation in species assemblages and abundances that differ among map units of the same alliance. On an annual basis, most of the water-balance variables were no better correlated with production than actual evapotranspiration (AET).

Production can increase or decrease with precipitation depending on elevation. Production increases with precipitation at lower, water limited elevations, but at the highest elevations production decreases with precipitation because much of the annual precipitation falls as snow, and deep or lingering snowpacks shorten the growing season. Production is always positively related to AET (where there are significant relationships), because AET represents the simultaneous availability of water and heat needed for growth regardless of elevation.

Some vegetation types respond more strongly to seasonal weather than annual conditions. For these plants, warming temperatures in the spring initiate growth. Then, as soil moisture decreases throughout the growing season, other variables, such as water deficit or rain, become important. Depending on the species, most growth may occur in spring or late summer. Thus, the timing of seasonal water and energy availability may be more important to annual vegetation production than total annual water and energy availability (Barnes et al. 2016). These kinds of seasonal responses to weather are difficult to characterize on an annual basis with a single variable because the important climate drivers switch seasonally and there may be long-term legacy effects from earlier growing seasons that affect current-year production (Thoma et al. 2016).

In other words, multiple aspects of climate and water balance act over both short and long periods to affect annual production. Thus, a simple linear-regression approach that considers single-variable influences on production over the course of an entire year is an oversimplification of important vegetation-climate relations. This may explain coefficients of determination < 0.5 (Figure 9), which may seem unimpressive but are similar to species responses to single variables in plot studies (Munson et al. 2011).

Nevertheless, there is value in determining single-variable regressions because they can identify important drivers that result in increases or decreases in annual production and represent a practical way to derive critical water needs and drought-stress indicators (Thoma et al. 2019; Munson et al. 2016) that can be tracked using data from weather stations. The best single-variable indicator of annual vegetation production can be determined by alliance group from visual inspection of Figure 9 (tallest bar = best relationship), or by polygon from Table S-2 in Thoma (2024).

Actual evapotranspiration was the only variable positively correlated with upland vegetation production in every alliance group where it was statistically significant. The only exception was a single polygon in the Riparian alliance group (polygon CURE_6525; Horseweed - Thistle - Prickly Lettuce Wet Meadow) located on the southeastern shoreline, which is strongly affected by reservoir levels rather than meteoric weather. Actual evapotranspiration is used in the following sections that further explore climate-vegetation relationships. Multiple predictors and time lags of annual production response are considered in a later section.

3.6 Pivot points

3.6.1 Pivot points indicate drought tolerance

Plant species with smaller pivot points for water-abundance variables (e.g., precipitation, rain, snow, actual evapotranspiration, soil moisture) demonstrated a higher degree of drought tolerance, because less water was needed to achieve above-average production (Tables S-2 and S-4 in Thoma 2024).[4] Conversely, larger pivot points for variables representing heat, unmet water need, or atmospheric dryness also indicated a higher degree of drought tolerance, because more drought was tolerated before production dropped below average.

At Curecanti NRA, the most drought-tolerant alliance group (i.e., the one with the highest water deficit pivot point) was Wet Meadow, but only one polygon in this alliance group had a significant relationship with water deficit (Figure 10). The next most drought-tolerant alliance groups were Pinyon-Juniper and Riparian. The high deficit pivot points for Wet Meadow and Riparian alliance groups are likely due to their location in low-lying places where accumulation of water from upslope positions makes these alliance groups less drought prone in low-precipitation years. Because these alliance groups collect water from upslope, they can have above average performance even when annual precipitation is low or when water deficit is high in surrounding areas. The water-balance model used in this report does not accumulate flow from upslope positions, so it cannot account for the process of flow accumulation that is likely the cause of drought tolerance in these alliance groups. Nevertheless, the physical processes that collect water in these low-lying locations will continue to

[4] The pivot points differed among water-abundance variables because they represent different pools, periods and magnitudes of water availability. For example, soil moisture is only a fraction of total precipitation (P), because some P runs off and is not available to plants. Similarly, rain and snow represent fractions of total P that supply water for vegetation at different times of the year. Thus, each variable represents a different "pool" and phase of water (solid, liquid, or gas) that may be seasonally active or present during different seasons.

collect water in the future, which will likely make these alliance groups less susceptible to drought than other upland alliance groups.

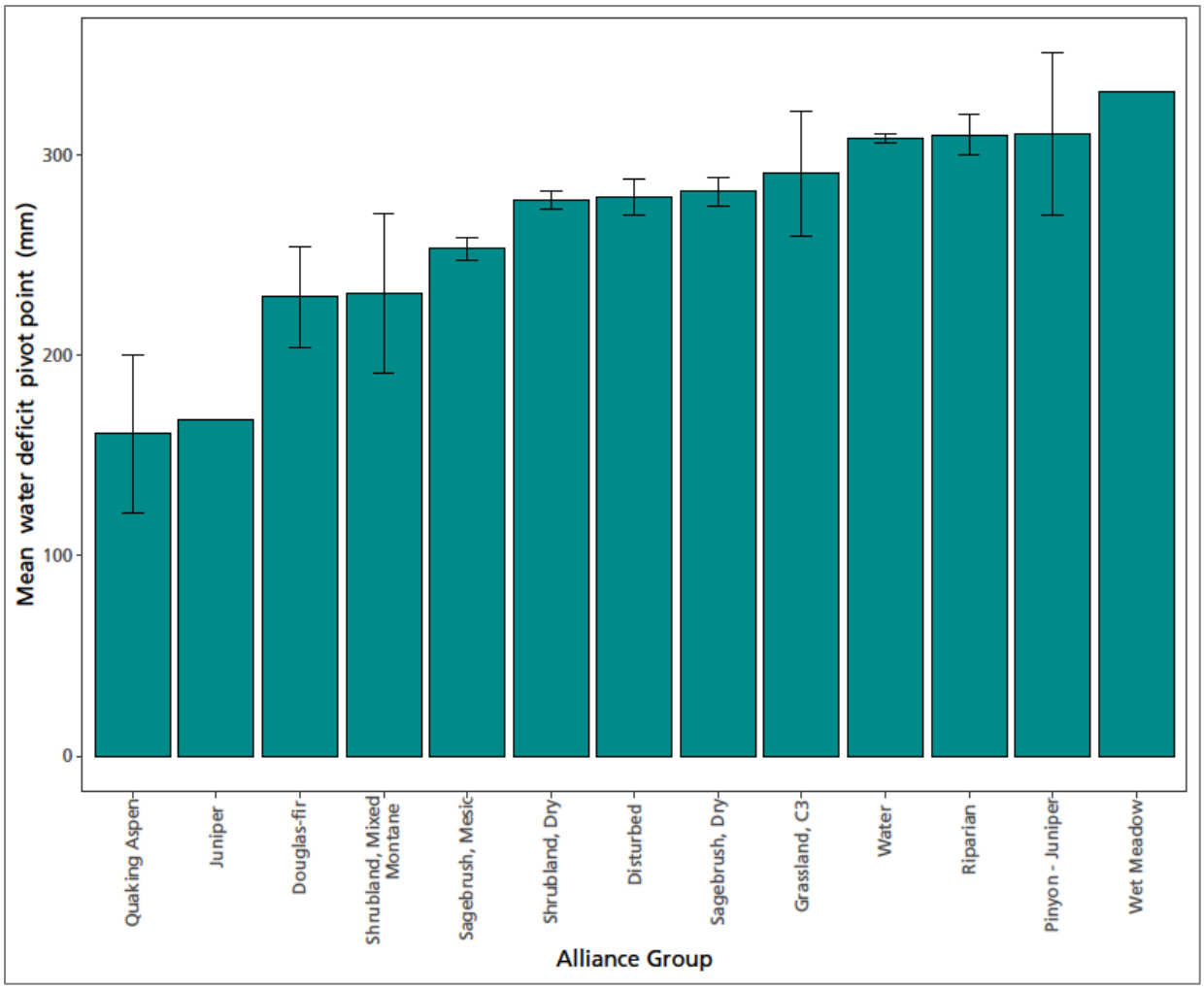

Figure 10. The mean water deficit pivot-point values shown here represent drought tolerance for the different alliance groups. Standard error bars indicate the range in variability of pivot points among polygons of an alliance group if more than one polygon had a statistically significant relationship ($p < 0.05$) with water deficit. Pivot points identify the critical water need that achieves average production for each alliance group. NPS / DAVID THOMA

Pivot points for a specific geographic area are related to, but not always equal to, the mean annual climate value where a pivot point is determined. For this reason, spatial patterns in pivot points often but not always follow precipitation and temperature gradients with elevation. A study in the southwestern US found that found soil properties explained more than 70% of the spatial pattern of pinyon mortality caused by the 2003–2004 drought (Peterman et al. 2013). Interactions between vegetation and precipitation that are modified by site conditions affecting water storage, such as aspect and soil properties, are an important part of this study and were considered by using water balance variables as indicators of climate. For this reason, soil moisture pivot points and pivot points

for other water balance variables that integrate the effects of temperature and precipitation, like annual evapotranspiration, are included in the appendix figures (see Appendix A) and supplemental tables (see Tables S-2 and S-4 in Thoma 2024).

3.6.2 Spatial patterns of drought tolerance

The map of water deficit pivot points (Figure 11) shows the amount of drought stress that causes a change in production from the previous year. Deficit pivot points generally decreased with elevation. This pattern stemmed from the distribution of vegetation groups that generally followed changes in mean climate values. More specifically, it reflected the tendency of water availability and use (soil moisture and evapotranspiration) to increase with elevation (low near the reservoir and higher at higher elevations), and unmet water need (deficit) to decrease with elevation (Stephenson 1998).

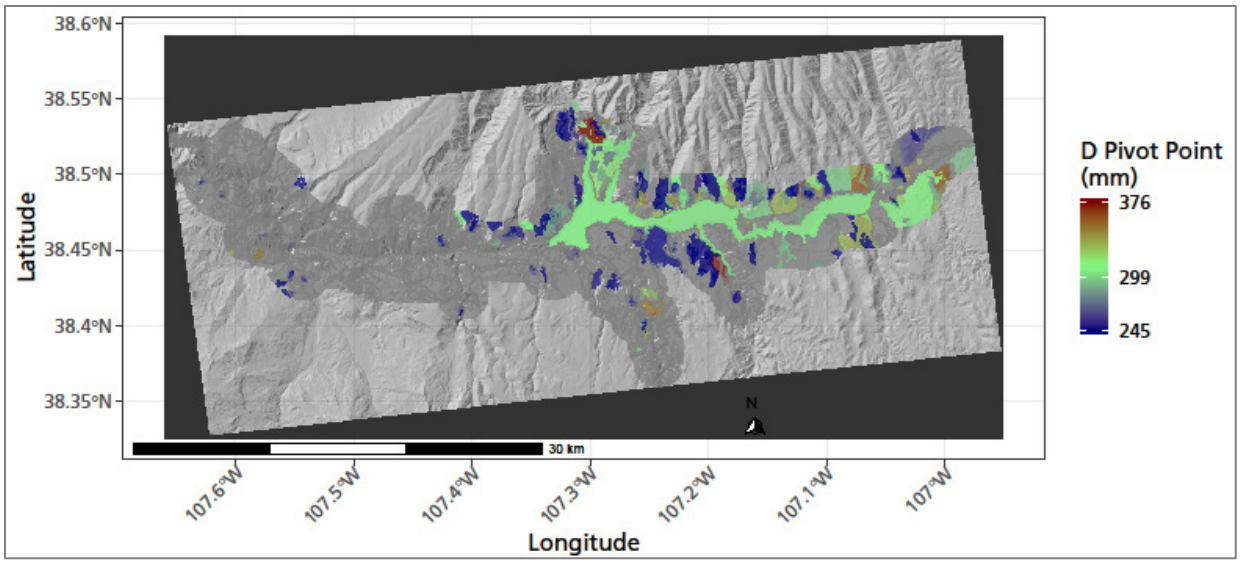

Figure 11. Water deficit (D) pivot points for polygons with a significant relationship (p-value < 0.05) between water-year annual water deficit and change in annual vegetation production, assessed as the interannual difference in iSAVI. The mean water deficit pivot-point values shown here represent spatial patterns in drought tolerance. A higher pivot point indicates higher levels of drought tolerance, and therefore, red areas are most drought tolerant. Gray areas are polygons that did not have a significant relationship between iSAVI and water deficit. Pivot points for other water balance variables can be found in Appendix A and Tables S-2 and S-4 in Thoma (2024). NPS / DAVID THOMA

3.6.3 Pivot points for other climate variables

Pivot points for other climate and water-balance variables generally reflected the average climate conditions where alliance groups were found (Figure 12; Appendix A, Figures 32 to 55). However, the range in pivot points within alliance groups, and the variation in species assemblages within and between polygons of each alliance group, reflected some variation beyond a pattern purely determined by elevation gradient. In low elevation semi-arid environments, pivot points for variables AET, P, SOIL, RAIN, and SNOW are generally lower than the pivot point for D, an indicator of drought. This is because vegetation in these environments is adapted to handle relatively low water availability and high drought stress. However, at Curecanti NRA, AET is higher than D in many

alliance groups, which is indicative of a transitional environment that lies between purely water limited low elevation areas and purely temperature limited high elevation areas. This is the most likely reason why AET (which incorporates both temperature and moisture in a single variable) is consistently and positively correlated with production at Curecanti NRA (see Figure 9).

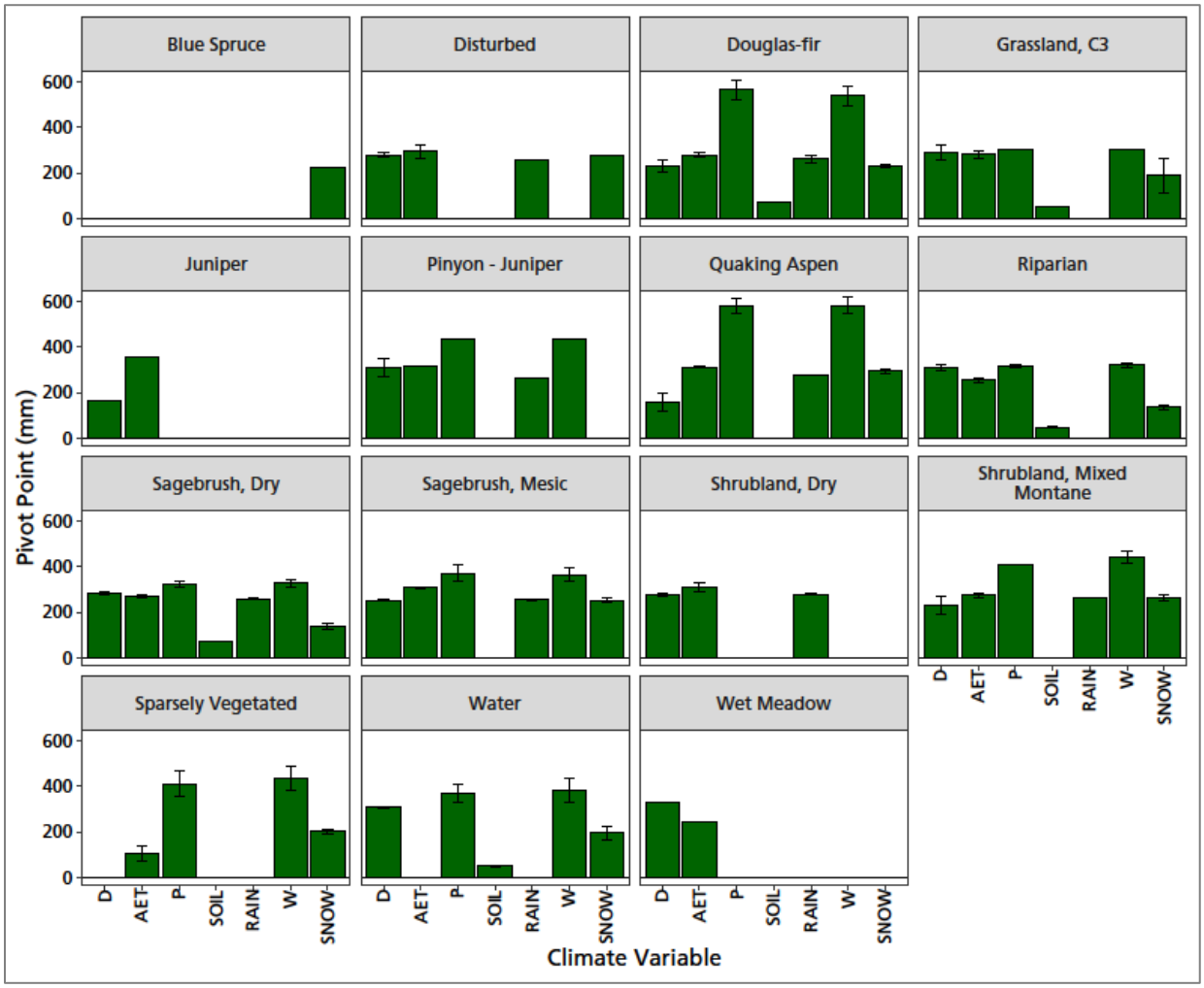

Figure 12. Significant ($p < 0.05$) water-related pivot points by alliance group. See Tables S-2 and S-4 in Thoma (2024) for the pivot point values. The magnitude of each pivot point reflects generally average conditions for polygons in each alliance group. The mean pivot-point values are the critical values where annual production switches from below- to above-average (relative to the previous year) for the different alliance groups. D = water deficit (mm), AET = actual evapotranspiration (mm), P = precipitation (mm), SOIL = average soil moisture (mm), RAIN = precipitation as rain (mm), W = snowmelt plus rain (mm), and SNOW = precipitation as snow (mm). NPS / DAVID THOMA

All results shown in Figure 12 are statistically significant. For this reason, any of these alliance group-level pivot points can be compared against historic, present, or future projected growing-season climate conditions to determine if those conditions are likely to result in below- or above-average vegetation production. Pivot points for each climate variable by polygon are provided in Table S-2, and by alliance group in Table S-4, of Thoma (2024). These can be used with data on

climate exposure to identify conditions conducive to above- or below-average growth—information useful in vulnerability assessments associated with Climate Smart Conservation planning (NPS 2021; Stein et al. 2014) (see Section 4).

3.7 Vegetation response

3.7.1 Vegetation response and climate sensitivity

When they interact with climate, plant traits determine which species grow under different conditions of water availability. The result is a spatial organization of alliance groups that reflects local climate and the sensitivity of vegetation to climate (Figure 13). The interactions between plant traits, site characteristics, and climate-determined patterns of vegetation distribution in the past will determine how vegetation in Curecanti NRA will be shaped by climate in the future.

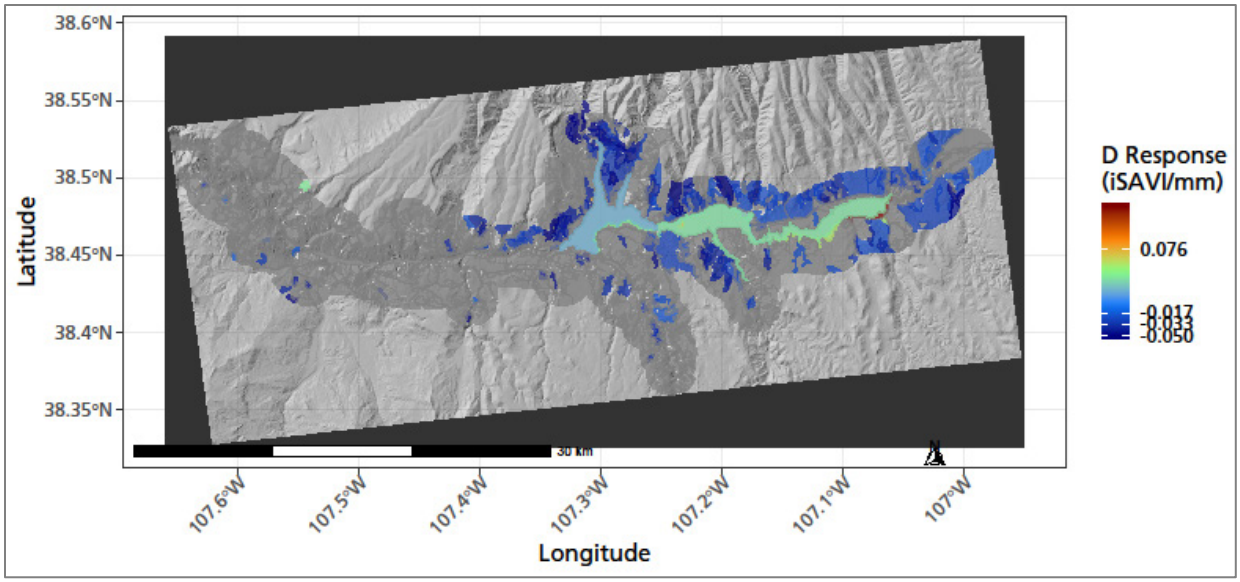

Figure 13. Sensitivity of growing-season vegetation production to annual water-year deficit (D). This figure shows which areas will experience change first. Areas with the largest positive or negative D response rates are most likely to see change happen first and fastest as the climate shifts. Response is the slope of the linear-regression relationship between annual water deficit and iSAVI change from the previous year. It is the change in iSAVI expected per millimeter of change in annual water deficit. Areas without color were either smaller than the minimum area required for mapping (< 8.3 ha) or did not have a significant relationship with annual water deficit; however, areas that were not significantly related to water deficit may be related to other climate metrics. Statistics for the sensitivity of each polygon to each climate metric, including the quality of relationships and regression coefficients, can be found in Table S-2 of Thoma (2024). NPS / DAVID THOMA

Vegetation response is a formal component of vegetation vulnerability assessments used in Planning for a Changing Climate (NPS 2021). The importance of response is related to the need to understand which vegetation groups may respond sooner or more strongly to a given amount of climate exposure. While a unit change in iSAVI is not quantitatively linked to vegetation cover or biomass in this analysis, it is representative of change in both of those attributes. In this way, the iSAVI response indicates where change is likely to happen first and fastest as the climate shifts.

At Curecanti NRA, the Disturbed alliance group had the greatest response rate and sensitivity to water deficit (Figure 14). Riparian areas that were mostly classified as cottonwood-dominated and Water areas that were largely insensitive to changes in water deficit responded positively. This is because vegetation in riparian areas has access to water that is not included in the water balance model, which does not consider ground or river water or water from upslope positions. The strong positive response in the Water alliance group is an artifact of running the terrestrial water balance model on polygons labeled Water where a water holding capacity of 100 mm was assumed. This assumption was made prior to running the model to potentially evaluate changing reservoir levels. The positive response to deficit in Water, Riparian and some Quaking Aspen alliance group polygons may suggest a positive change in iSAVI due to temperature that has a strong effect on water deficit in the water balance model. For this reason, results for these alliance groups need to be considered with caution and should be interpreted on a case-by-case basis. Most of the other alliance groups had negative responses to increasing water deficit. Alliance-group sensitivities to other water-balance variables can be found in Appendix A, Figures 56 to 79.

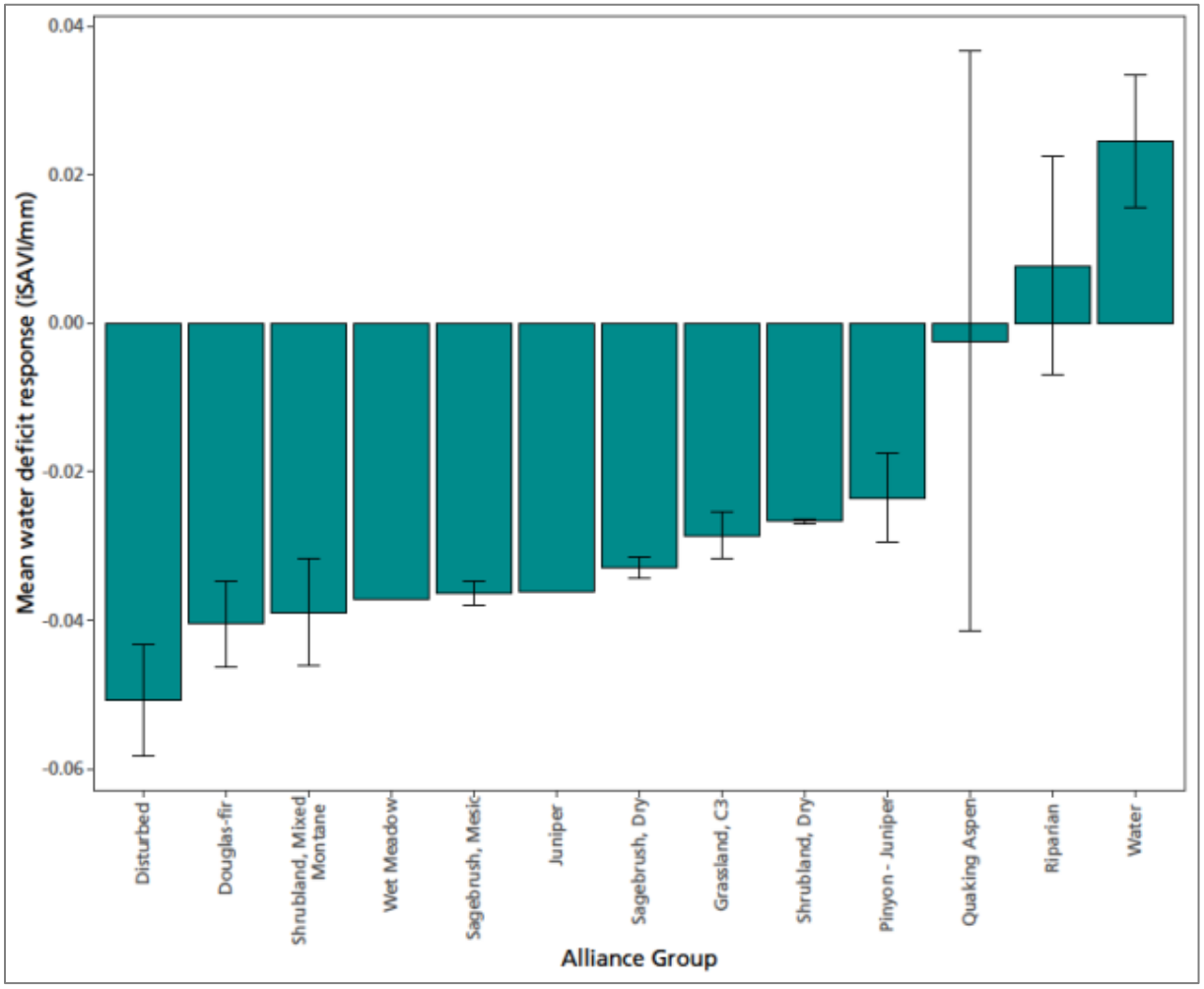

Figure 14. Responses of different vegetation alliance groups to water deficit. Standard error bars indicate the range in variability of responses among polygons of an alliance group if more than one polygon had a statistically significant relationship ($p < 0.05$) with water deficit. NPS / DAVID THOMA

If a disturbance, such as fire or drought, replaced the woodland alliance groups with grassland or shrubland, then the response would shift to reflect the dominant vegetation structure. Additional response maps, found in Appendix A, illustrate spatial patterns in the sensitivity of alliance groups to deficit and soil moisture.[5]

3.7.2 Influence of site characteristics

Spatial patterns in soil and site properties, including percent sand and clay, depth to root-restrictive layers, water-holding capacity, slope, and aspect, influenced drought tolerance and sensitivity to climate variables. This was apparent from close examination of patterns in the soil-properties maps (Figure 15) and the response maps (e.g., Figure 13). This correspondence was further evidence of the interactions between climate, site properties, and vegetation traits (deep- or shallow-rooted, perennial or annual) that influence vegetation condition, trends, and sensitivity to climate. However, more careful analyses are likely necessary using the data in Table S-2 of Thoma (2024) and Appendix A, Figures 80 and 81.

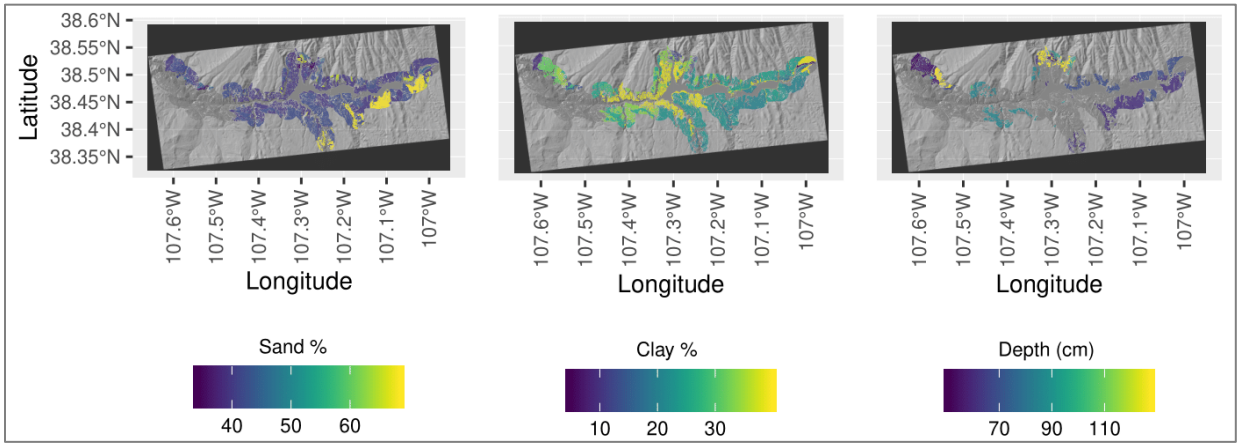

Figure 15. Maps of percentage sand and clay content in the top meter of soil, and depth to restrictive layer, in Curecanti National Recreation Area. Spatial patterns of soil properties correspond with patterns in vegetation response to climate. Areas with gray fill indicate missing soil properties data or depth greater than 100 centimeters. NPS / DAVID THOMA

By relating pivot points and responses with site properties (see Table S-2 in Thoma 2024), we can quantify the strength of influence that site properties have in modifying climate effects. Steeper regression slopes between vegetation responses or pivot points and site properties (such as those in Appendix A, Figures 80 and 81) indicate a stronger effect of a given site property on either the pivot point or response to climate. For example, there is evidence that Dry Sagebrush is less sensitive to precipitation (Table S-6 in Thoma 2024; P pivot point = 4.71 × clay % + 195.94; $r^2 = 0.5652$) and

[5] Response to soil moisture is greater than sensitivity to precipitation or deficit because incremental changes in soil moisture in this analysis are expressed as a water-year mean, whereas precipitation and deficit are sums (see Table 2). However, the pattern in response to soil moisture is tied to spatial variation in soil properties that play important roles in storing precipitation between events.

less drought tolerant (Table S-6 in Thoma 2024; P response = −0.0009 × clay % + 0.0453; r^2 = 0.2014) as clay content increases. These trends suggest that soil texture plays a role in determining how Dry Sagebrush alliance groups may be affected by climate change. In other words, to achieve average production, Dry Sagebrush growing on soil with the highest clay content needed 80 mm more annual precipitation than Dry Sagebrush growing on soil with the least clay content. Soil with higher clay content can hold more water, but when water is scarce clay particles hold water more tightly than more coarsely textured soils, making it more difficult for plants to use. Site properties affected drought tolerance and sensitivity to climate by influencing water retention and distribution in the soil profile, as well as heat-loading due to the slope and aspect of the site relative to the sun. These site-specific properties locally modified the influence of climate and were important determinants of vegetation condition and patterns on the landscape. They can be quantitatively introduced into vulnerability assessments at the polygon scale using a water-balance model that accounts for these complex interactions and using the data in Table S-4 of Thoma (2024).

3.7.3 Patterns within alliance groups

While pivot points and responses provide different information, they are linked by plant traits: as actual evapotranspiration (AET) pivot points decrease (i.e., cross the horizontal “no change” line further to the left), response rates may increase (Figure 16). Individual polygons that show a response opposite that of other polygons in an alliance group usually are affected by disturbance or a non-climate factor, as demonstrated in the case of the single Riparian alliance group polygon of shore-line vegetation among this cottonwood-dominated alliance group (i.e., the single line with a negative slope in Figure 16). Fluctuating ground water elevation associated with reservoir management can represent a disturbance not linked to the local climate conditions that are considered in the water balance model. Alliance groups with steeper slopes are considered more responsive to changes in water availability. These groups increase production with lower AET, demonstrating that responsiveness to AET is greatest where vegetation is most drought tolerant.

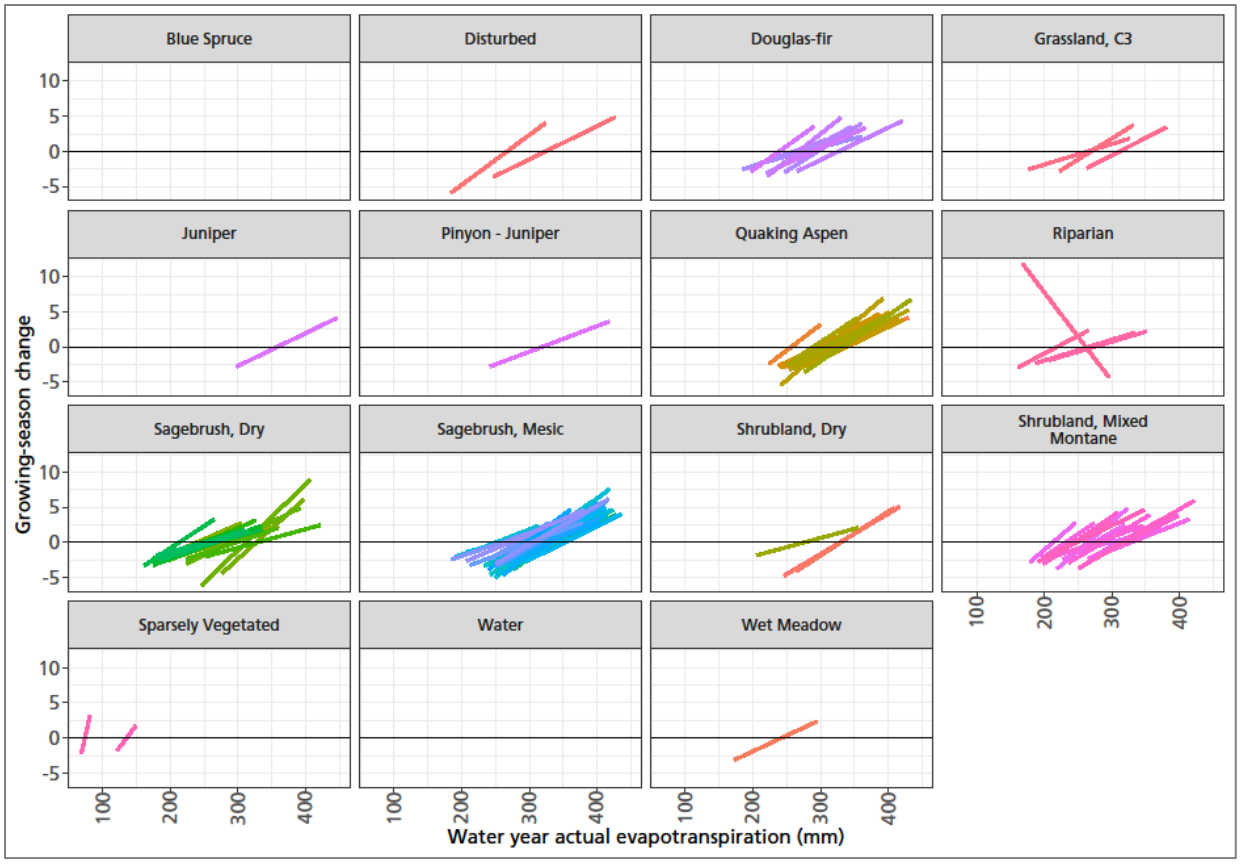

Figure 16. Graphical depiction of the relationship between pivot points and responses in polygons that had a significant relationship (p-value < 0.05) between iSAVI and water-year actual evapotranspiration (e.g., critical water need on the x-axis versus rate of growing season iSAVI change per mm actual evapotranspiration on the y-axis). Polygon-level pivot points and responses are provided in Table S-2 of Thoma (2024). Alliance groups with steeper slopes are considered more responsive to changes in water availability. Alliance groups, and polygons within alliance groups, that cross the horizontal axis further to the left are more drought resistant. This is because they shift to above-average condition at lower values of actual evapotranspiration. Only significant relationships are shown. Panels without lines represent alliance groups with no significant relationships between iSAVI and actual evapotranspiration. Colors help differentiate individual polygons within alliance groups. NPS / DAVID THOMA

There was a large range in pivot points and responses, reflecting a wide range of plant traits responding differently to climate variability across the NRA. The patterns of pivot points and responses quantify unique climatic habitats occupied by the different alliance groups in the park, and can serve as a guide to anticipate what, where, when, and why vegetation change may occur. For example, this analysis suggests that the positive growth response to the same value of actual evapotranspiration will be greater in Mesic Sagebrush (0.05 iSAVI/mm) than in Dry Sagebrush (0.04 iSAVI/mm) alliance groups (Table S-2 in Thoma 2024).

Tracking weather conditions during the growing season allows a view into vegetation condition at the polygon or alliance-group scale, depending on management interest (Tables S-2 and S-4 in Thoma 2024). The degree of responsiveness was determined by traits that allowed plants to either

resist drought or rapidly respond to water availability. The result was that vegetation response to climate could be considered coarsely at the alliance-group level, but at higher spatial resolution, and often with higher accuracy, at the polygon level. For example, in the Mesic Sagebrush alliance group, actual evapotranspiration explained 24% of interannual variation in production. But by polygon (n = 40), actual evapotranspiration explained between 16% and 45% of interannual variation in production. Multiple factors can introduce additional variability in pivot points and responses within alliance groups. These include differences in species assemblages, spacing between plants, and soil properties that affect the retention and distribution of water in the soil profile that is accessible to different growth forms (e.g., plants with shallow or deep roots) (Lauenroth 2012; Schlaepfer et al. 2012; Lauenroth and Bradford 2009).

3.7.4 Production response to water and non-water variables

Assemblages with higher responses (steeper regression slopes) were more sensitive to climate. Depending on the climate variable, the slope could be positive (as with semi-arid environments and water variables, such as precipitation and actual evapotranspiration), or negative (in response to water deficit or potential evapotranspiration, which are related to temperature) (Figure 17; also see Tables S-2 and S-4 in Thoma 2024).

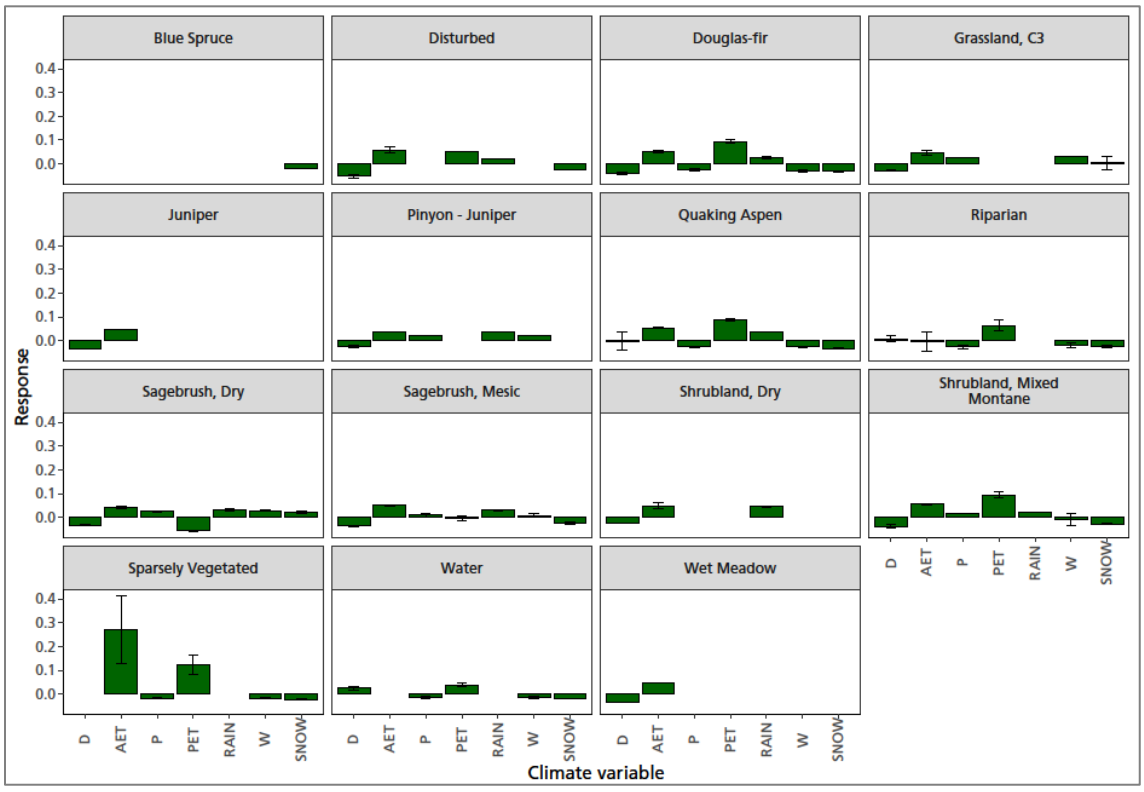

Figure 17. Vegetation response to summed water flux variables (regression slopes from iSAVI versus the annual water flux climate-variable sum). Statistics for these relationships and all other variables can be found in Tables S-3 and S-4 of Thoma (2024). D = deficit (mm), AET = actual evapotranspiration (mm), P = precipitation (mm), PET = potential evapotranspiration (mm), RAIN = precipitation as rain (mm), W = combination of rain and snowmelt (mm), SNOW = precipitation as snow (mm of water). NPS / DAVID THOMA

Direct comparison of water variables to non-water variables, such as GDD and VPD, is difficult due to their different units of measure. Similarly, it is important to note that response to change in an average annual value, such as soil moisture, is strong partly because this variable is averaged (because soil has an upper limit of water-holding capacity), which weights its effect on vegetation more per unit change than other climate variables that are summed (see Table 2). Therefore, small changes in average soil moisture have a larger effect than small changes in annual precipitation. Responses to temperature variables GDD and T should also be considered similarly, because GDD is a summed variable, while T is averaged. Variable importance is considered in the following sections.

3.8 Multi-variable indicators of annual vegetation production

Pivot points and responses are ecological measures of annual production, but production is affected by multiple aspects of weather before and during a growing season, as well as conditions in prior growing seasons that set the stage for production potential in the current year (Sala et al. 2012).[6]

In the multi-model comparison of climate correlates with interannual differences in growing-season iSAVI across all alliance groups, climate indicators of annual production showed that regardless of alliance group, most (76%) polygons were influenced by three years of actual evapotranspiration (Figure 18). The next most-common indicators of production were three years of actual evapotranspiration and current year water deficit considered together (Figure 18). These patterns generally held within alliance groups, with two-to-three years of soil moisture or actual evapotranspiration commonly ranking as the best models of growing-season production in most alliance groups (Figures 19 and 20). A list of top-performing models (AICc < 4) by polygon can be found in Table S-5 of Thoma (2024).

[6] This is one reason why the annual relationships described above are not as strong as monthly relationships described in some of our earlier work (e.g., Thoma et al. 2016).

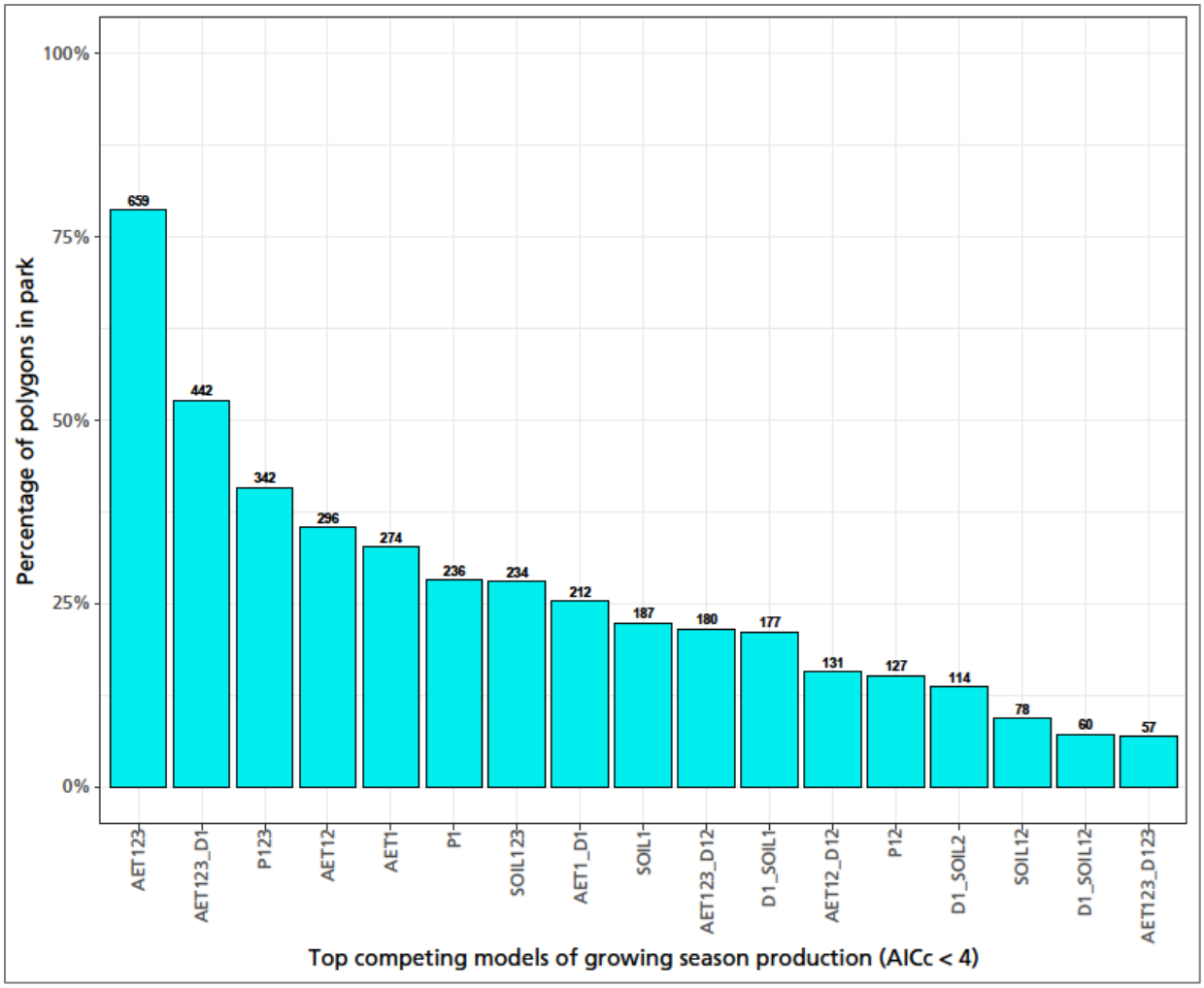

Figure 18. Top models in a multi-model comparison of climate correlates with interannual differences in growing-season iSAVI across all alliance groups. Percentages indicate the proportion of polygons where each model was competitive. Numbers above bars indicate the number of polygons in which each model was competitive. Each polygon may have more than one competitive model; thus, the sum of percentages exceeds 100% across all models. The x-axis labels refer to the a priori climate models described in Table 3. SOIL = annual average soil moisture; D = annual deficit; AET = annual evapotranspiration; P = annual precipitation. The number following the x-axis labels indicates the current and prior years included in each model: 1 = current year; 12 = current and previous year; 123 = current and previous two years. NPS / DAVID THOMA

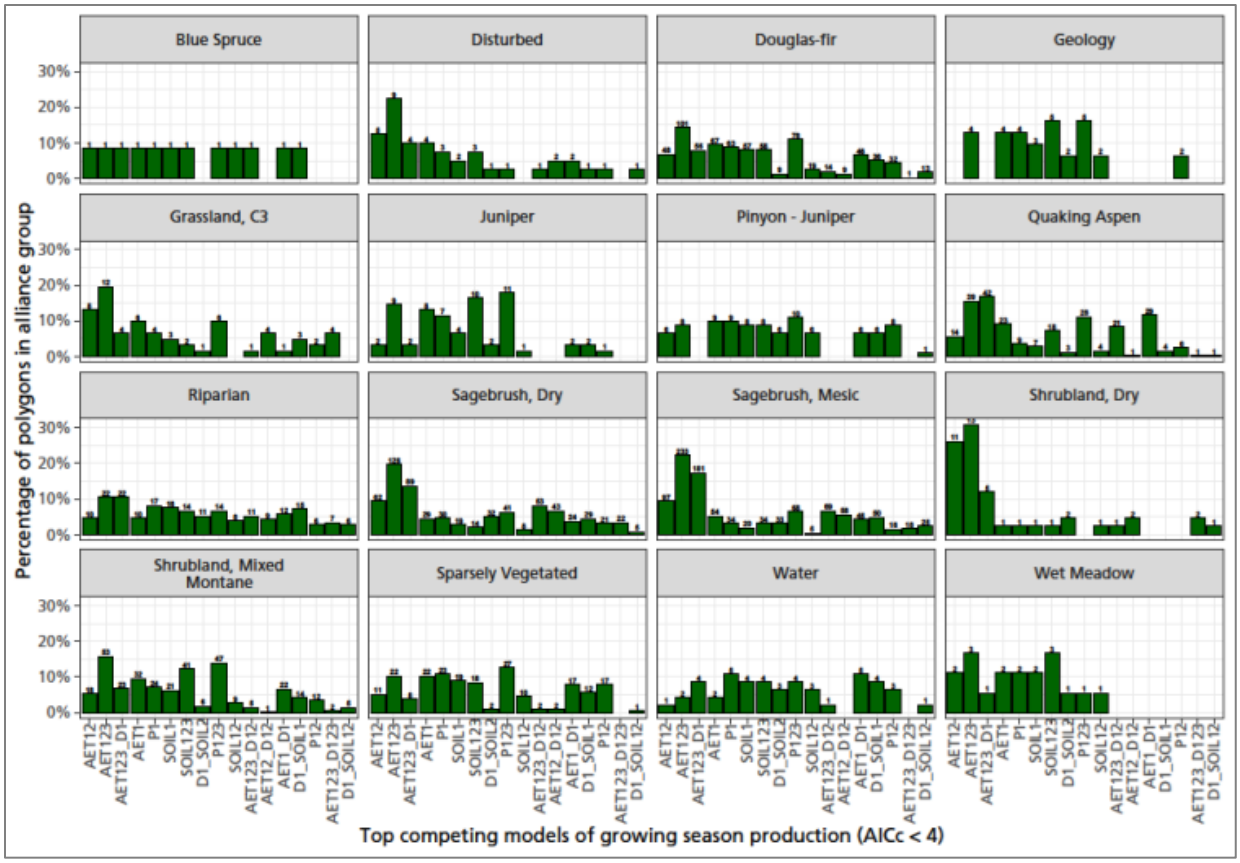

Figure 19. Top models of growing-season production by alliance group in multi-model comparisons of climate correlates with interannual differences in growing season iSAVI. The x-axis labels refer to the a priori climate models described in Table 3. The y-axis represents the proportion of polygons in each alliance group where each model was competitive. Numbers above bars indicate the number of polygons in each alliance group in which each model was competitive. Each polygon may have more than one competitive model; thus, the sum of percentages can exceed 100% across all models. SOIL = annual average soil moisture, D = annual deficit, AET = annual evapotranspiration, P = annual precipitation. The number following the x-axis labels indicates the years included in each model: 1 = current year; 12 = current and previous year; 123 = current and previous two years. NPS / DAVID THOMA

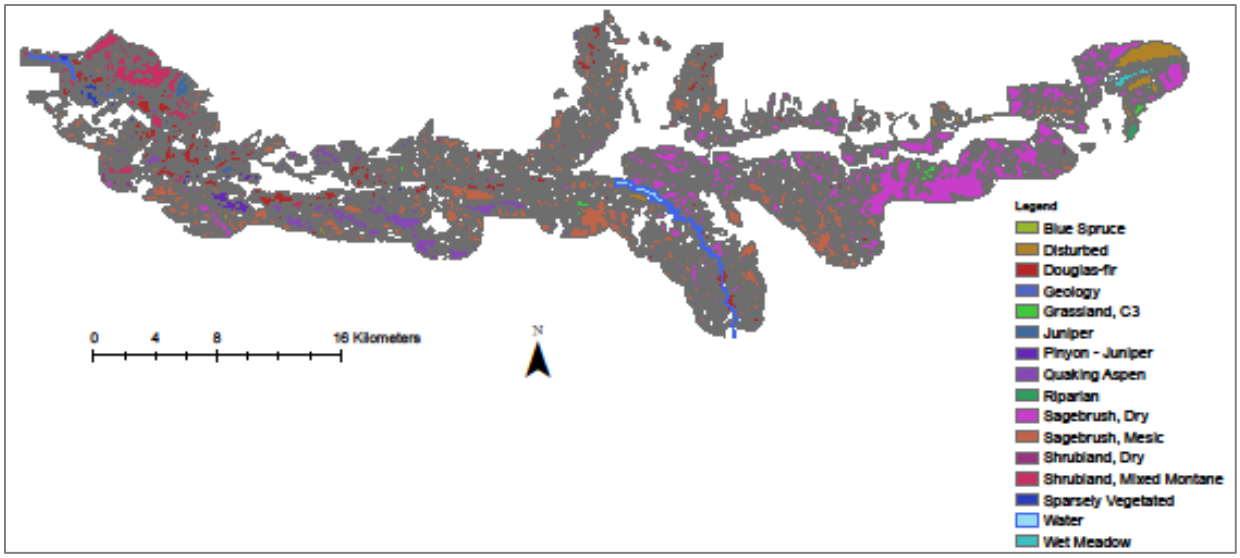

Figure 20. Alliance map units that had a significant relationship between growing season production and three years of actual evapotranspiration. Equations for relationships by polygon can be found in Table S-5 of Thoma (2024). NPS / DAVID THOMA

Most alliance groups responded to multiple years of actual evapotranspiration from soil, a variable that incorporates both heat and water in its calculation, highlighting the importance of legacy effects across years in an environment that could be limited by water or temperature in any given year (Bisigato et al. 2013). Evidence for the role that weather variability (i.e., wet years interspersed with dry years) plays in determining which variables are important comes from the finding that the second most important combination of variables at the park scale includes three years of actual evapotranspiration and one year of water deficit (Figure 18).

3.9 Land-surface phenology trends at Curecanti National Recreation Area

At the park scale the start of growth occurred 4.7 days later and the end of growth occurred 7.8 days later, collectively resulting in a growing season that was on average 3.1 days longer by the end of the study. The lengthening of the growing season occurred across 26.2% of the study area (Table 6). The biggest increase in growing season length (16 days) was in the Water alliance group. This is likely a response to increasing water temperature or changes in reservoir nutrient status that causes change in lake productivity. Although the SAVI remote sensing index is designed for terrestrial applications, it uses wavelengths that are also sensitive to chlorophyll in water. Another potential explanation of the change in season length for the Water alliance group could be related to vegetation infill into areas previously occupied by water as reservoir levels fall. Although a significant trend in temperature was not found, a longer growing season is consistent with warming temperature in this non-water limited alliance group. A trend in later start of growing season occurred in all alliance groups except for Wet Meadow (Table 6; Appendix A, Figures 82 and 83). In recent years, the growing season was ending later for most alliance groups, but four days earlier for Blue Spruce (Table 6).

Table 6. Trends in phenology averaged across polygons in the same alliance group. Changes in the start date of growing season (ΔSOS), end date of growing season (ΔEOS), length of growing season (ΔLOS), and the timing of peak growth (ΔPOP) are given in days.

Alliance Group	Hectares	Polygon Count	% Area	ΔSOS	ΔEOS	ΔLOS	ΔPOP
Sagebrush, Mesic	12,114.8	280	31.1	9.0	7.5	−2.4	7.1
Sagebrush, Dry	9,547.7	157	24.5	7.0	6.7	−1.9	7.5
Douglas-fir	3,644.0	129	9.4	4.5	8.3	3.4	7.6
Water	3,366.4	7	8.6	0.2	14.9	16.6	9.8
Quaking Aspen	3,017.5	64	7.7	8.6	4.9	−4.3	5.9
Shrubland, Mixed Montane	2,692.1	64	6.9	8.5	7.4	−0.6	7.2
Disturbed	1,372.4	10	3.5	6.6	0.2	−5.2	7.0
Riparian	1,108.6	37	2.8	7.4	10.6	4.4	4.0
Sparsely Vegetated	535.1	32	1.4	2.2	9.2	7.4	7.1
Grassland, C3	400.0	14	1.0	2.1	15.2	8.9	3.6
Pinyon - Juniper	360.7	10	0.9	1.9	12.6	11.1	20.9
Juniper	350.8	12	0.9	6.9	8.2	1.8	10.2
Shrubland, Dry	233.8	13	0.6	2.9	4.4	2.5	9.7
Wet Meadow	138.3	3	0.4	0.0	2.7	2.4	0.9
Geology	71.8	5	0.2	0.6	15.7	13.1	10.8
Blue Spruce	9.7	1	0.0	7.3	−4.0	−7.8	3.7

These changes were consistent with rising temperatures and increasing annual growing degree days that can extend the growing season if moisture is available. They were also consistent with increasing CO_2 concentrations that increase vegetation production through a process known as CO_2 fertilization (Sorokin et al. 2017) that increases water use efficiency.

Changes in land-surface phenology result from interactions between temperature, moisture, plant traits that control growth rates, and CO_2 concentrations that affect water-use efficiency. Generally, warming reduces growth rates in semi-arid environments, while elevated CO_2 increases water-use efficiency of production for the same amount of water. Thus, warming may initiate an earlier start to the growing season and elevated CO_2 may increase water-use efficiency, resulting in a longer growing season. But efficiency is ultimately limited if conditions become sufficiently dry and growth ceases. For this reason, and given projected drying on the Colorado Plateau, increases in efficiency may be small and short-lived in the face of disturbance caused by drought or wildfire (Allen et al. 2015). Tracking changes in phenology in NCPN parks, and linking those changes to seasonal changes in temperature and CO_2 concentrations, could help further clarify the vulnerability of semi-arid vegetation to multiple aspects of climate change (Sorokin et al. 2017).

3.10 Drivers of green-up

3.10.1 A priori model selection method

At the scale of both the park and alliance group, the most common a priori competitive model of green-up timing (see Table 4) was growing degree days and cumulative precipitation between January 1 to the SOS date (Figures 21 and 22). Other competitive models included precipitation (as rain or snow) and day of complete snow melt. At the alliance group level, growing degree days and precipitation were the only variables important in every alliance group (Figure 22).

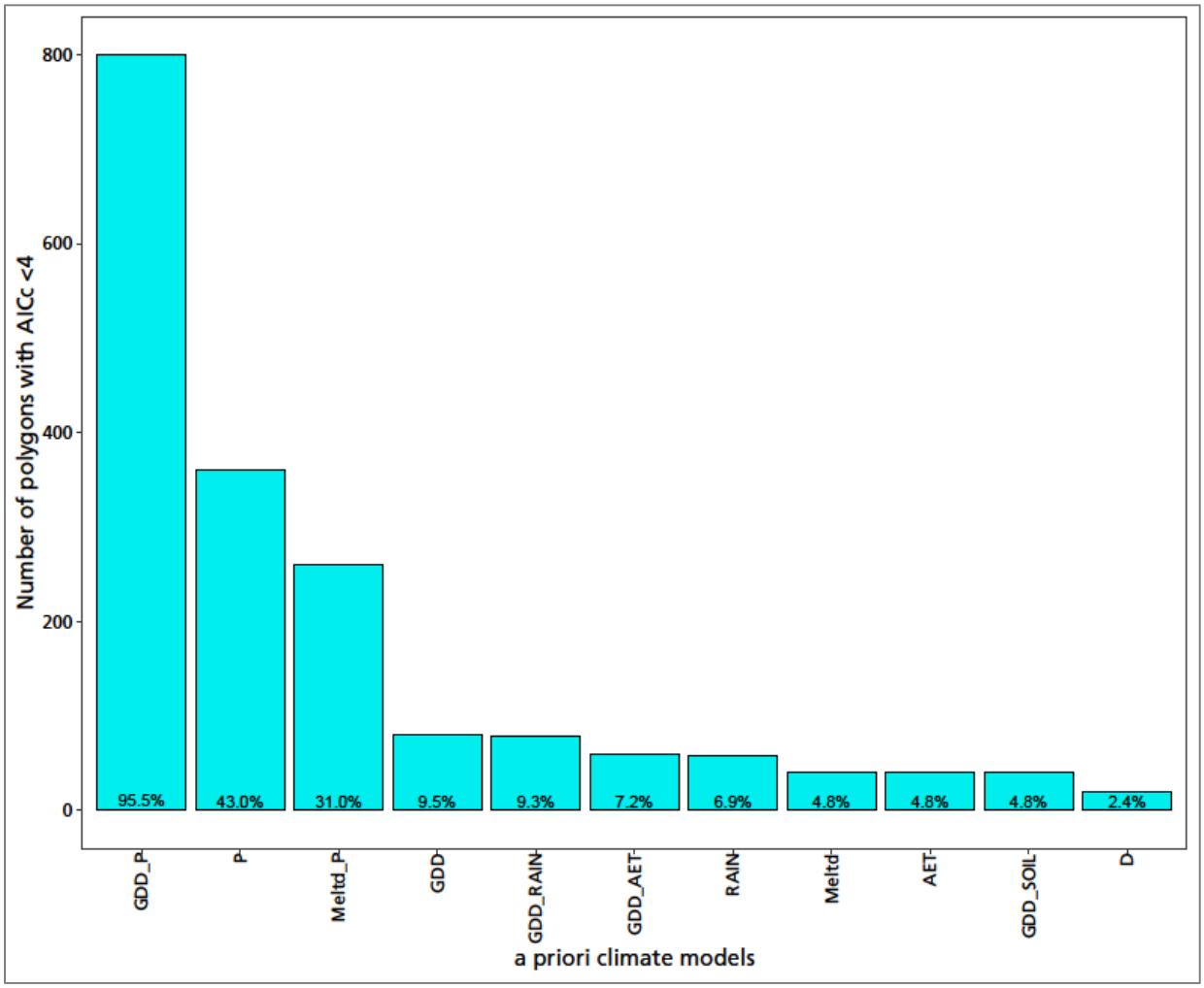

Figure 21. Top models in multi-model comparisons of climate correlates with the start of the growing season at the whole-park scale. The x-axis labels refer to a priori climate models as determinants of green-up, or start of season. GDD = growing degree days, SOIL = soil moisture, RAIN = precipitation as rain, Meltd = day of complete snowmelt, AET = actual evapotranspiration, P = precipitation, D = deficit. NPS / DAVID THOMA

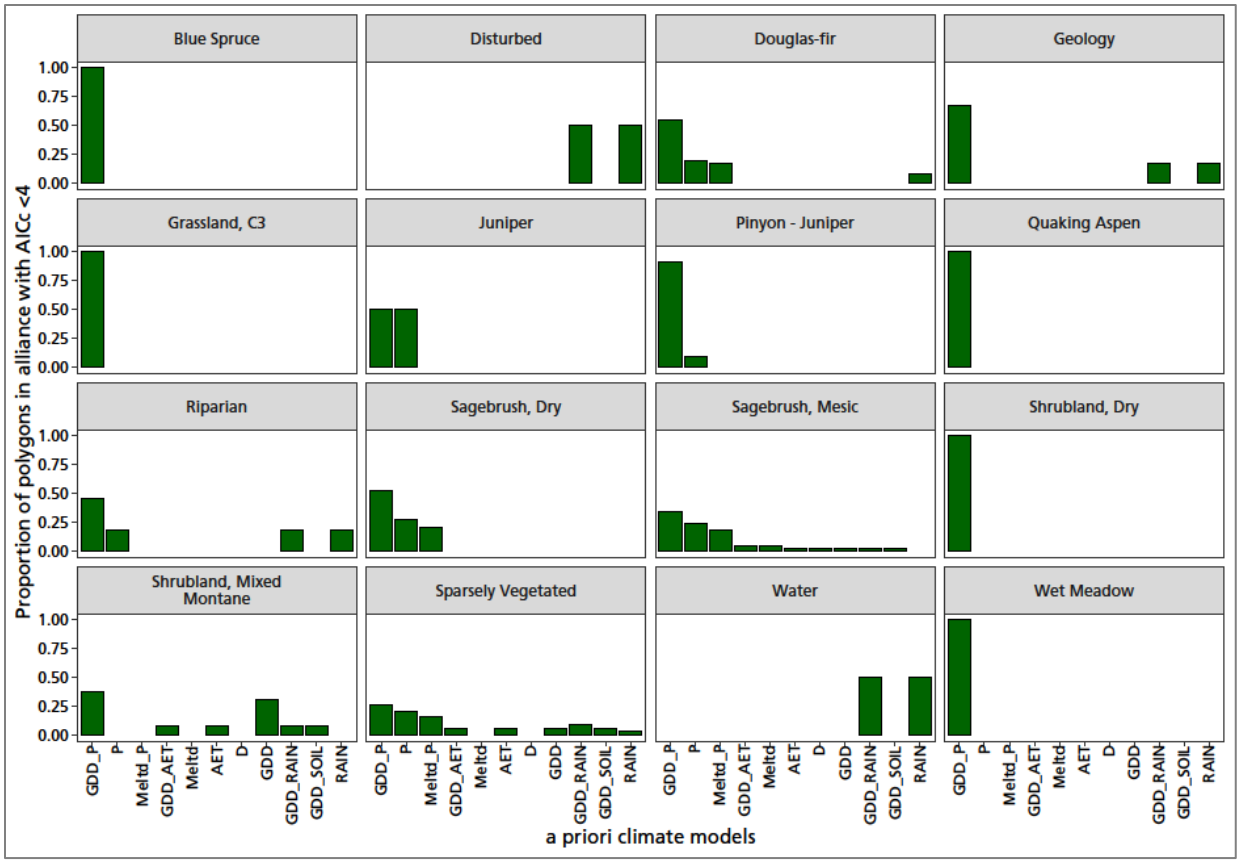

Figure 22. Top models in multi-model comparisons of climate correlates with the start of the growing season at the alliance-group scale. The x-axis labels refer to a priori climate models as determinants of green-up, or start of season. GDD = growing degree days, SOIL = soil moisture, RAIN = precipitation as rain, Meltd = day of complete snowmelt, AET = actual evapotranspiration, P = precipitation, D = deficit. NPS / DAVID THOMA

Growing degree days are important because spring soil moisture is typically at its highest level of the year after the winter recharge period, and warming temperatures are necessary to break dormancy. The importance of precipitation during the calendar year may indicate that the soil water holding capacity requires spring accumulation of snow or rain to fill the soil moisture storage capacity. Otherwise, insufficient precipitation may be a limiting factor for initiating growth. This may be a consequence of typically dry fall and winter periods that would result in low moisture levels being a co-limiting factor to temperature in spring in the absence of spring precipitation. It was surprising that day of complete snowpack melt was not a competitive a priori model in this cold and snowy environment (see next section).

3.10.2 Random-forests method

Variable importance plots showed the best predictors of SOS (start-of-season) were date of snowpack melt, growing degree days and precipitation (Figure 23). These findings were similar to those in the multi-variable regression models, except that date of complete snowmelt and growing degree days were more important than precipitation.

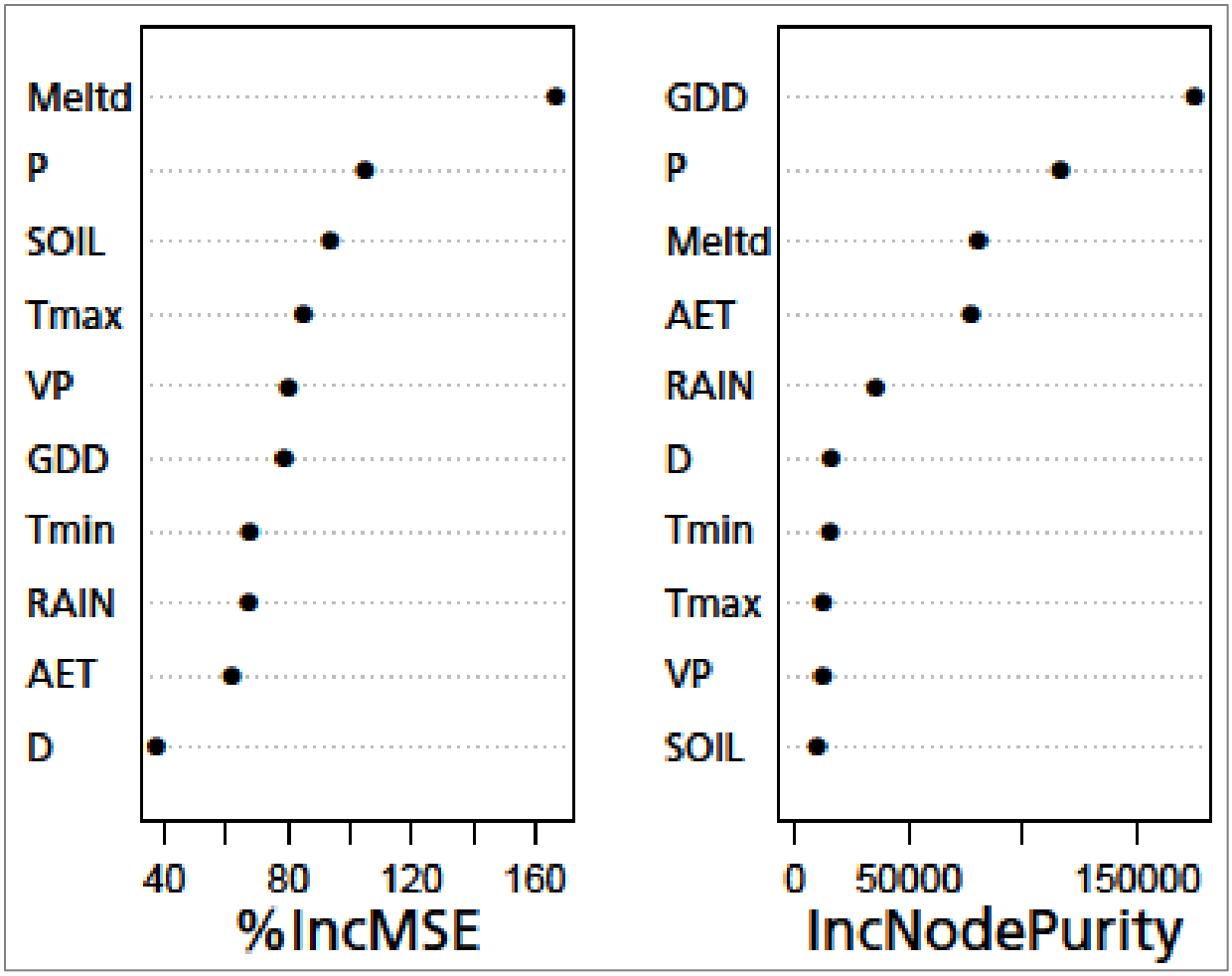

Figure 23. Variable importance in the random-forests model of climate drivers of the start of the growing season. Percent increase in mean square error (%IncMSE) is a measure of model performance with each variable. Increase in node purity (IncNodePurity) is the difference in residual sum of squares in regression with or without each variable. NPS / DAVID THOMA

Findings from the two modeling methods suggested that a combination of snow melt and warming spring temperature are important indicators of SOS, as is expected in cold environments. The loss of snow cover that exposes vegetation to warming and solar radiation in spring makes intuitive sense as a driver for the start of growth at higher elevations where snow accumulates over winter, but the effect of spring precipitation is less intuitive unless the soil moisture was not sufficiently replenished over winter to meet plant needs as a cue for growth. Alternatively, spring precipitation in the form of snow could delay loss of snow cover and the start of green-up.

The random-forests model obtained from the training dataset was used to model SOS in the validation dataset to determine predictive performance. It predicted SOS date at the park scale with a

mean absolute error of ± 2.2 days (Figure 24). When separated by alliance group, the model performed equally well (Figure 25).[7]

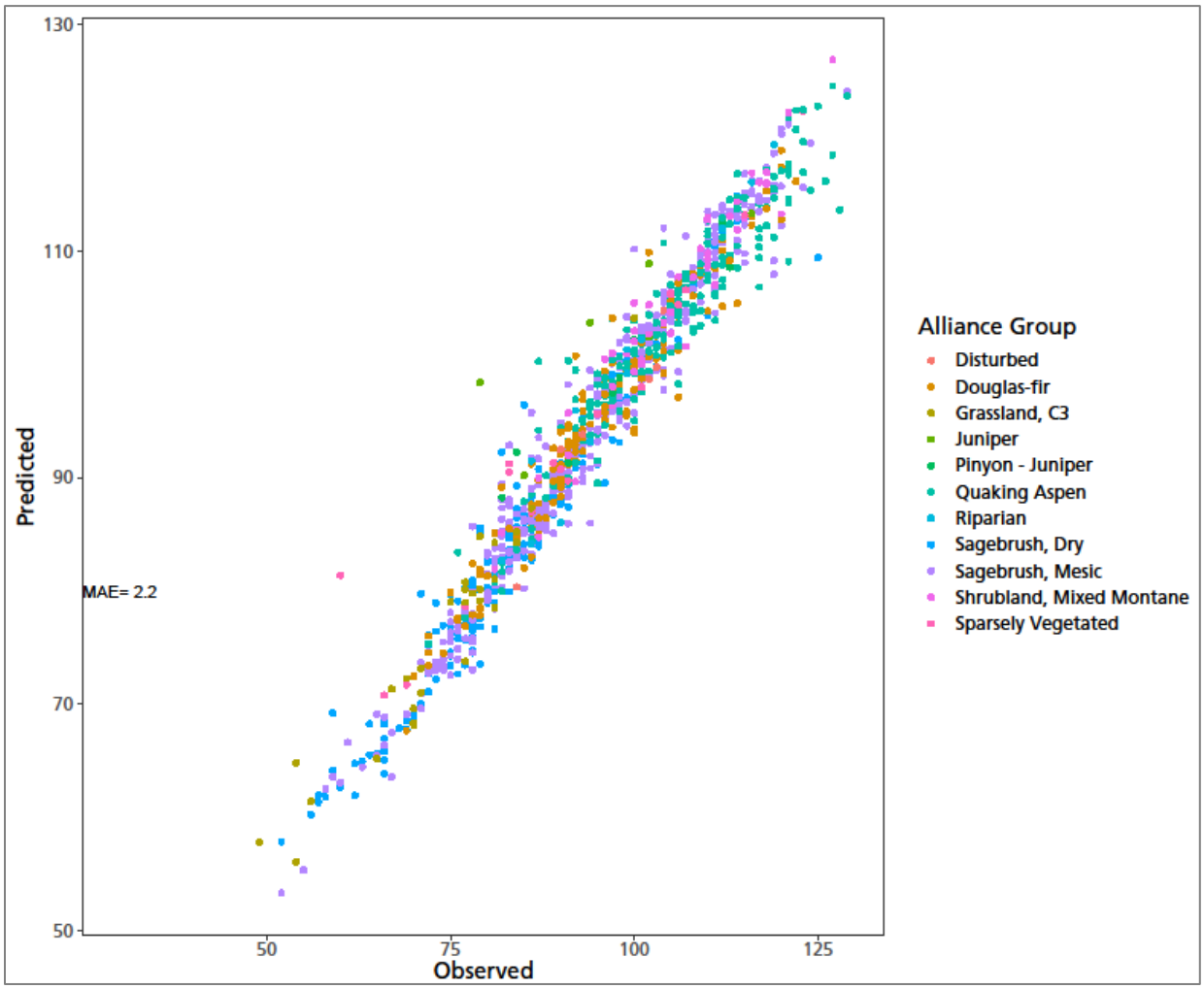

Figure 24. Predicted start-of-season date versus observed start-of-season date in the holdout dataset used for validation of the random-forests model for all polygons in Curecanti NRA. MAE is mean absolute error of prediction in days. Polygons with annual peaks in production occurring between November 1 and April 1 were removed prior to this analysis to minimize the effects of vegetation shadows that confound determination of phenology (Norris and Walker 2020). NPS / DAVID THOMA

[7] The analysis was conducted at the park scale, rather than by polygon (as in Section 3.7.2) to increase sample size for the random forests modeling process.

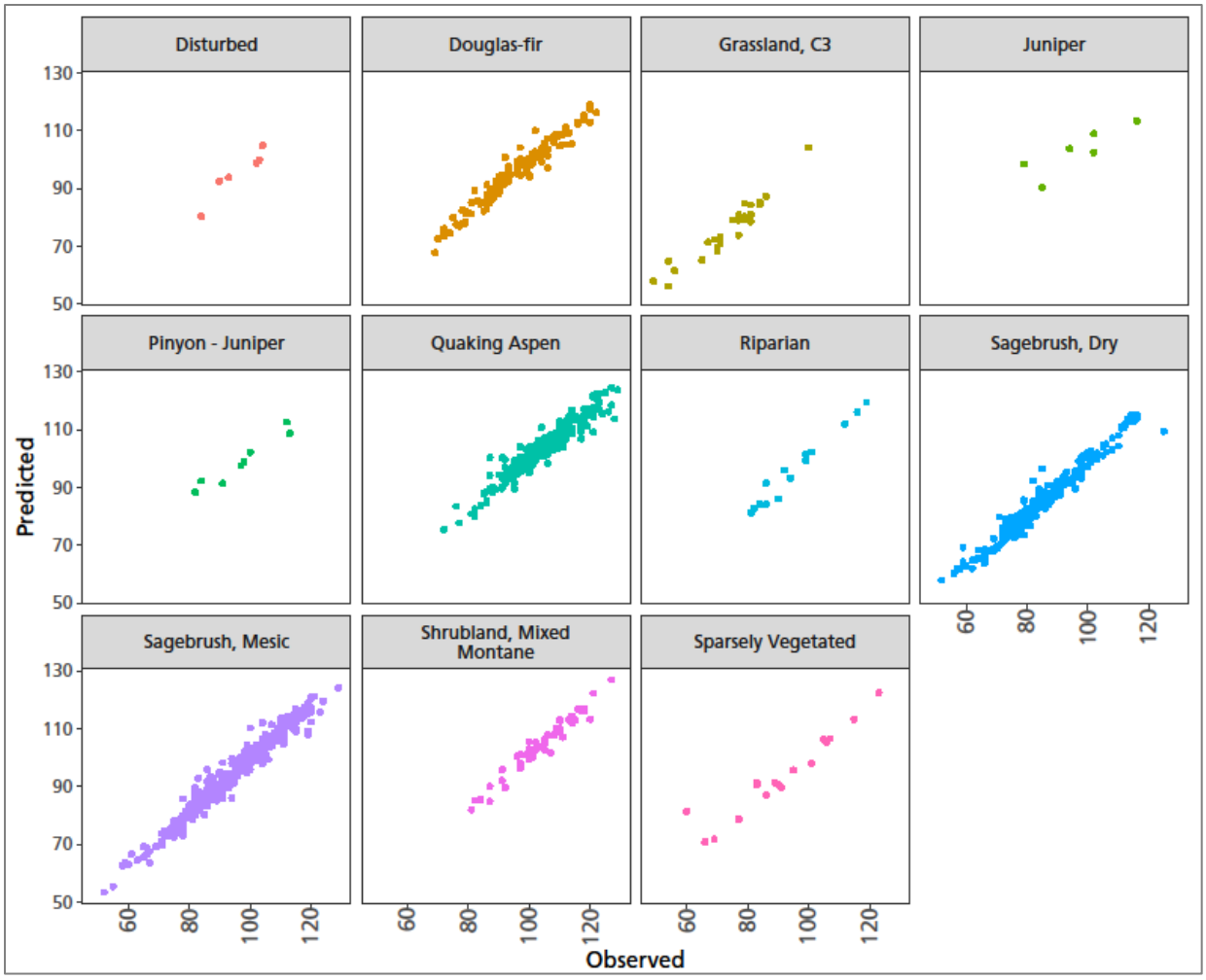

Figure 25. Predicted start-of-season date versus observed start-of-season date in the holdout dataset used for validation of the random-forests model for alliance groups. Polygons with annual peaks in production occurring between November 1 and April 1 were removed from this analysis. Outliers are likely due to the difficulty in discriminating SOS when SAVI changes monotonically during a growing season in low productivity years. NPS / DAVID THOMA

Inspection of SOS outliers in Figures 24 and 25 suggests they may have resulted from low amplitude and monotonic increases (straight line with minimal amplitude fluctuation) in SAVI in some years. This combination makes it difficult to identify meaningful SOS dates using the derivative method that relies on change in the acceleration of growth rate in spring to determine when growth starts. Even though polygon/year combinations with winter SAVI peaks were screened out of the analysis (per Norris and Walker 2020), it is not clear how SOS may be affected by the shadowing noted in pinyon-juniper and shrubland habitats by Norris and Walker. This is because the shadowing effect is partially dependent on vegetation structure and spacing, which is a continuum of conditions across landscapes. For this reason, modeled SOS dates should be considered with skepticism in the Pinyon-Juniper, Juniper and all shrubland alliance groups, as well as in polygons that yield outliers in the model of SOS.

Despite these potential shortcomings, the validation demonstrates a strong predictive model of SOS using climate data for most of the Curecanti NRA landscape. This means climate projections could be used to model SOS dates in the future. This could be helpful in assessing potential vulnerabilities caused by phenological mismatches between pollinators and flowering species, as well as potential impacts to migrating birds and mammals, such as deer. Mule deer in some western states "surf the green wave" of vegetation as it greens up progressively across gradients of latitude and elevation (Aikens et al. 2017; Merkle et al. 2016; van Wijk et al. 2012). Presently, it is unknown if animal species in NCPN parks time their movements with SOS or the green wave thereafter, but this information could be used to help assess if animals are keyed into this land-surface process.

3.11 Climate patterns

Annual temperature, precipitation, and estimates of actual evapotranspiration (AET), climatic water deficit, and soil moisture derived from the water-balance model for 1980–2019 exhibited high interannual variability (Figure 26; Appendix A, Figures 84 to 93). This variation caused large interannual changes in annual vegetation production. An interesting decadal oscillation in precipitation was evident: peaks in the middle of each decade since 1980 translated to similar peaks in other water-balance variables. The same pattern was apparent in soil moisture, AET, and water deficit (Appendix A, Figures 88 to 93), although for deficit the peaks (maximum drought stress) coincided with the times of least precipitation (Appendix A, Figures 90 and 91). If the periodicity of these cycles continues in the future, it could serve as a useful guide for timing restoration efforts that require substantial planning efforts, long-term investments, and multiple years of minimal drought stress for germination and establishment.

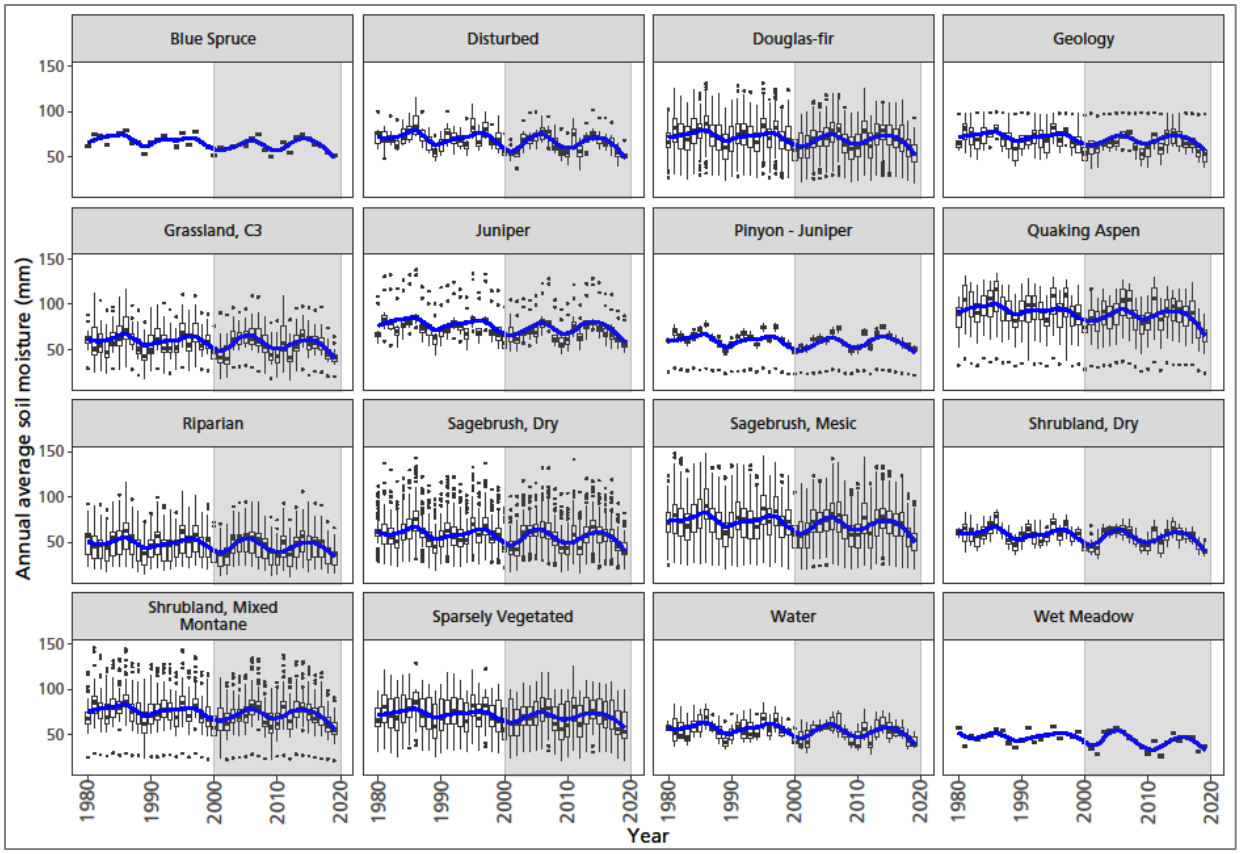

Figure 26. Long-term temporal patterns in soil moisture in vegetation alliance groups. Box plots demonstrate the range of variation by year. The line is a loess smooth with a 25% span to illustrate multi-year patterns. The gray shaded area includes the period between 2000 and 2019, investigated for relationships between production and climate when satellite imagery and climate data were both available. Study-period trends and associated statistics for the other water-balance variables are presented in Appendix A, Figures 84 to 93. NPS / DAVID THOMA

From 2000–2019, there was a weak, though statistically insignificant ($p > 0.05$), increase in soil moisture of less than one millimeter per year (Figure 27). Average annual temperature remained stable during the study period (see Appendix A, Figures 86 and 87). An increase in precipitation during the study period (see Appendix A, Figure 85) resulted in a corresponding increase in AET of 1–2 millimeters per year. The effect of these seemingly small changes was important, as illustrated by the significant upward trends in production in some of the alliance groups shown in Section 3.3 and the relationship between AET and production shown in Section 3.8.

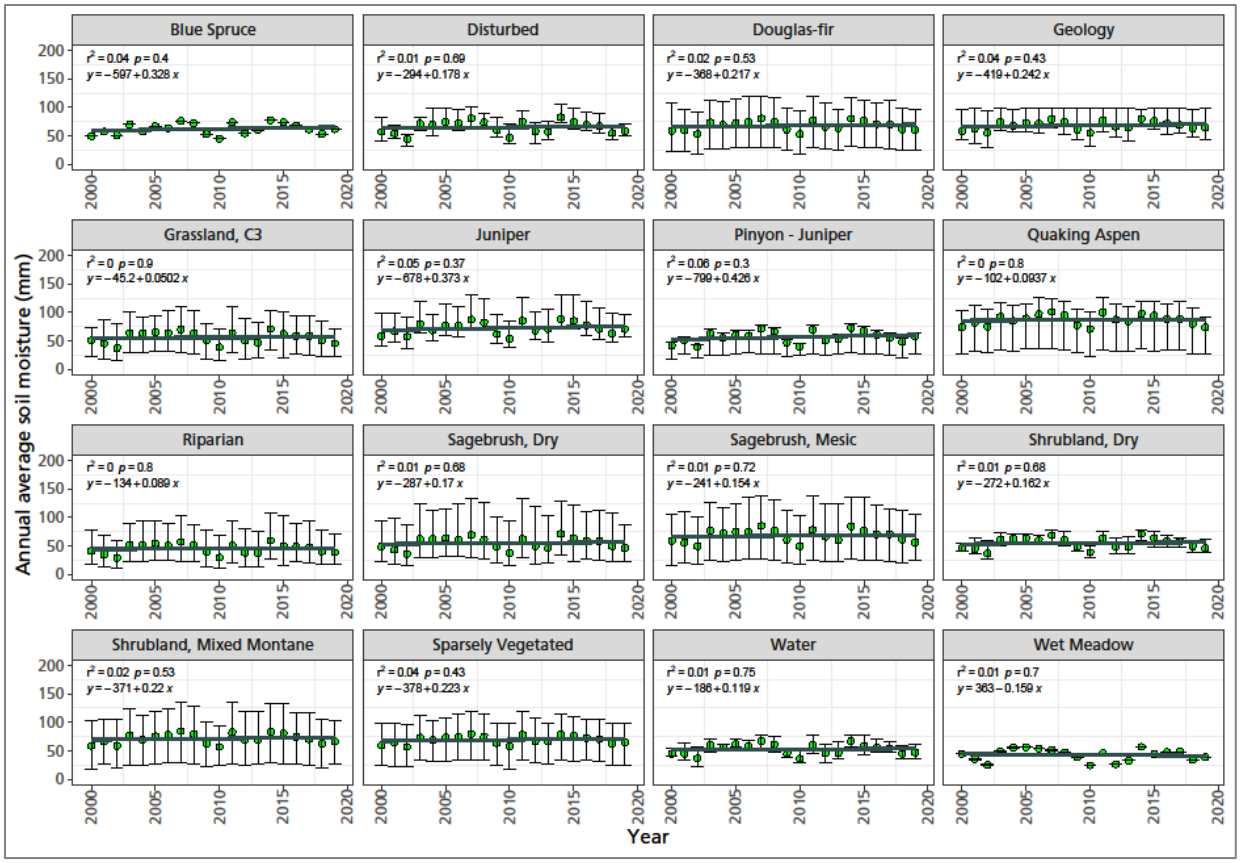

Figure 27. Annual average soil moisture trend over time, 2000–2019. Bars are standard error. NPS / DAVID THOMA

4 How to Use this Report when Planning for a Changing Climate

This report provides information that feeds directly into the Planning for a Changing Climate Framework (Figure 28), the process used by the NPS Climate Change Response Program (CCRP) and other federal agencies to make climate-adaptation plans based on plausible future climate and resource responses in climate-scenario planning (NPS 2021; Stein et al. 2014). Results from this report inform Step 2 (Figure 28), which is an assessment of vegetation vulnerability to climate change that defines climate exposure, vegetation sensitivity, and vulnerability of vegetation to climate change considering inherent adaptive capacity and management actions that help reduce vulnerability (adapted from NPS 2021).

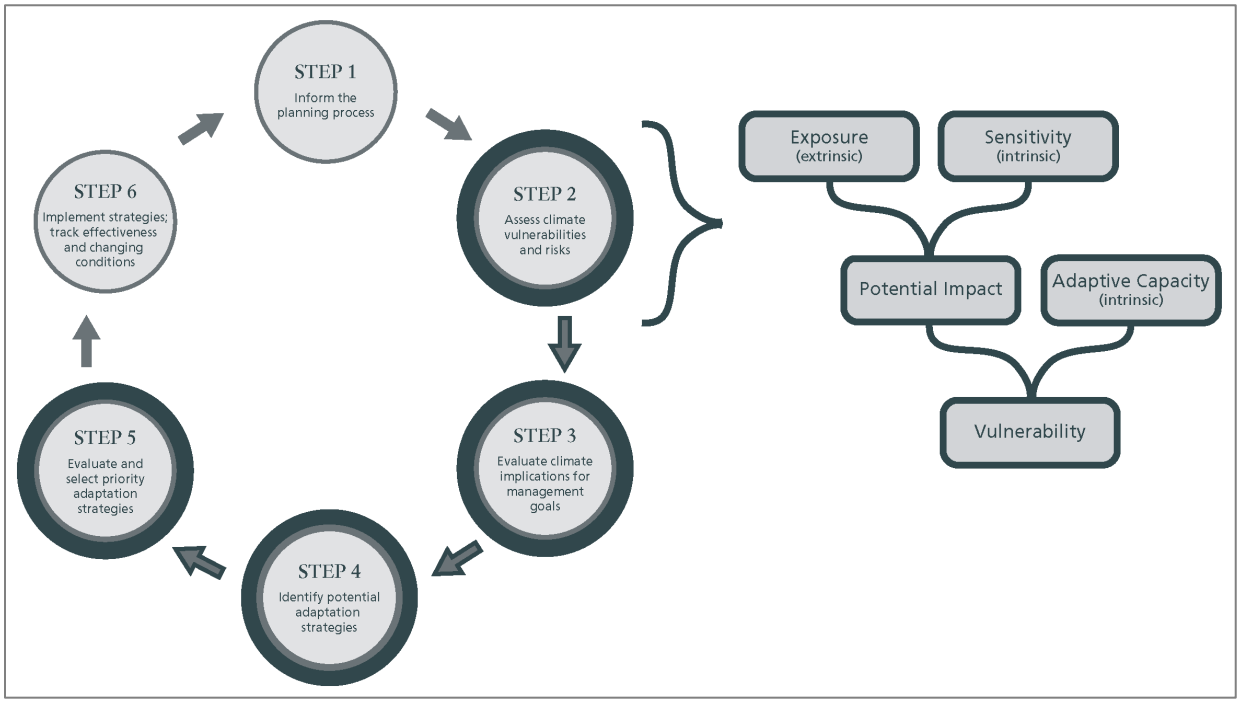

Figure 28. Framework for Planning for a Changing Climate. The concentric circles represent different scenarios that can guide the planning process. NPS

4.1 Identifying management goals

The first step in Planning for a Changing Climate is to identify management goals that will inform the planning process. This is usually an iterative process where initial goals are periodically re-evaluated based on values, vulnerability, and adaptive management. Goals may be determined via planning processes, by current threats, or by changes that have already occurred. Clearly defined goals help make the rest of the process more efficient. In addition to vulnerability and values, management goals may also consider management paradigms of resisting, accepting, or directing change (NPS 2021; Schuurman et al. 2020). The appropriate paradigm depends on the goals

informed by values and vulnerability assessments. It may be necessary to implement strategies that reflect more than one paradigm to achieve goals.

4.2 Vulnerability assessment

This report advances understanding of climate as a driver of vegetation production and phenology at alliance-polygon, alliance-group, and whole-park scales at Curecanti NRA. The historical perspective in this report provides the necessary background for understanding the range in variability of climate and vegetation response while also informing how vegetation is likely to respond to weather in the near term and climate change in the long-term. Specifically, results identify how vegetation condition and sensitivity are linked to incremental changes in weather and climate. Thus, this report can be used to determine how vegetation production and phenology may change (increasing or decreasing production) if the relationships described here carry into the future. Disruption of those relationships can be caused by gradual transitions of native vegetation, exotic species invasions, disturbance, or land-use change.

Vegetation response in this report is synonymous with the concept of climate sensitivity in Planning for a Changing Climate (see Figure 28), which is a critical step in determining vulnerability to climate change. Sensitivity to climate determines how much, and how rapidly, vegetation production changes with climate. Sensitivity is obtained from the slope of the regression line in the relationship between interannual variation in growing season iSAVI (a surrogate for change in annual production) and any one climate variable (see Figure 3; Tables S-2 and S-4 in Thoma 2024).

Quantitative vulnerability assessments can help determine where, when, and which alliance groups, and which polygons, are likely to change as vegetation responds to climate change according to its sensitivity to climate (see Figures 13 and 14). The information in Tables S-2 and S-4 of Thoma (2024) is designed for use as a landscape- and polygon-scale vegetation vulnerability assessment. A vulnerability assessment evaluates climate exposure and vegetation sensitivity, and how they will likely interact in the future to affect vegetation condition. Historic and future exposure to many climate variables are included in this report (Appendix A, Figures 84 to 93; Christensen et al. 2021). Pivot points and sensitivity by polygon or alliance group are summarized in maps, charts, and tables (Appendix A, Figures 32 to 79; Tables S-2 and S-4 in Thoma 2024), as is the role of site characteristics, such as soil properties, that modify sensitivity (see Figure 15). Future vulnerability is determined by comparing different climate projections (the climate scenarios in Christensen et al. 2021) to pivot points for each polygon (in Table S-2 in Thoma 2024). This quantifies how frequently production falls below average conditions. If future production consistently falls below historic average conditions, then one vegetation assemblage is likely to transition into another better-suited to the new climate conditions. Section 4.4 demonstrates how to use data in this report for a polygon-level vulnerability assessment.

4.3 Using pivot points and responses in climate-adaptation planning

The annual pivot points and responses described here are useful for understanding how different aspects of climate (water availability, water use, water need, and temperature) affect vegetation. Additionally, pivot points and responses are integrative, useful ecological variables that complement

assessments of exposure and sensitivity used for climate-adaptation planning. They combine effects of temperature, precipitation, and plant traits with site characteristics into single-variable descriptions of water use (AET) and unmet water need (D) (Tercek et al. 2021) that are place-based and uniquely identified for each alliance polygon.

Water-balance pivot points and responses are well-suited for applications that benefit from the simplicity of single-variable descriptions of climate exposure (such as temperature and precipitation) but are more biophysically related to natural-resource response (Thoma et al. 2020; Stephenson 1998). The quantitative assessment of vegetation sensitivity to climate and water-balance variables on an annual basis is a good starting point for the initial phase of long-range climate-adaptation planning.

4.4 Example vulnerability assessment

Below, an example of a quantitative vulnerability assessment for Curecanti NRA is presented using a pivot point and two future scenarios. Rather than considering all possible climate futures (currently 24 scenarios are available for consideration), which can be overwhelming, two scenarios shown in Christensen et al. (2021) were intentionally selected to bracket a wide range of plausible future conditions at Curecanti NRA. These include a best-case scenario of warming and increasing precipitation, and a worst-case scenario of warming and reduced precipitation. Climate exposure at Curecanti NRA will increase over time (Christensen et al. 2021) as declines in soil moisture and increases in water deficit play out under both a warmer and wetter and warmer and drier future. This is because the rate of warming under either scenario will result in drying that will outstrip projected changes in precipitation, even for the wetter scenario. The interaction of temperature and precipitation in both scenarios will result in earlier and longer dry seasons (Christensen et al. 2021).

For illustrative purposes, a vulnerability analysis for a single Dry Sagebrush polygon in Curecanti NRA identifies exposure (change in climate over time), drought tolerance (pivot point determined from remote sensing), and vulnerability (frequency of pivot-point exceedance) in the future (Figure 29). The vulnerability assessment for this polygon, located near the center of the NRA, was made by comparing pivot points (the critical water need) to future water-balance conditions at Curecanti NRA. In this case, the annual water deficit pivot point for polygon CURE_1684 was 312 millimeters (calculated as the mean Gridmet deficit, which is the historic climate dataset appropriate for use with climate projections).

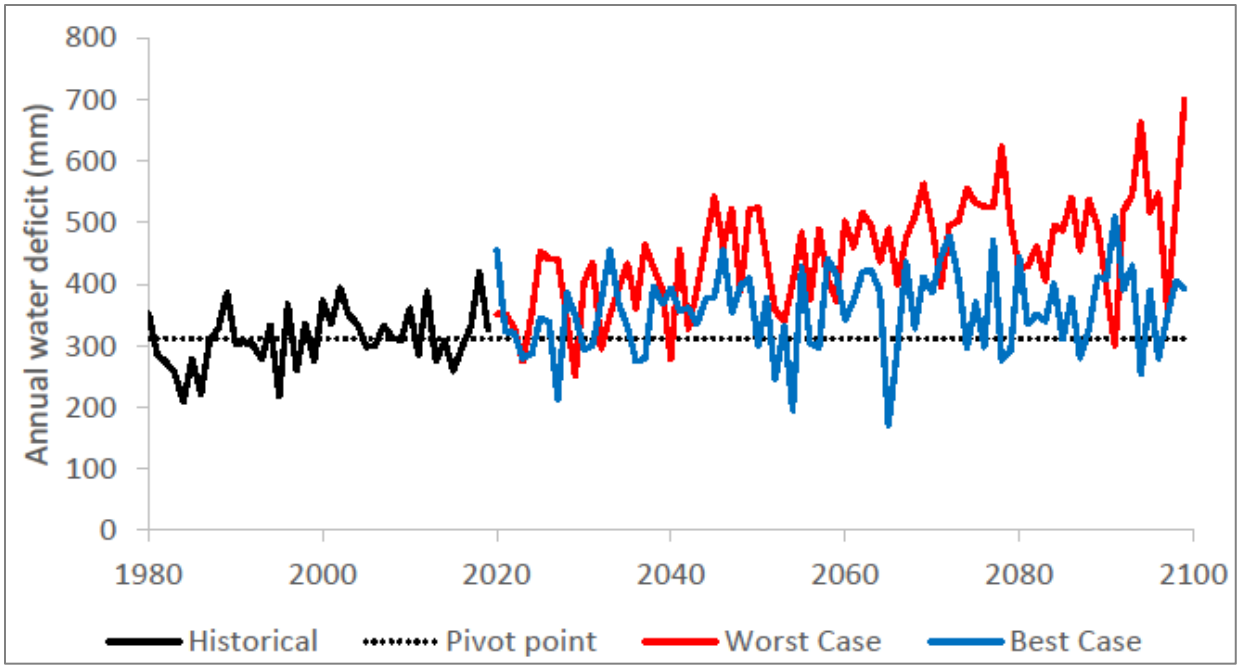

Figure 29. Quantitative vulnerability analysis for a single polygon. Here, the projected change in annual water deficit relative to the pivot point is shown for a location at the park centroid (polygon CURE_1684), which falls in a Dry Sagebrush alliance group. The deficit pivot point for this polygon was determined as 312 millimeters per year from the historical Gridmet climate dataset compatible with climate projections (retrieved from the page Summary Layers for the NPS Gridded Water Balance Model). The best- and worst-case scenarios were selected from a range of many plausible futures derived from temperature and precipitation projections from the World Climate Research Program CMIP5 experiments. The temperature and precipitation data were passed through the water-balance model to generate future projections of the water-balance variables. The warming-and-wetting scenario is the "best" case in this example. The projection data used to build this figure were from the climate exposure analysis summary used to create the report in Christensen et al. (2021). NPS / DAVID THOMA

Under the warm-and-wet (best-case) scenario, annual water deficit will remain near the historic range of variability until mid-century, but will rise after that time. However, even before mid-century, multiple years of drought that exceed the water deficit pivot point may exceed the adaptive capacity of the Dry Sagebrush alliance group, leading to transition in vegetation assemblage due to acute drought or fire disturbance. The effect of consecutive years of below-normal soil moisture and above-average deficit was made clear by the widespread juniper mortality in southeast Utah noted by NCPN resource managers in 2019, following two years of high deficit (Figure 30). This drought was sufficiently long and deep to kill trees that have multiple drought-resistance mechanisms via osmotic regulation and stomatal closure (Dickman et al. 2015).

Figure 30. A patch of dying junipers with the Abajo Mountains in the background, Cedar Mesa, Utah, 2019. In the two years before this photo was taken, water deficit was higher than at any time since 1980. NPS / DANA WITWICKI

From this analysis, it may seem that anything is possible—from no change to complete transition—which could lead to inaction due to uncertainty. However, the greatest uncertainty in this analysis is the representative concentration pathway (RCP) (RCP4.5, the best-case, or RCP8.5, the worst-case) that models CO_2 emissions resulting from societal choices to reduce greenhouse gas emissions—far more so than the uncertainty in vegetation response to climate. For this reason, the next decade will be important to determining the trajectory of exposure.

The analysis demonstrated here can be recreated to determine site-specific vulnerability for any polygon in Curecanti NRA. Until such analyses using climate projections are quantitatively linked to pivot points in this report (as in Figure 29), users can gain a sense of vulnerability by sorting on pivot or slope in Tables S-3 and S-4 of Thoma (2024) to identify the most sensitive and most drought tolerant polygons and alliance groups.

4.5 Identifying and implementing management actions

In planning for the future, the importance of vulnerability assessments for understanding and managing climate change is underscored by statements from the Intergovernmental Panel on Climate

Change (IPCC). As the summary for policymakers in their recent report states, "Global surface temperature will continue to increase until at least the mid-century under all emissions scenarios considered. Global warming of 1.5°C and 2°C will be exceeded during the 21st century unless deep reductions in carbon dioxide (CO_2) and other greenhouse gas emissions occur in the coming decades." It goes on to say, "Continued global warming is projected to further intensify the global water cycle, including its variability, global monsoon precipitation and the severity of wet and dry events" (IPCC 2021).

Vulnerability assessments can help identify the timing and type of management actions needed to achieve management goals in the face of an uncertain future. Additionally, they can help determine if existing actions are likely to achieve existing goals, if new management strategies are needed to achieve goals, or if management goals are unrealistic and need to be revised. After management goals and vulnerability assessments are reconciled, management options likely to achieve management goals can be identified and implemented (Steps 3–6 in Figure 28).

4.6 Tools to inform near-term management

Tracking weather conditions that lead up to or surpass pivot points during the growing season is a useful climate-based tool for assessing vegetation condition—but it provides an indirect assessment. Additional tools can provide real-time assessments of vegetation condition by identifying both trends in vegetation greenness and the vegetation anomaly (a comparison of current growing conditions versus past conditions). With these tools, users can iteratively identify the spatial pattern and strength of trends, and where disturbance or unusual events are happening in near-real time.[8]

Interpreting the link between those patterns and climate requires contemporaneous climate data. The gridded climate data used in this report were created from weather-station data, typically in the year following a full year of data collection at weather stations. Weather-station data are better suited to investigations of real-time change in conditions, especially extreme events that garner interest as they happen or soon after—as was the case when park managers noted juniper mortality in 2018 and 2019.

The NCPN supports The Climate Analyzer, which makes accessing weather-station data intuitive and easy. Data from the park weather station and other sources can be used to determine how weather and vegetation condition vary together in near real-time. This could be the basis for real-time condition assessments used in the tactical decisions needed to achieve long-range management goals. Care must be taken when analyzing trends from weather-station data due to missing values and outliers. Nevertheless, over the period of time analyzed in this report, the upward trend in station precipitation and lack of trend in average temperature were consistent with the trends found using Daymet, the gridded climate data used in the analysis for this report.

[8] More information on these tools can be obtained by emailing the author of this report.

5 Conclusions

Since 2000, a very dry period, primary production has increased in 98% of the area in and near Curecanti NRA. This increase coincided with a slight increase in precipitation over the same period. However, between 2000 and 2019, there were dry years and dry periods extending for several years that resulted in substantial declines in vegetation cover that largely rebounded by the end of the study.

The variation in vegetation condition across wet and dry years was evaluated to identify which alliance groups were most drought-tolerant (Pinyon-Juniper, Riparian and a single polygon of Wet Meadow), and which were least drought tolerant (Quaking Aspen, Douglas-fir, Mixed Montane Shrubland and a single polygon of Juniper). Similarly, variation in climate over the study period was used to determine that Disturbed areas, Douglas-fir and Mixed Montane Shrubland were the alliance groups most sensitive to water deficit.

The climate variable most strongly correlated with vegetation production was three years of actual evapotranspiration. Timing of snowmelt, growing degree days and calendar year precipitation were the primary determinants of green-up timing. Over the study period, the start of the growing season shifted later, and the length of growing season increased for most alliance groups, likely due to slight warming and an increase in precipitation during the study period, although the changes in these climate variables were not significant.

The variation in weather conditions and corresponding vegetation response provide a window into the past that will inform understanding and management of vegetation that always has responded, and will continue to respond, to climate at Curecanti NRA. Much of the information in this report will soon be outdated. However, some of the findings described here have long-term value and are unlikely to change until vegetation composition changes in the future, such as pivot points and the sensitivity of vegetation to weather and climate. This is because drought tolerance and response to weather are factors inherent to the natural history traits of vegetation and where it grows. However, climate is changing rapidly, and extreme weather events are becoming more frequent. The tools developed for these analyses can help National Park Service managers to anticipate and plan for climate change—and to manage change as it happens. This report demonstrates how combining satellite observations of vegetation condition with climate data can help determine the right time and place for action needed in the near-term to help achieve long-range management goals for stewarding park resources through continuous change.

6 Literature Cited

Aikens, EO, MJ Kauffman, JA Merkle, SPH Dwinnell, GL Fralick, and KL Monteith. 2017. The greenscape shapes surfing of resource waves in a large migratory herbivore. Ecology Letters 20:741–750. https://doi.org/10.1111/ele.12772

Allen, CD, DD Breshears, and NG McDowell. 2015. On underestimation of global vulnerability to tree mortality and forest die-off from hotter drought in the Anthropocene. Ecosphere 6:1–55. https://doi.org/10.1890/ES15-00203.1

Barger, NN, SR Archer, JL Campbell, C Huang, JA Morton, and AK Knapp. 2011. Woody plant proliferation in North American drylands: A synthesis of impacts on ecosystem carbon balance. Journal of Geophysical Research-Biogeosciences 116:G00K07. https://doi.org/10.1029/2010JG001506

Barnes, ML, MS Moran, RL Scott, TE Kolb, GE Ponce-Campos, DJP Moore, MA Ross, B Mitra, and S Dore. 2016. Vegetation productivity responds to sub-annual climate conditions across semiarid biomes. Ecosphere 7:e01339. https://doi.org/10.1002/ecs2.1339

Bisigato, AJ, L Hardtke, and HF del Valle. 2013. Soil as a capacitor: Considering soil water content improves temporal models of productivity. Journal of Arid Environments 98:88–92. https://doi.org/10.1016/j.jaridenv.2013.08.004

Breiman, L. 2001. Random forests. Machine Learning 45:5–32. https://doi.org/10.1023/A:1010933404324

Bunting, EL, SM Munson, and JB Bradford. 2019. Assessing plant production responses to climate across water-limited regions using Google Earth Engine. Remote Sensing of Environment 233:111379. https://doi.org/10.1016/j.rse.2019.111379

Christensen, J, D Thoma, M Tercek, and J Gross. 2021. Historical and projected water balance report for Curecanti National Recreation Area. Unpublished report. https://irma.nps.gov/DataStore/Reference/Profile/2306218

de Beurs, KM, and GM Henebry. 2010. Spatio-temporal statistical methods for modelling land surface phenology. Pages 177–208 in IL Hudson and MR Keatley, eds., Phenological research: Methods for environmental and climate change analysis. Springer Science+Business Media BV. https://doi.org/10.1007/978-90-481-3335-2

Dickman, LT, NG McDowell, S Sevanto, RE Pangle, and WT Pockman. 2015. Carbohydrate dynamics and mortality in a piñon-juniper woodland under three future precipitation scenarios. Plant, Cell, & Environment 38(4):729–739. https://doi.org/10.1111/pce.12441

Didan, K, AB Munoz, R Solano, and A Huete. 2015. MODIS vegetation index user's guide (Collection 6). University of Arizona, Tucson, AZ.

Dunn, AH, and KM de Beurs. 2011. Land surface phenology of North American mountain environments using moderate resolution imaging spectroradiometer data. Remote Sensing of Environment 115(5):1220–1233. https://doi.org/10.1016/j.rse.2011.01.005

Federal Geographic Data Committee (FGDC). 2008. National Vegetation Classification Standard, Version 2. February. U.S. Geological Survey, Reston, Virginia. http://usnvc.org/wp-content/uploads/2011/02/NVCS_V2_FINAL_2008-02.pdf

Forkel, M, and T Wutzler. 2015. greenbrown - land surface phenology and trend analysis. https://greenbrown.r-forge.r-project.org/

Forkel, M, N Carvalhais, J Verbesselt, MD Mahecha, CSR Neigh, and M Reichstein. 2013. Trend change detection in NDVI time series: Effects of inter-annual variability and methodology. Remote Sensing 5(5):2113–2144. https://doi.org/10.3390/rs5052113

Fu, Y, H Zhang, W Dong, and W Yuan. 2014. Comparison of phenology models for predicting the onset of growing season over the northern hemisphere. PLoS ONE 9(10):e109544. https://doi.org/10.1371/journal.pone.0109544

Garroutte, EL, AJ Hansen, and RL Lawrence. 2016. Using NDVI and EVI to map spatiotemporal variation in the biomass and quality of forage for migratory elk in the Greater Yellowstone ecosystem. Remote Sensing 8(5):404. https://doi.org/10.3390/rs8050404

Gremer, JR, C Andrews, JR Norris, LP Thomas, SM Munson, MC Duniway, and JB Bradford. 2018. Increasing temperature seasonality may overwhelm shifts in soil moisture to favor shrub over grass dominance in Colorado Plateau drylands. Oecologia 188:1195–1207. https://doi.org/10.1007/s00442-018-4282-4

Grossiord, C, TN Buckley, LA Cernusak, KA Novick, B Poulter, RTW Siegwolf, JS Sperry, and NG McDowell. 2020. Plant responses to rising vapor pressure deficit. New Phytologist 226:1550–1566. https://doi.org/10.1111/nph.16485

Huete, AR. 1988. A soil-adjusted vegetation index (SAVI). Remote Sensing of Environment 25(3):295–309. https://doi.org/10.1016/0034-4257(88)90106-X

Intergovernmental Panel on Climate Change (IPCC). 2021. Summary for policymakers, in Climate change 2021: The physical science basis. Contribution of Working Group I to the Sixth Assessment Report of the Intergovernmental Panel on Climate Change, V Masson-Delmotte, P Zhai, A Pirani, SL Connors, C Péan, S Berger, N Caud, Y Chen, L Goldfarb, MI Gomis, M Huang, K Leitzell, E Lonnoy, JBR Matthews, TK Maycock, T Waterfield, O Yelekçi, R Yu, and B Zhou, eds. https://www.ipcc.ch/report/ar6/wg1/downloads/report/IPCC_AR6_WGI_SPM_final.pdf

Jennings, MD, D Faber-Langendoen, OL Loucks, RK Peet, and D Roberts. 2009. Standards for associations and alliances of the US National Vegetation Classification. Ecological Monographs 79:173–199. https://doi.org/10.1890/07-1804.1

Johnson, HE, DD Gustine, TS Golden, LG Adams, LS Parrett, EA Lenart, and PS Barboza. 2018. NDVI exhibits mixed success in predicting spatiotemporal variation in caribou summer forage quality and quantity. Ecosphere 9:e02461. https://doi.org/10.1002/ecs2.2461

Kariyeva, J, and WJD van Leeuwen. 2011. Environmental drivers of NDVI-based vegetation phenology in Central Asia. Remote Sensing 3(2):203–246. https://doi.org/10.3390/rs3020203

McMaster, GS, and WW Wilhem. 1997. Growing degree-days: One equation, two interpretations. Agricultural and Forest Meteorology 87(4):291–300. https://doi.org/10.1016/S0168-1923(97)00027-0

Mendez-Barroso, LA, ER Vivoni, CJ Watts, and JC Rodriguez. 2009. Seasonal and interannual relations between precipitation, surface soil moisture and vegetation dynamics in the North American monsoon region. Journal of Hydrology 377(1–2):59–70. https://doi.org/10.1016/j.jhydrol.2009.08.009

Merkle, JA, KL Monteith, EO Aikens, MM Hayes, KR Hersey, AD Middleton, BA Oates, H Sawyer, BM Scurlock, and MJ Kauffman. 2016. Large herbivores surf waves of green-up during spring. Proceedings of the Royal Society B: Biological Sciences 283:1–8. https://doi.org/10.1098/rspb.2016.0456

Munson, SM. 2013. Plant responses, climate pivot points, and trade-offs in water-limited ecosystems. Ecosphere 4(9):1–15. https://doi.org/10.1890/ES13-00132.1

Munson, SM, MC Duniway, and JK Johanson. 2016. Rangeland monitoring reveals long-term plant responses to precipitation and grazing at the landscape scale. Rangeland Ecology & Management 69(1):76–83. https://doi.org/10.1016/j.rama.2015.09.004

Munson, SM, RH Webb, J Belnap, JA Hubbard, DE Swann, and S Rutman. 2011. Forecasting climate change impacts to plant community composition in the Sonoran Desert region. Global Change Biology 18(3):1083–1095. https://doi.org/10.1111/j.1365-2486.2011.02598.x

Munson, SM, RH Webb, DC Housman, KE Veblen, KE Nussear, EA Beever, KB Hartney, MN Miriti, SL Phillips, RE Fulton, and NG Tallent. 2015. Long-term plant responses to climate are moderated by biophysical attributes in a North American desert. Journal of Ecology 103(3):657–668. https://doi.org/10.1111/1365-2745.12381

National Park Service (NPS). 2021. Planning for a changing climate: Climate-smart planning and management in the National Park Service. NPS Climate Change Response Program, Fort Collins, Colorado. https://irma.nps.gov/DataStore/Reference/Profile/2279647

Norris, JR, and JJ Walker. 2020. Solar and sensor geometry, not vegetation response, drive satellite NDVI phenology in widespread ecosystems of the western United States. Remote Sensing of Environment 249:112013. https://doi.org/10.1016/j.rse.2020.112013

Noy-Meir, I. 1973. Desert ecosystems: Environment and producers. Annual Review of Ecology, Evolution, and Systematics 4:25–51. https://doi.org/10.1146/annurev.es.04.110173.000325

Oudin, L, F Hervieu, C Michel, C Perrin, V Andréassian, F Anctil, and C Loumagne. 2005. Which potential evapotranspiration input for a lumped rainfall-runoff model? Part 2 - Towards a simple and efficient potential evapotranspiration model for rainfall-runoff modelling. Journal of Hydrology 303(1–4):290–306. https://doi.org/10.1016/j.jhydrol.2004.08.026

Paruelo, JM, M Oesterheld, CM Di Bella, M Arzadum, J Lafontaine, M Cahuepé, and CM Rebella. 2000. Estimation of primary production of subhumid rangelands from remote sensing data. Applied Vegetation Science 3(2):189–195. https://doi.org/10.2307/1478997

Peterman, W, RH Waring, T Seager, and WL Pollock. 2013. Soil properties affect pinyon pine - juniper response to drought. Ecohydrology 6(3):455–463. https://doi.org/10.1002/eco.1284

Qi, J, A Chehbouni, AR Huete, YH Kerr, and S Sorooshian. 1994. A modified soil adjusted vegetation index. Remote Sensing of Environment 48(2):119–126. https://doi.org/10.1016/0034-4257(94)90134-1

Reed, BC, JF Brown, D VanderZee, TR Loveland, JW Merchant, and DO Ohlen. 1994. Measuring phenological variability from satellite imagery. Journal of Vegetation Science 5(5):703–714. https://doi.org/10.2307/3235884

Sala, OE, LA Gherardi, L Reichmann, E Jobbagy, and D Peters. 2012. Legacies of precipitation fluctuations on primary production: theory and data synthesis. Philosophical Transactions of the Royal Society B: Biological Sciences 367(1606):3135–3144. https://doi.org/10.1098/rstb.2011.0347

Schlaepfer, DR, WK Lauenroth, and JB Bradford. 2012. Ecohydrological niche of sagebrush ecosystems. Ecohydrology 5(4):453–466. https://doi.org/10.1002/eco.238

Schuurman, GW, C Hawkins-Hoffman, DN Cole, DJ Lawrence, JM Morton, DR Magness, AE Cravens, S Covington, R O'Malley, and NA Fisichelli. 2020. Resist-accept-direct (RAD)— a framework for the 21st-century natural resource manager. Natural Resource Report NPS/NRSS/CCRP/NRR—2020/2213. National Park Service, Fort Collins, Colorado. https://doi.org/10.36967/nrr-2283597

Seager, R, A Hooks, AP Williams, B Cook, J Nakamura, and N Henderson. 2015. Climatology, variability, and trends in the U.S. vapor pressure deficit, an important fire-related meteorological quantity. Journal of Applied Meteorology and Climatology 54(6):1121–1141. https://doi.org/10.1175/JAMC-D-14-0321.1

Sorokin, Y, TJ Zelikova, D Blumenthal, DG Williams, and E Pendall. 2017. Seasonally contrasting responses of evapotranspiration to warming and elevated CO_2 in a semiarid grassland. Ecohydrology 10(7):e1880. https://doi.org/10.1002/eco.1880

St. Peter, JR. 2015. A model for determining drivers of phenology in western United States rangelands. University of Montana, Graduate Student Theses, Dissertations, & Professional Papers. 4444. https://scholarworks.umt.edu/etd/4444/

Stein, BA, P Glick, N Edelson, and A Staudt. 2014. Climate-smart conservation: Putting adaption principles into practice. National Wildlife Federation, Washington, D.C. https://pubs.usgs.gov/publication/70093621

Stephenson, NL. 1990. Climatic control of vegetation distribution: The role of the water balance. The American Naturalist 135(5):649–670. https://doi.org/10.1086/285067

Stephenson, N. 1998. Actual evapotranspiration and deficit: Biologically meaningful correlates of vegetation distribution across spatial scales. Journal of Biogeography 25(5):855–870. https://doi.org/10.1046/j.1365-2699.1998.00233.x

Tercek, MT, D Thoma, JE Gross, K Sherrill, S Kagone, and G Senay. 2021. Historical changes in plant water use and need in the continental United States. PLoS ONE 16(9):e0256586. https://doi.org/10.1371/journal.pone.0256586

Thoma, D. 2024. Supplemental tables for report on landscape phenology, vegetation condition, and relations with climate at Curecanti National Recreation Area, 2000–2019. National Park Service. https://irma.nps.gov/DataStore/Reference/Profile/2306218

Thoma, DP, DW Bailey, DS Long, GA Nielsen, MP Henry, MC Breneman, and C Montagne. 2002. Short-term monitoring of rangeland forage conditions with AVHRR imagery. Journal of Range Management 55(4):383–389. https://doi.org/10.2307/4003475

Thoma, DP, SM Munson, KM Irvine, DL Witwicki, EL Bunting, and J Paruelo. 2016. Semi-arid vegetation response to antecedent climate and water balance windows. Applied Vegetation Science 19(3):413–429. https://doi.org/10.1111/avsc.12232

Thoma, DP, SM Munson, and DL Witwicki. 2019. Landscape pivot points and responses to water balance in national parks of the southwest US. Journal of Applied Ecology 56(1):157–167. https://doi.org/10.1111/1365-2664.13250

Thoma, D, J Norris, and P Lauck. 2017. Satellite-based vegetation condition and phenology, and snow cover extent monitoring protocol for the Northern and Southern Colorado Plateau Networks. Natural Resource Report. NPS/SCPN/NRR—2017/1533. National Park Service. Fort Collins, Colorado. https://irma.nps.gov/DataStore/Reference/Profile/2246068

Thoma, DP, MT Tercek, EW Schweiger, SM Munson, JE Gross, and ST Olliff. 2020. Water balance as an indicator of natural resource condition: Case studies from Great Sand Dunes National Park and Preserve. Global Ecology and Conservation 24:e01300. https://doi.org/10.1016/j.gecco.2020.e01300

Thornton, PE, MM Thornton, BW Mayer, Y Wei, R Devarakonda, RS Vose, and RB Cook. 2018. Daymet: Daily surface weather data on a 1-km grid for North America; Version 3.

van Wijk, RE, A Kölzsch, H Kruckenberg, BS Ebbinge, GJDM Müskens, and BA Nolet. 2012. Individually tracked geese follow peaks of temperature acceleration during spring migration. Oikos 121(5):655–664. https://doi.org/10.1111/j.1600-0706.2011.20083.x

Von Loh, JK, A Landgraf, T Evenden, S Owens, and MR Blauer. 2007. Vegetation classification and mapping project report, Bryce Canyon National Park. Natural Resource Technical Report NPS/NCPN/NRTR—2007/061. National Park Service, Fort Collins, Colorado. https://www.nps.gov/im/vmi-brca.htm

Wang, C, J Chen, Y Tang, TA Black, and K Zhu. 2018. A novel method for removing snow melting-induced fluctuation in GIMMS NDVI3g data for vegetation phenology monitoring: A case study in deciduous forests of North America. IEEE Journal of Selected Topics in Applied Earth Observations and Remote Sensing 11(3):800–807. https://doi.org/10.1109/JSTARS.2017.2778076

Witwicki, DL, SM Munson, and DP Thoma. 2016. Effects of climate and water balance across grasslands of varying C_3 and C_4 grass cover. Ecosphere 7(11):1–19. https://doi.org/10.1002/ecs2.1577

Workie, TG, and HJ Debella. 2018. Climate change and its effects on vegetation phenology across ecoregions of Ethiopia. Global Ecology and Conservation 13:e00366. https://doi.org/10.1016/j.gecco.2017.e00366

Yang, Y, T Wu, S Wang, J Li, and F Muhanmmad. 2019. The NDVI-CV method for mapping evergreen trees in complex urban areas using reconstructed Landsat 8 time-series data. Forests 10(2):139. https://doi.org/10.3390/f10020139

Appendix A. Supplemental Figures for Landscape Phenology, Vegetation Condition, and Relations with Climate at Curecanti National Recreation Area, 2000–2019

Figures 31 to 93 contain information about the landscape phenology, vegetation condition, and relations with climate that were observed in Curecanti National Recreation Area during the study period from 2000 to 2019.

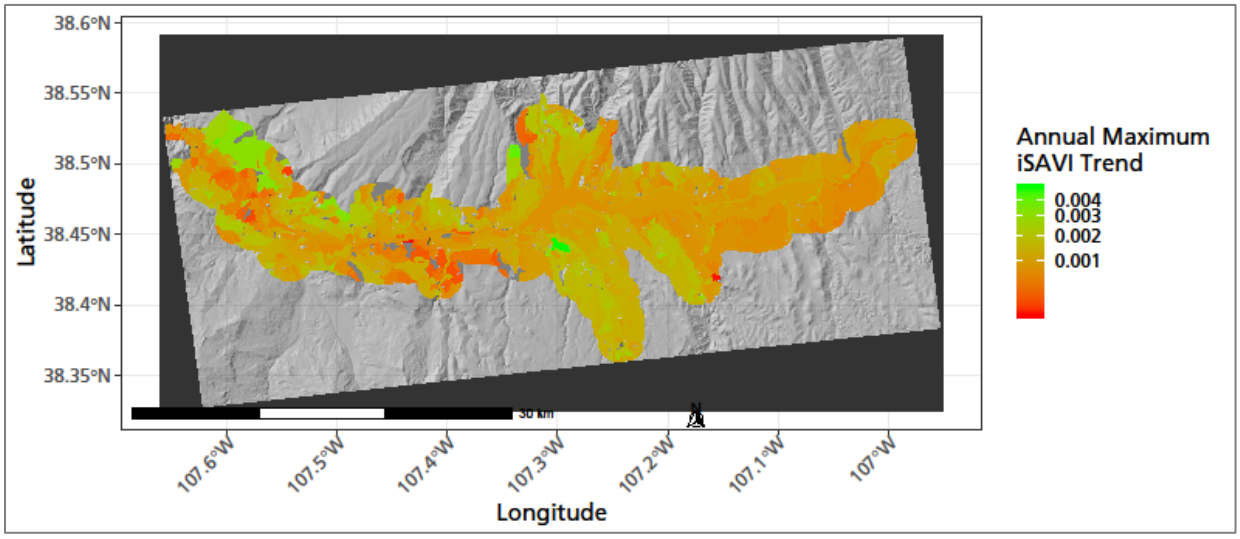

Figure 31. Spatial pattern of trends in maximum annual iSAVI in Curecanti NRA. Trend is average change in iSAVI per year for the period 2000–2019. NPS / DAVID THOMA

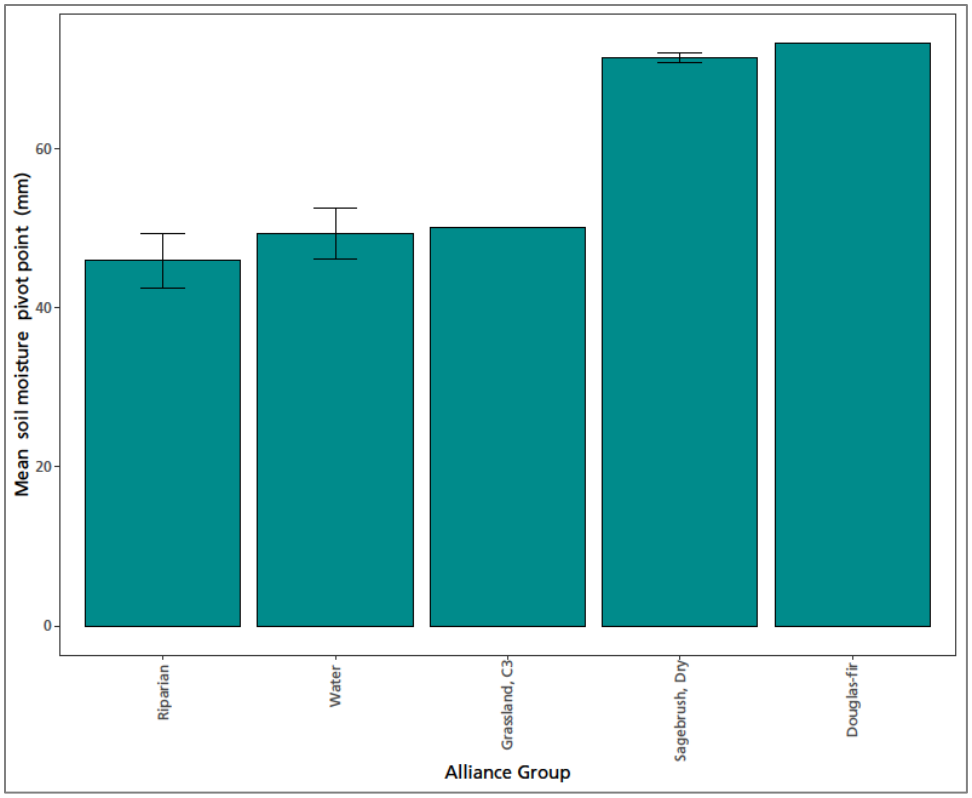

Figure 32. Pivot points for polygons in Curecanti NRA where soil moisture was significantly related to interannual variation in production (p-value < 0.05). Climate data summarized by water year. NPS / DAVID THOMA

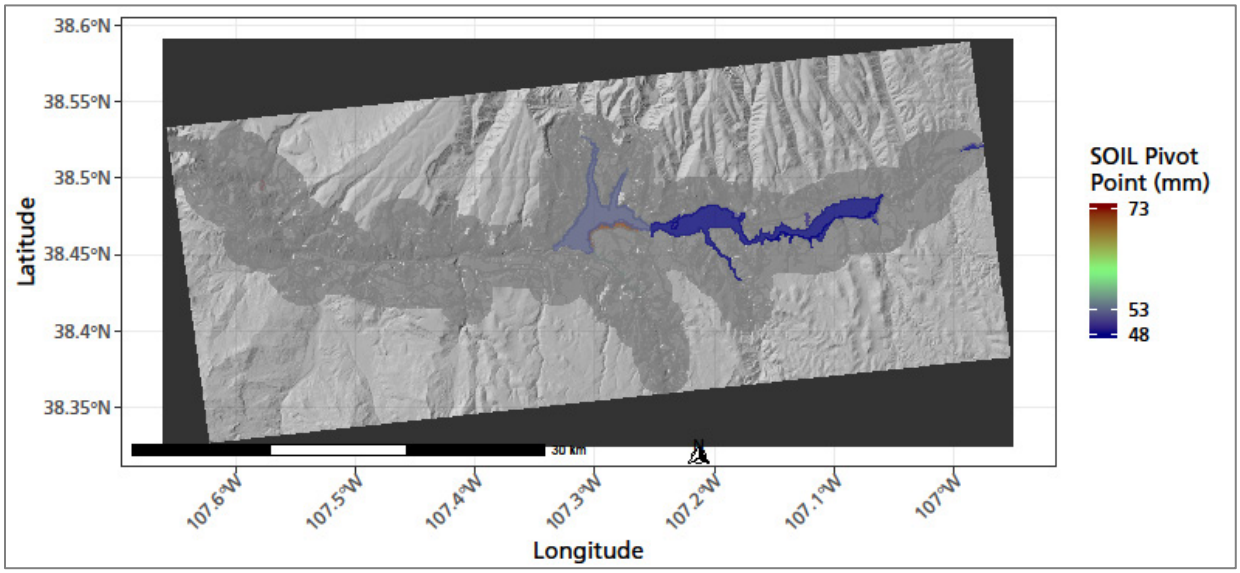

Figure 33. A map of Curecanti NRA showing the locations of polygons where soil moisture was significantly related to interannual variation in production (p-value < 0.05). Climate data summarized by water year. NPS / DAVID THOMA

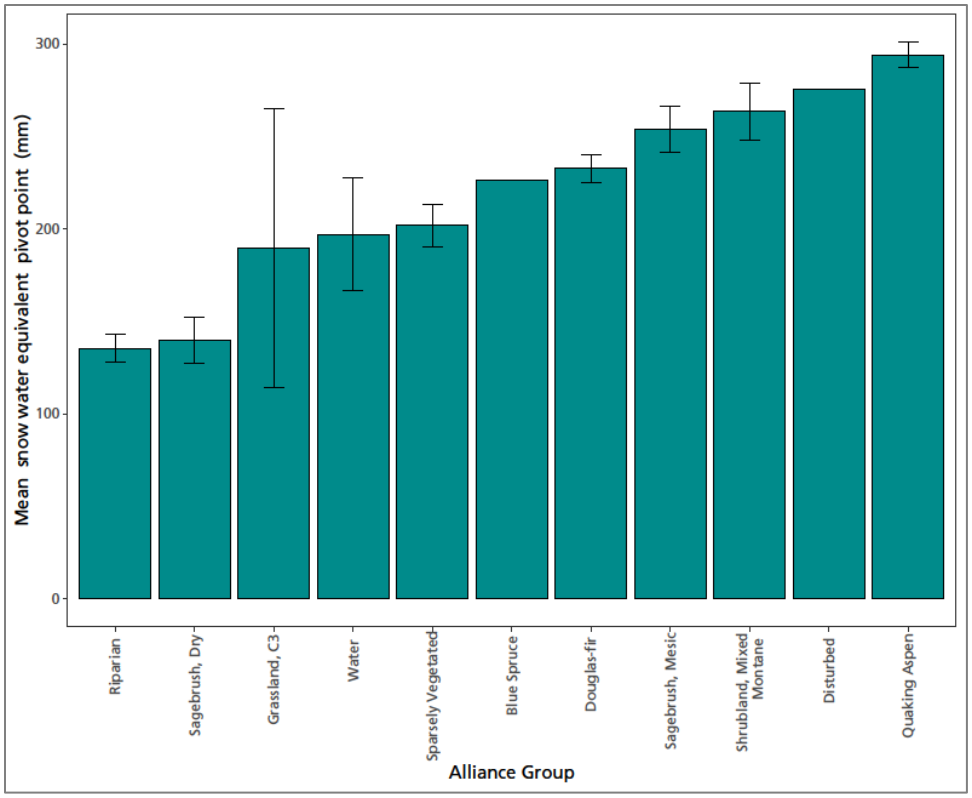

Figure 34. Pivot points for polygons in Curecanti NRA where snow water equivalent was significantly related to interannual variation in production (p-value < 0.05). Climate data summarized by water year. NPS / DAVID THOMA

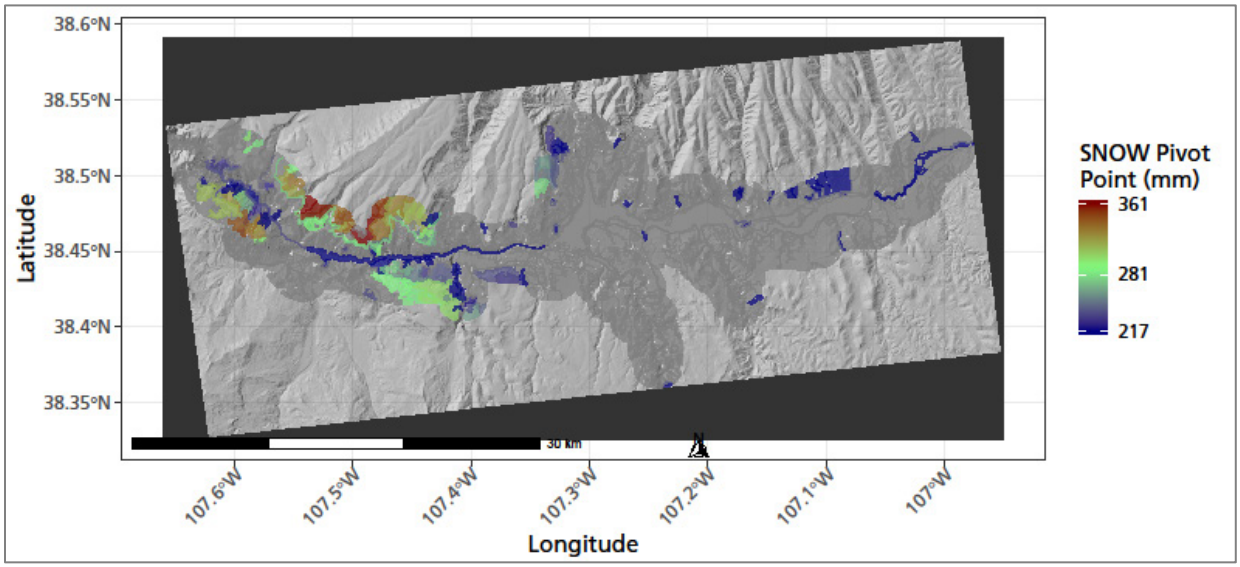

Figure 35. A map of Curecanti NRA showing the locations of polygons where snow water equivalent was significantly related to interannual variation in production (p-value < 0.05). Climate data summarized by water year. NPS / DAVID THOMA

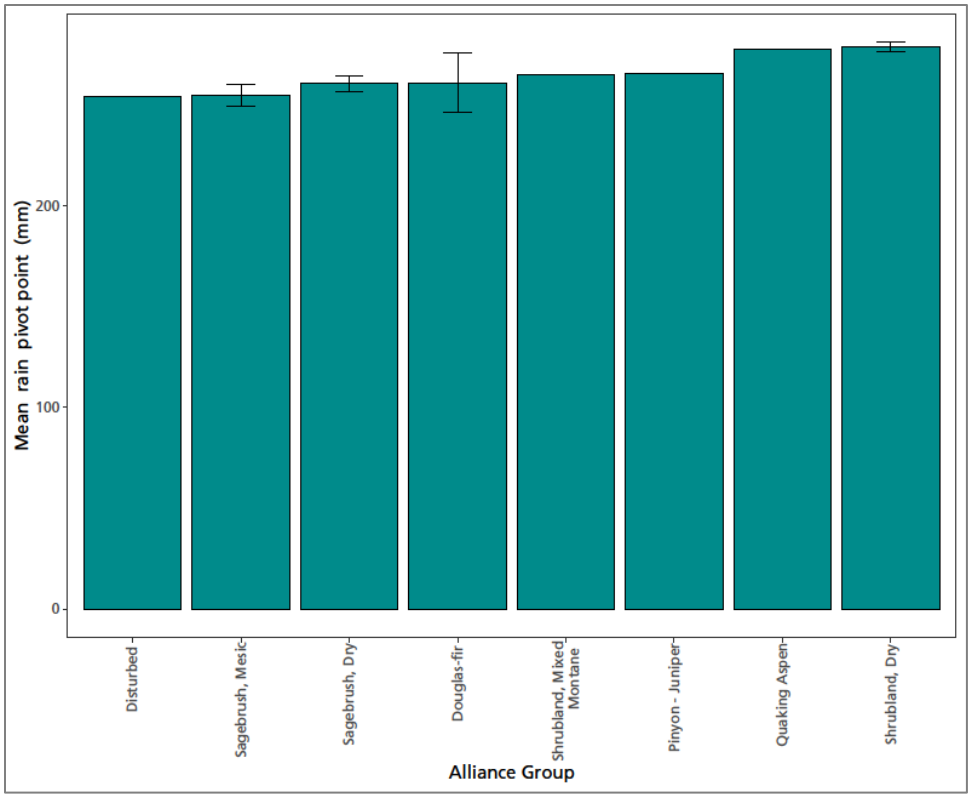

Figure 36. Pivot points for polygons in Curecanti NRA where rain was significantly related to interannual variation in production (p-value < 0.05). Climate data summarized by water year. NPS / DAVID THOMA

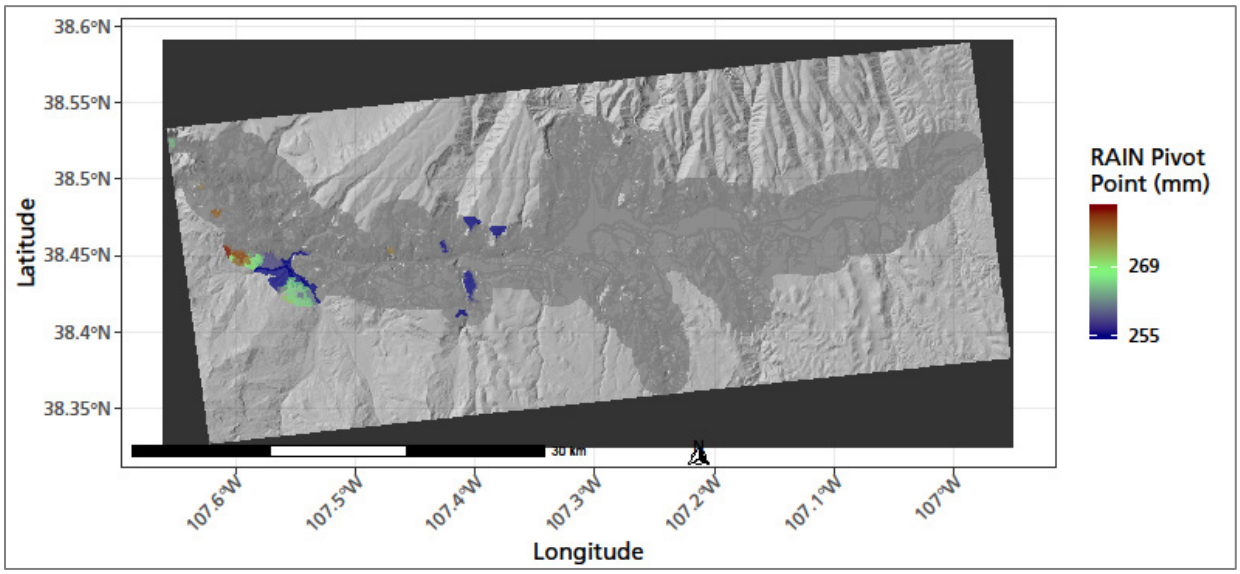

Figure 37. A map of Curecanti NRA showing the locations of polygons where rain was significantly related to interannual variation in production (p-value < 0.05). Climate data summarized by water year. NPS / DAVID THOMA

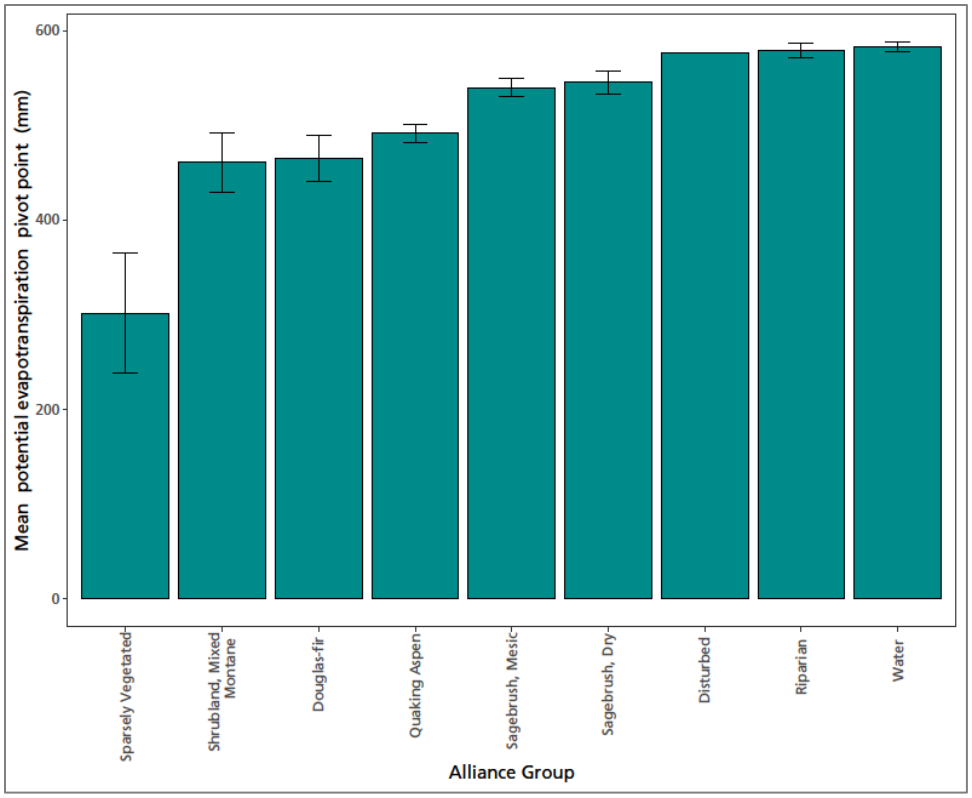

Figure 38. Pivot points for polygons in Curecanti NRA where potential evapotranspiration was significantly related to interannual variation in production (p-value < 0.05). Climate data summarized by water year. NPS / DAVID THOMA

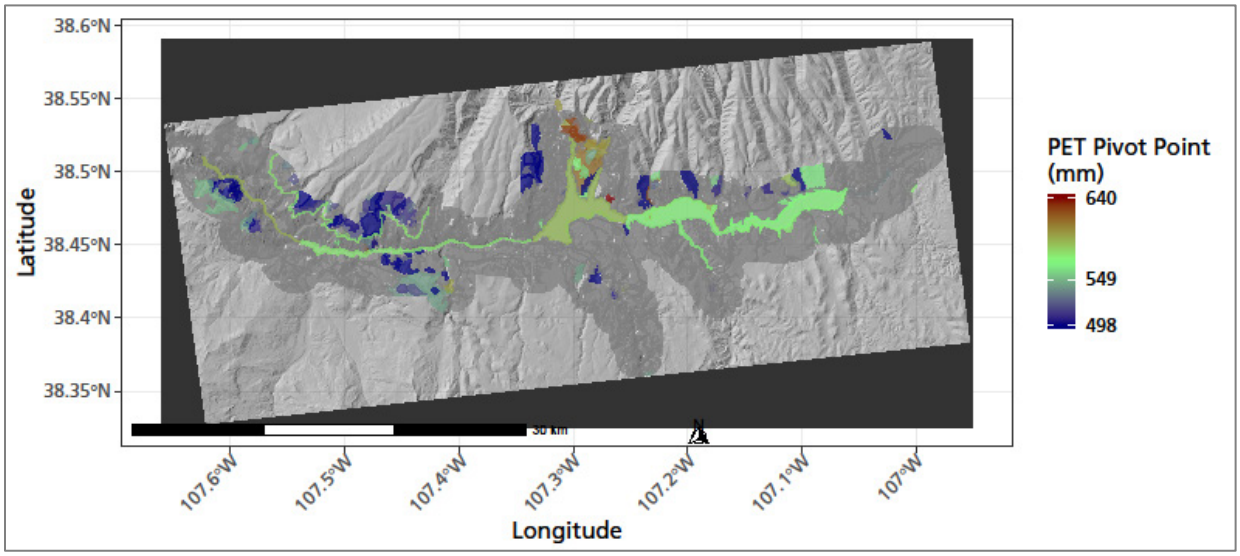

Figure 39. A map of Curecanti NRA showing the locations of polygons where potential evapotranspiration was significantly related to interannual variation in production (p-value < 0.05). Climate data summarized by water year. NPS / DAVID THOMA

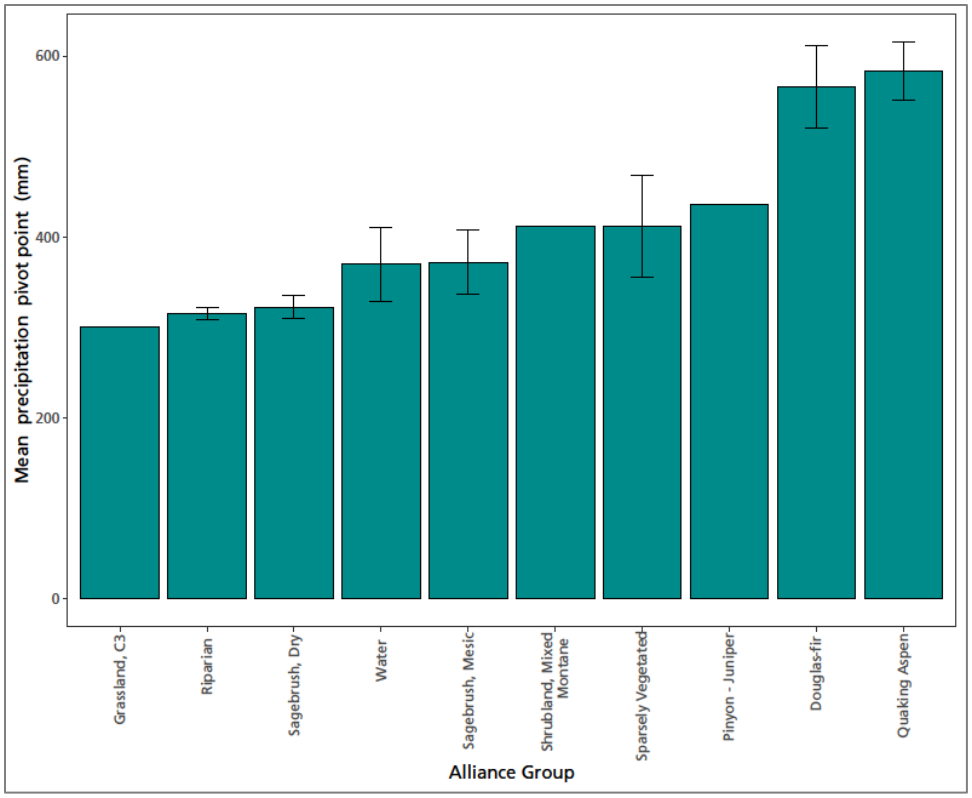

Figure 40. Pivot points for polygons in Curecanti NRA where precipitation was significantly related to interannual variation in production (p-value < 0.05). Climate data summarized by water year. NPS / DAVID THOMA

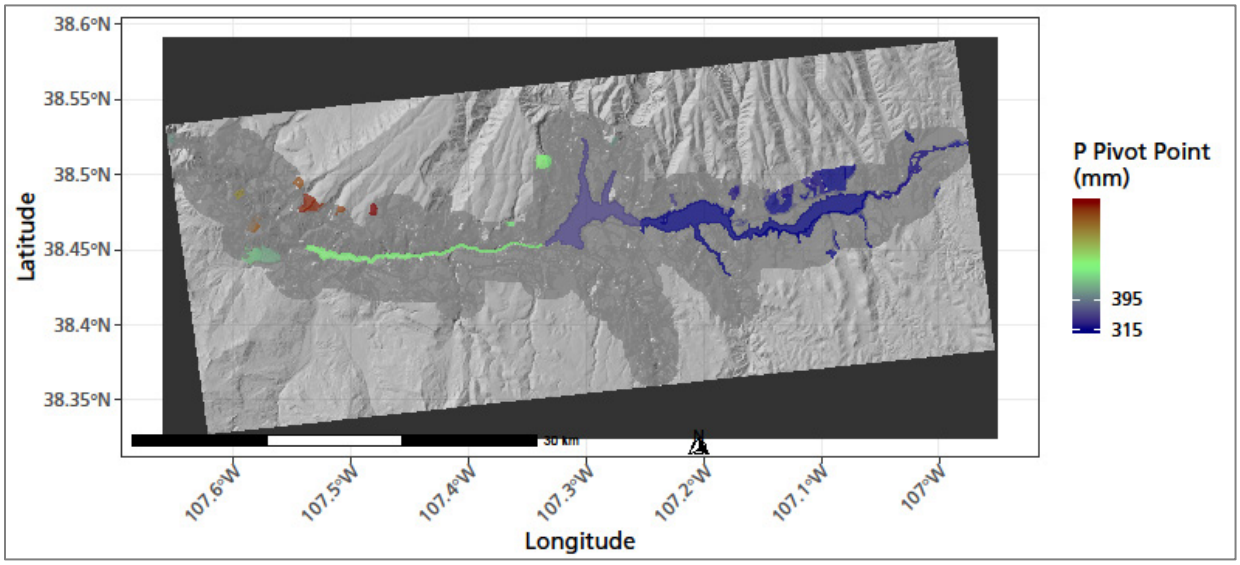

Figure 41. A map of Curecanti NRA showing the locations of polygons where precipitation was significantly related to interannual variation in production (p-value < 0.05). Climate data summarized by water year. NPS / DAVID THOMA

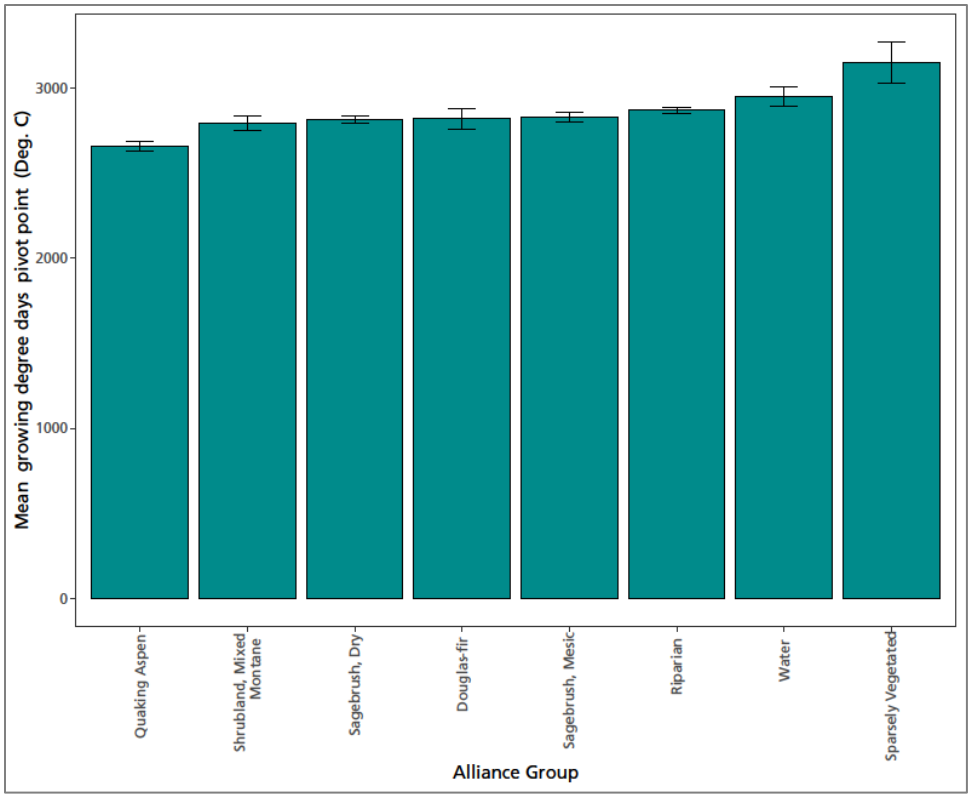

Figure 42. Pivot points for polygons in Curecanti NRA where growing degree days were significantly related to interannual variation in production (p-value < 0.05). Climate data summarized by water year. NPS / DAVID THOMA

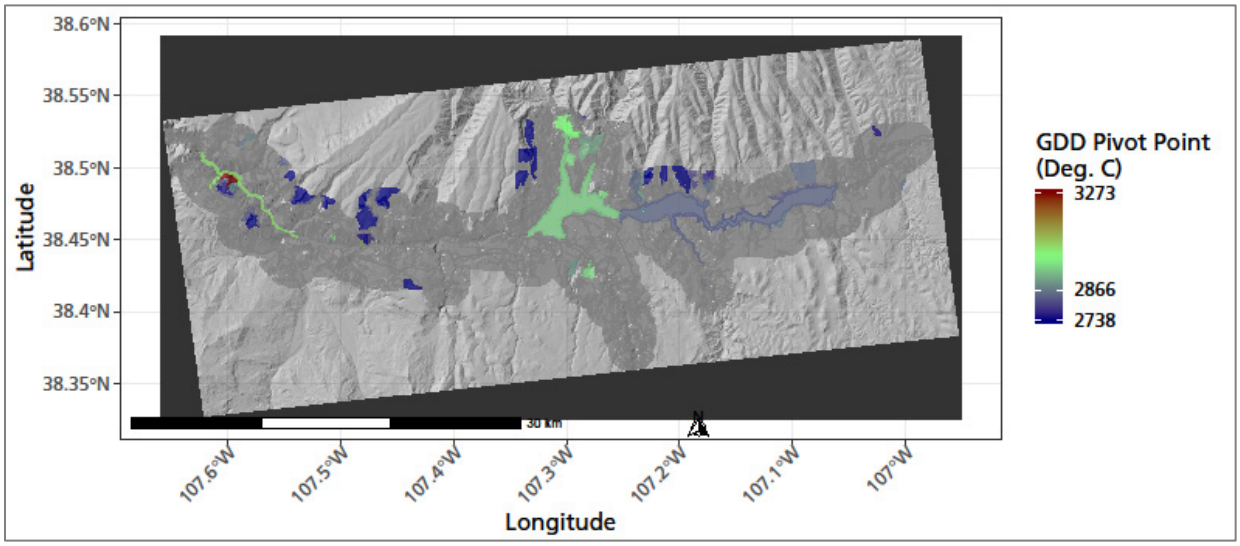

Figure 43. A map of Curecanti NRA showing the locations of polygons where growing degree days were significantly related to interannual variation in production (p-value < 0.05). Climate data summarized by water year. NPS / DAVID THOMA

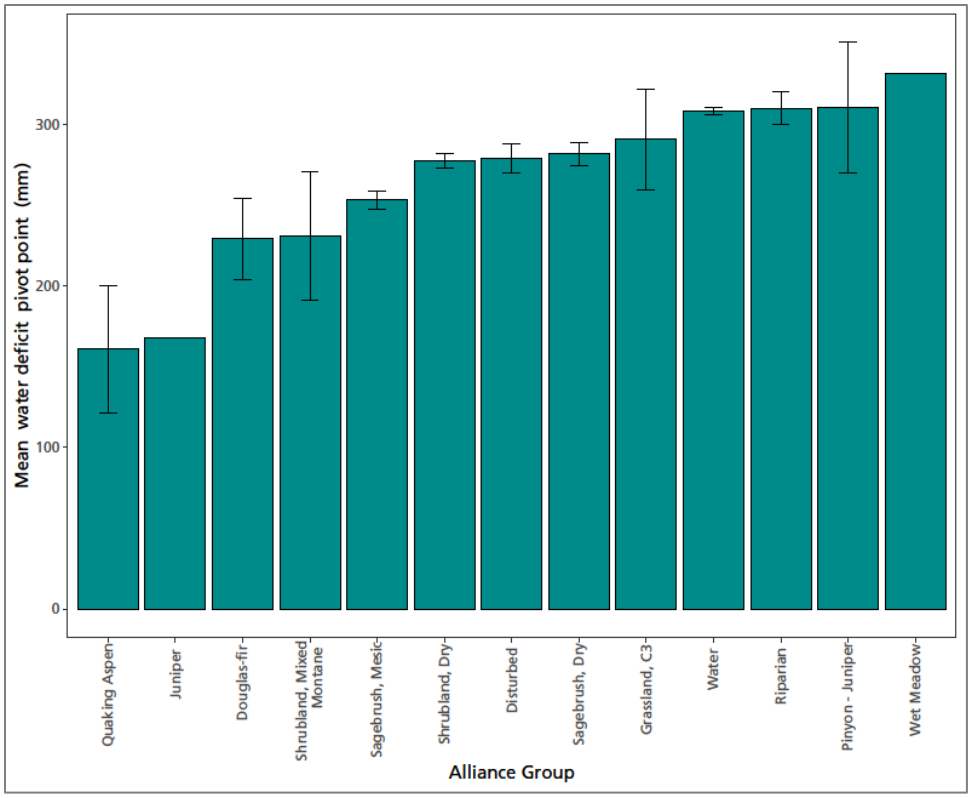

Figure 44. Pivot points for polygons in Curecanti NRA where water deficit was significantly related to interannual variation in production (p-value < 0.05). Climate data summarized by water year. NPS / DAVID THOMA

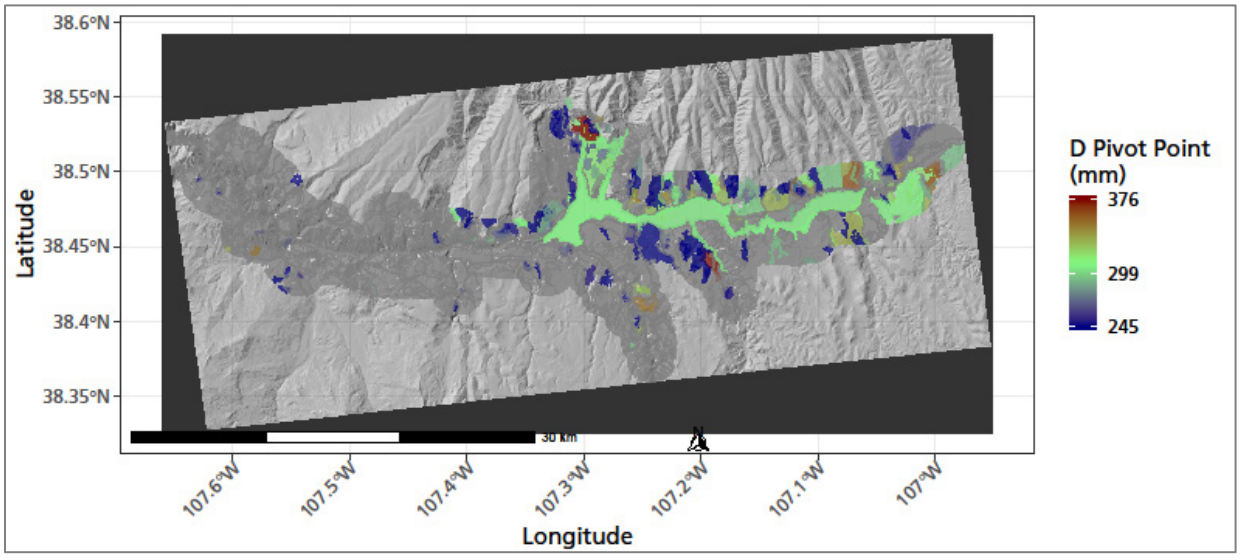

Figure 45. A map of Curecanti NRA showing the locations of polygons where water deficit was significantly related to interannual variation in production (p-value < 0.05). Climate data summarized by water year. NPS / DAVID THOMA

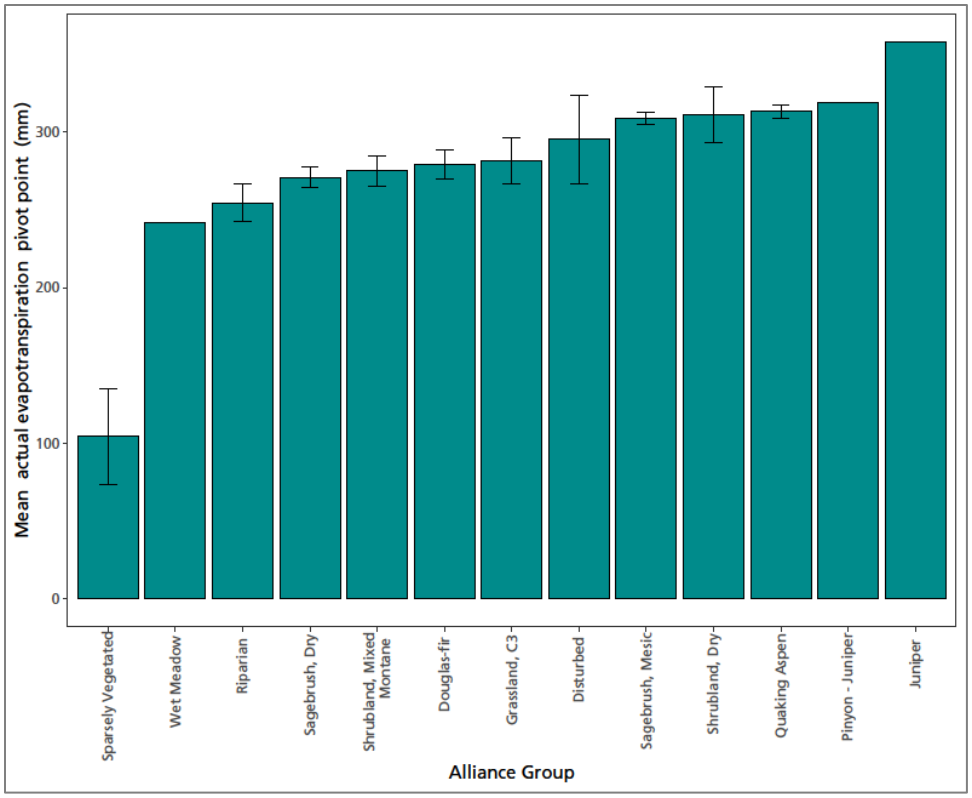

Figure 46. Pivot points for polygons in Curecanti NRA where actual evapotranspiration was significantly related to interannual variation in production (p-value < 0.05). Climate data summarized by water year. NPS / DAVID THOMA

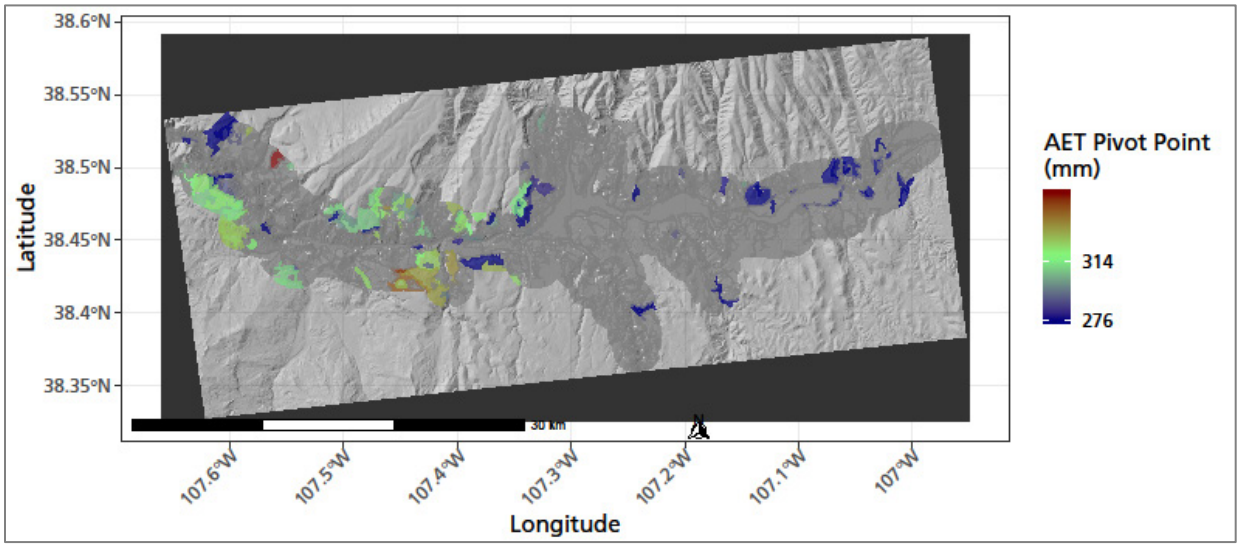

Figure 47. A map of Curecanti NRA showing the locations of polygons where actual evapotranspiration was significantly related to interannual variation in production (p-value < 0.05). Climate data summarized by water year. NPS / DAVID THOMA

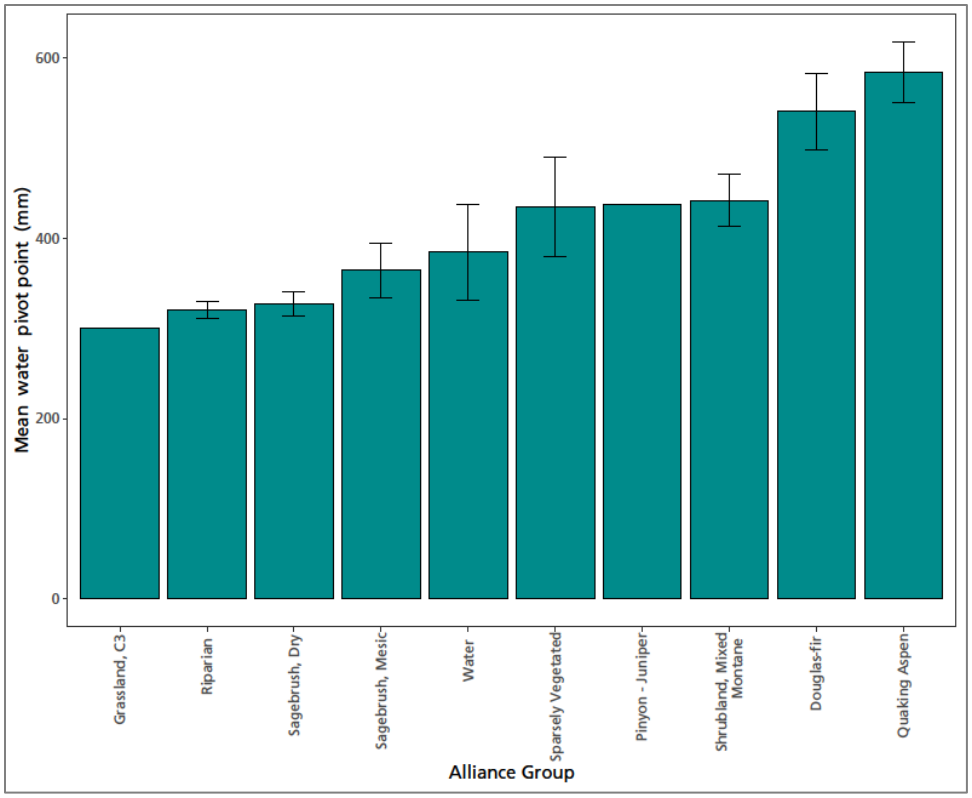

Figure 48. Pivot points for polygons in Curecanti NRA where water was significantly related to interannual variation in production (p-value < 0.05). Climate data summarized by water year. NPS / DAVID THOMA

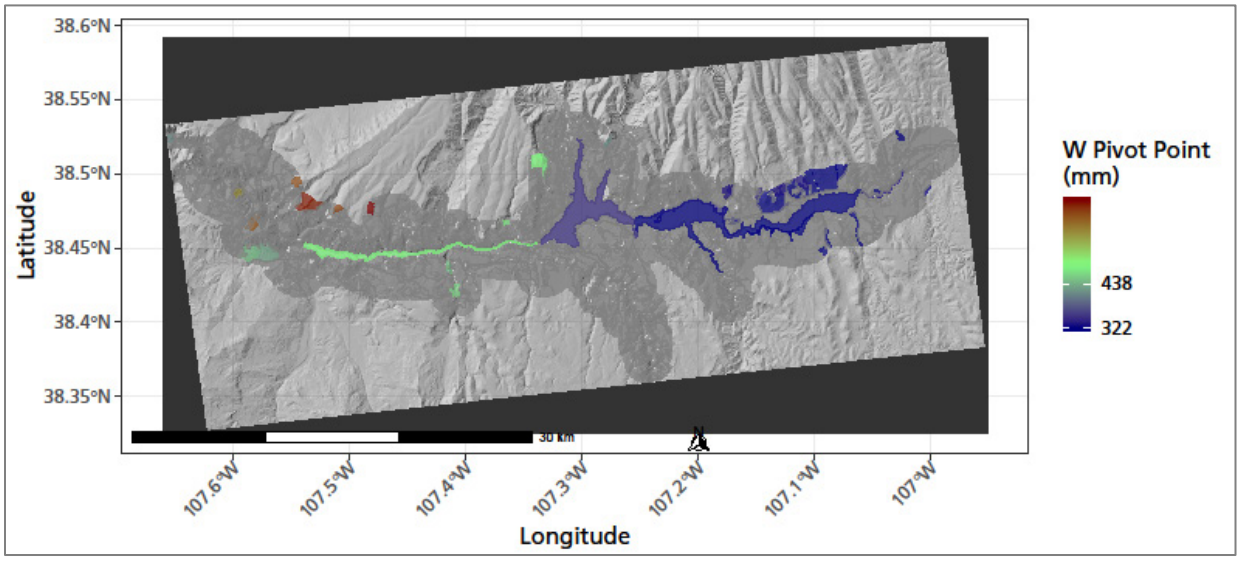

Figure 49. A map of Curecanti NRA showing the locations of polygons where water was significantly related to interannual variation in production (p-value < 0.05). Climate data summarized by water year. NPS / DAVID THOMA

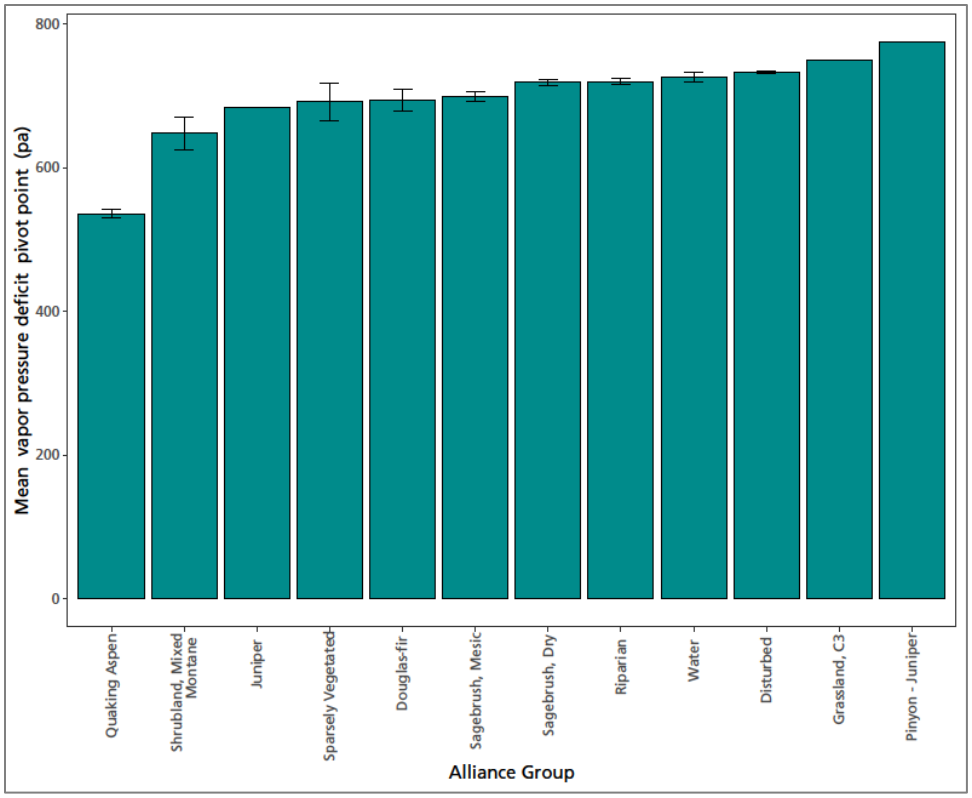

Figure 50. Pivot points for polygons in Curecanti NRA where vapor pressure deficit was significantly related to interannual variation in production (p-value < 0.05). Climate data summarized by water year. NPS / DAVID THOMA

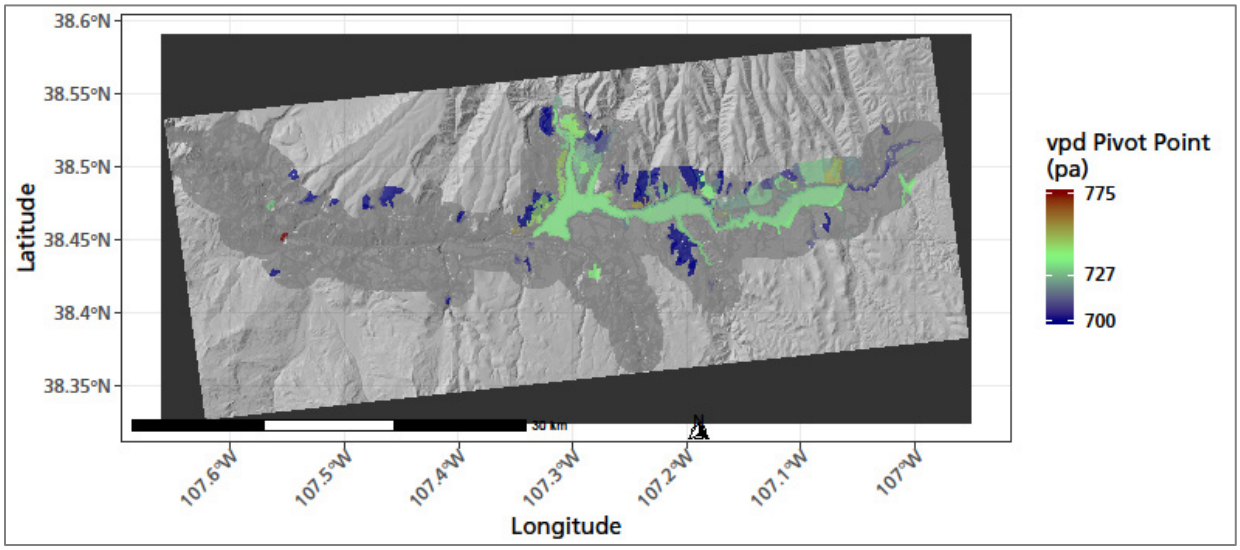

Figure 51. A map of Curecanti NRA showing the locations of polygons where vapor pressure deficit was significantly related to interannual variation in production (p-value < 0.05). Climate data summarized by water year. NPS / DAVID THOMA

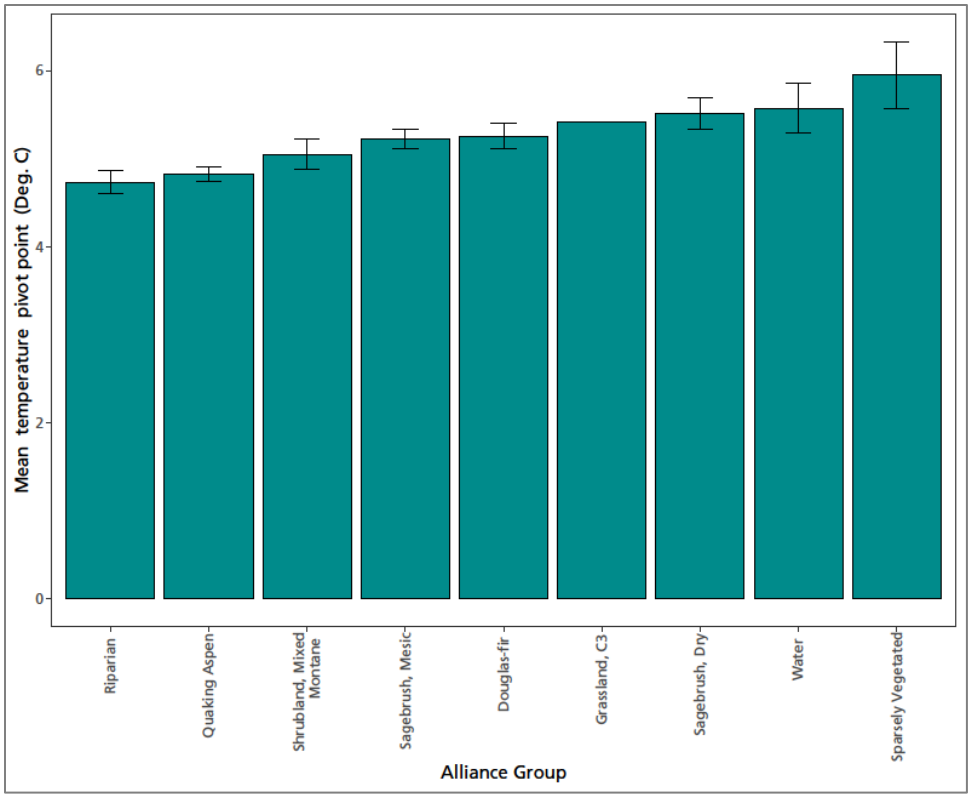

Figure 52. Pivot points for polygons in Curecanti NRA where temperature was significantly related to interannual variation in production (p-value < 0.05). Climate data summarized by water year. NPS / DAVID THOMA

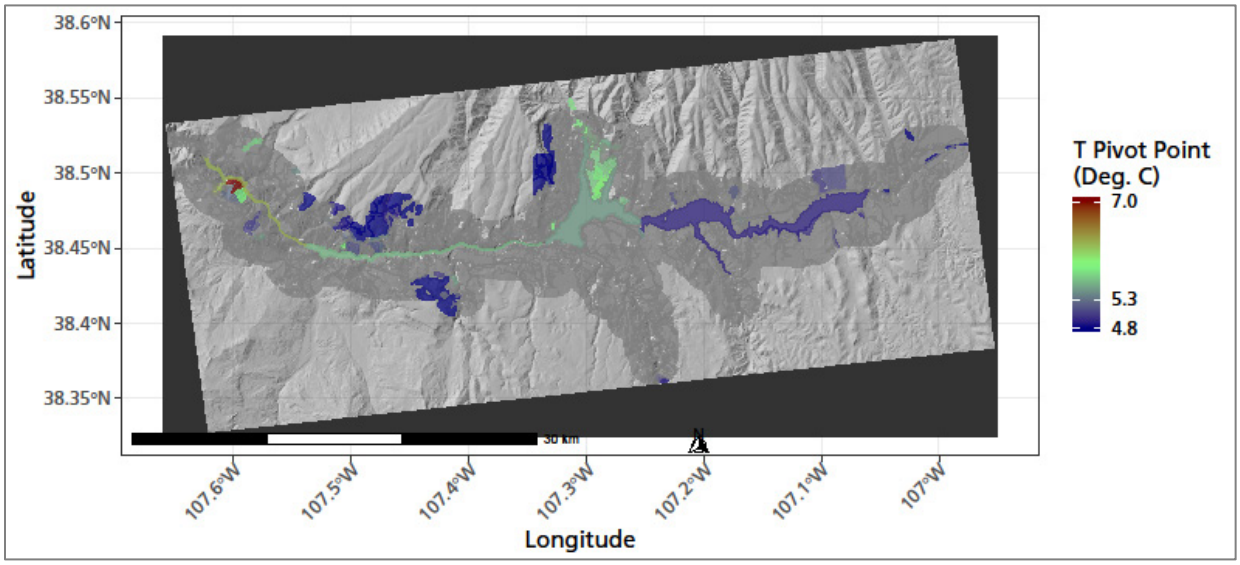

Figure 53. A map of Curecanti NRA showing the locations of polygons where temperature was significantly related to interannual variation in production (p-value < 0.05). Climate data summarized by water year. NPS / DAVID THOMA

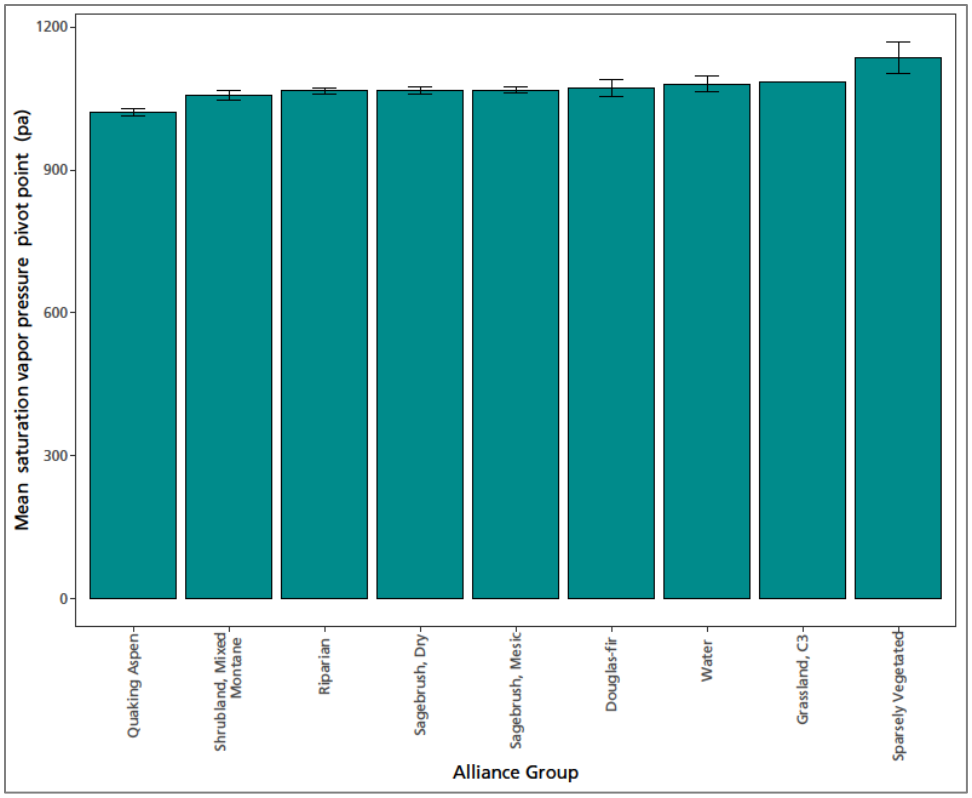

Figure 54. Pivot points for polygons in Curecanti NRA where saturation vapor pressure was significantly related to interannual variation in production (p-value < 0.05). Climate data summarized by water year. NPS / DAVID THOMA

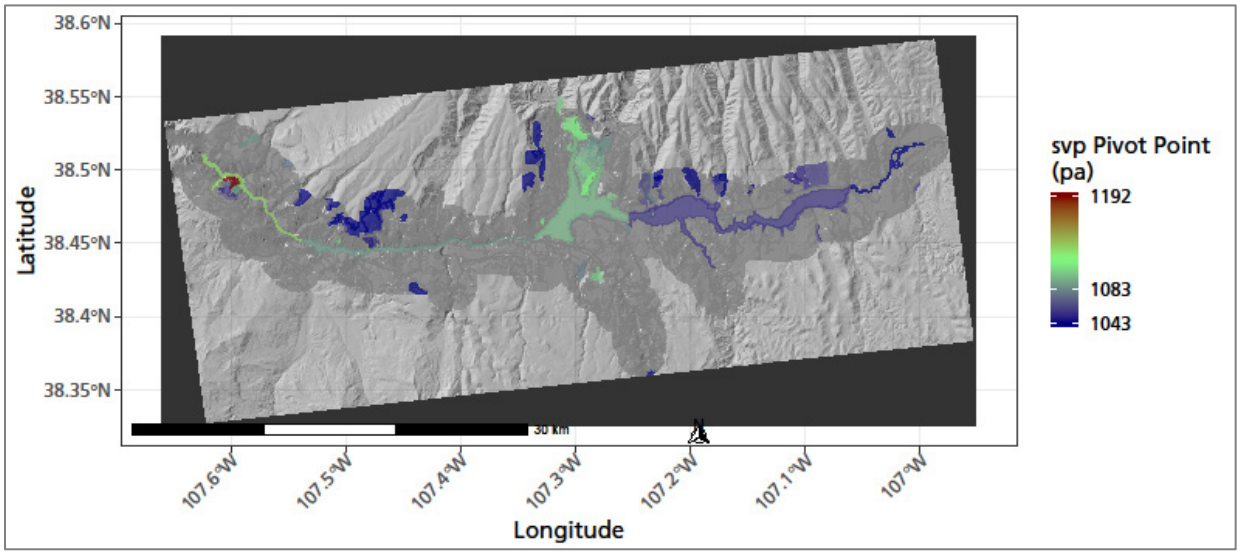

Figure 55. A map of Curecanti NRA showing the locations of polygons where saturation vapor pressure was significantly related to interannual variation in production (p-value < 0.05). Climate data summarized by water year. NPS / DAVID THOMA

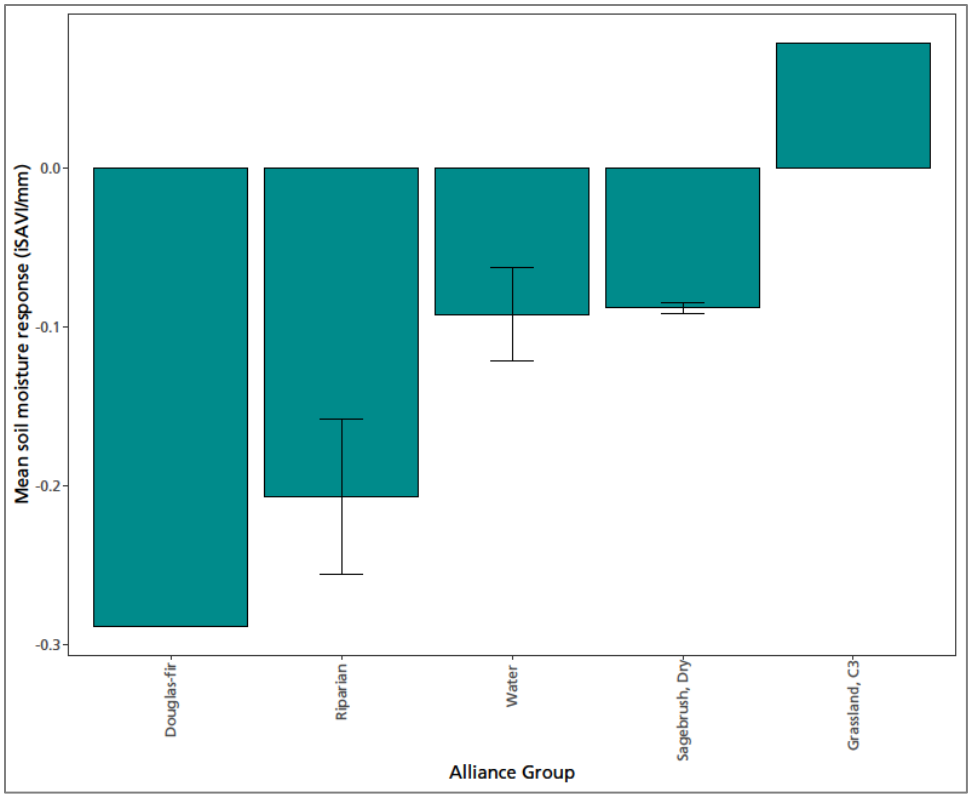

Figure 56. Sensitivity of growing season vegetation production to soil moisture in polygons at Curecanti NRA where the relationship was significant (p-value < 0.05). Climate data summarized by water year. NPS / DAVID THOMA

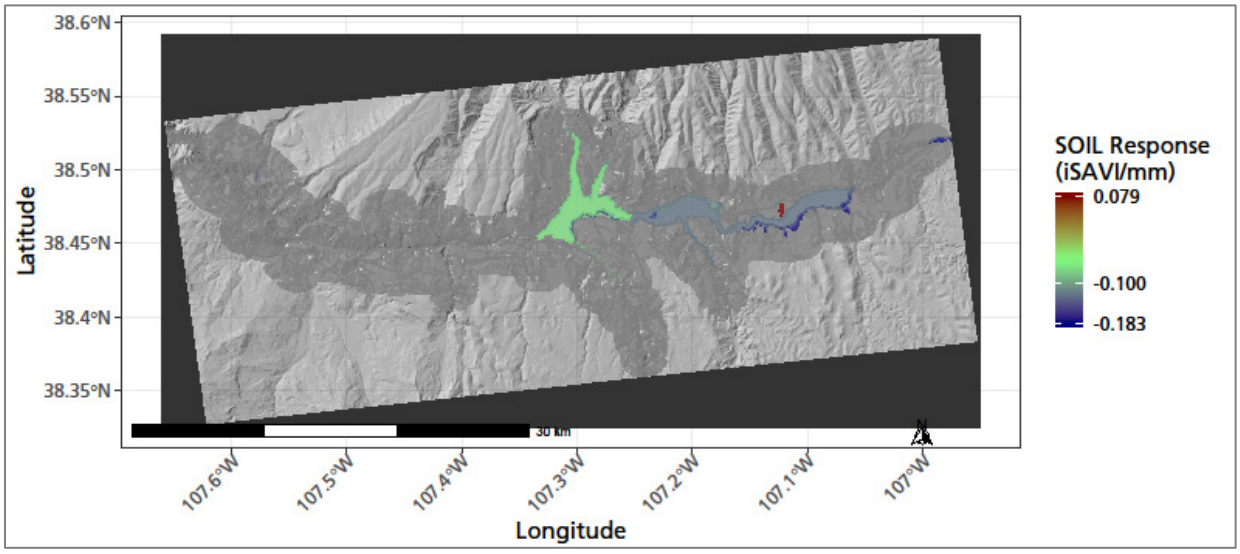

Figure 57. A map of Curecanti NRA showing the sensitivity of growing season vegetation production to soil moisture in polygons where the relationship was significant (p-value < 0.05). Climate data summarized by water year. NPS / DAVID THOMA

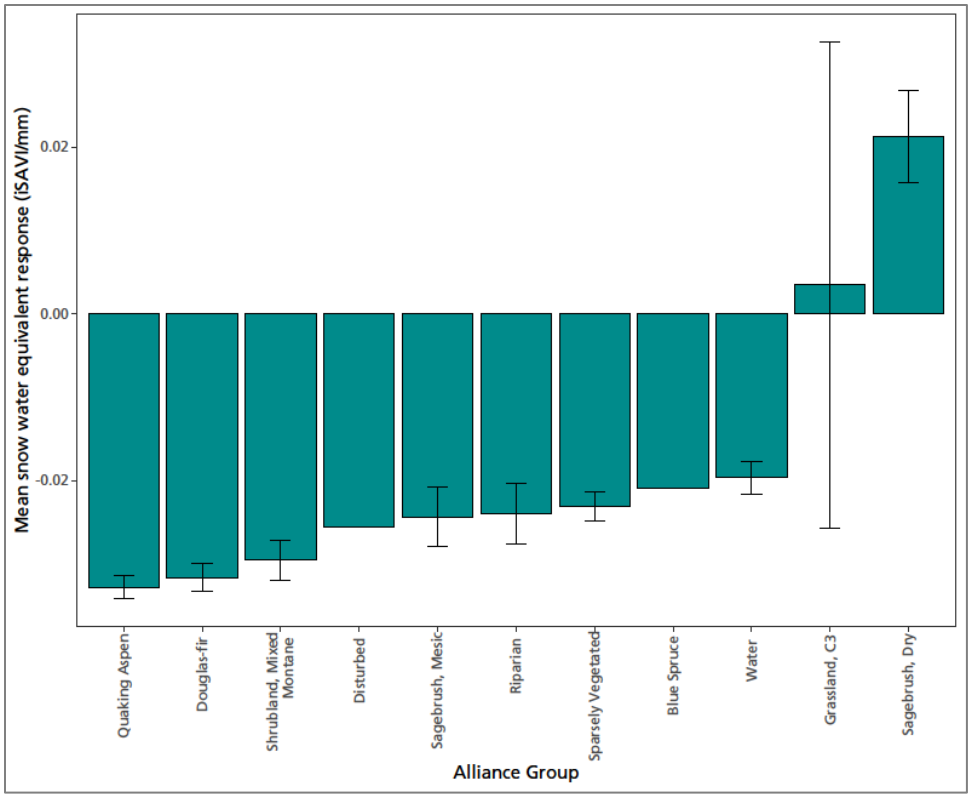

Figure 58. Sensitivity of growing season vegetation production to snow water equivalent in polygons at Curecanti NRA where the relationship was significant (p-value < 0.05). Climate data summarized by water year. NPS / DAVID THOMA

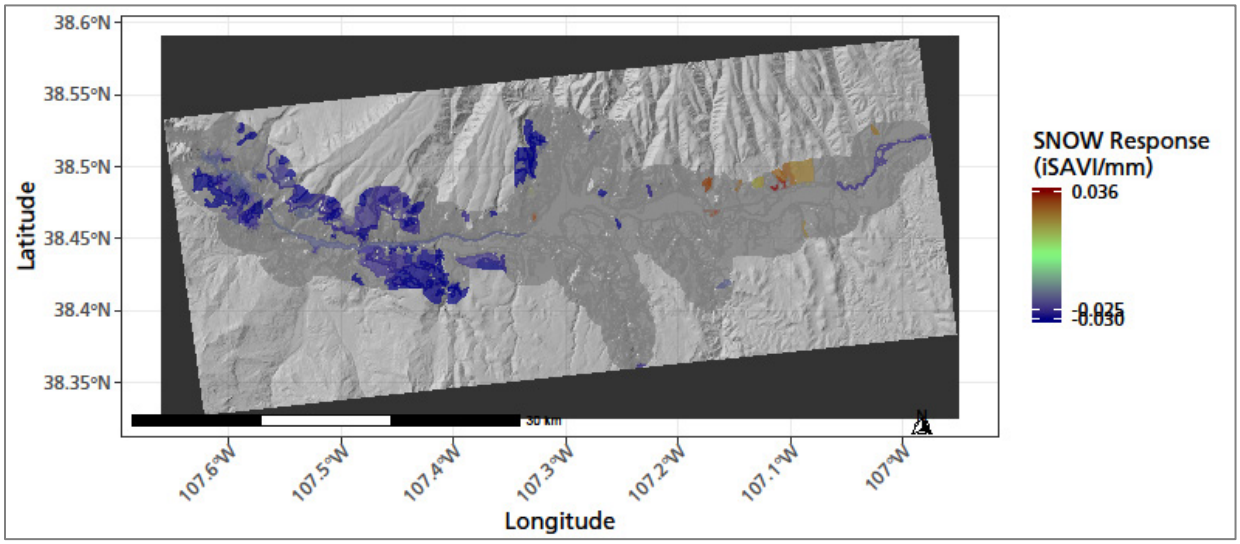

Figure 59. A map of Curecanti NRA showing the sensitivity of growing season vegetation production to snow water equivalent in polygons where the relationship was significant (p-value < 0.05). Climate data summarized by water year. NPS / DAVID THOMA

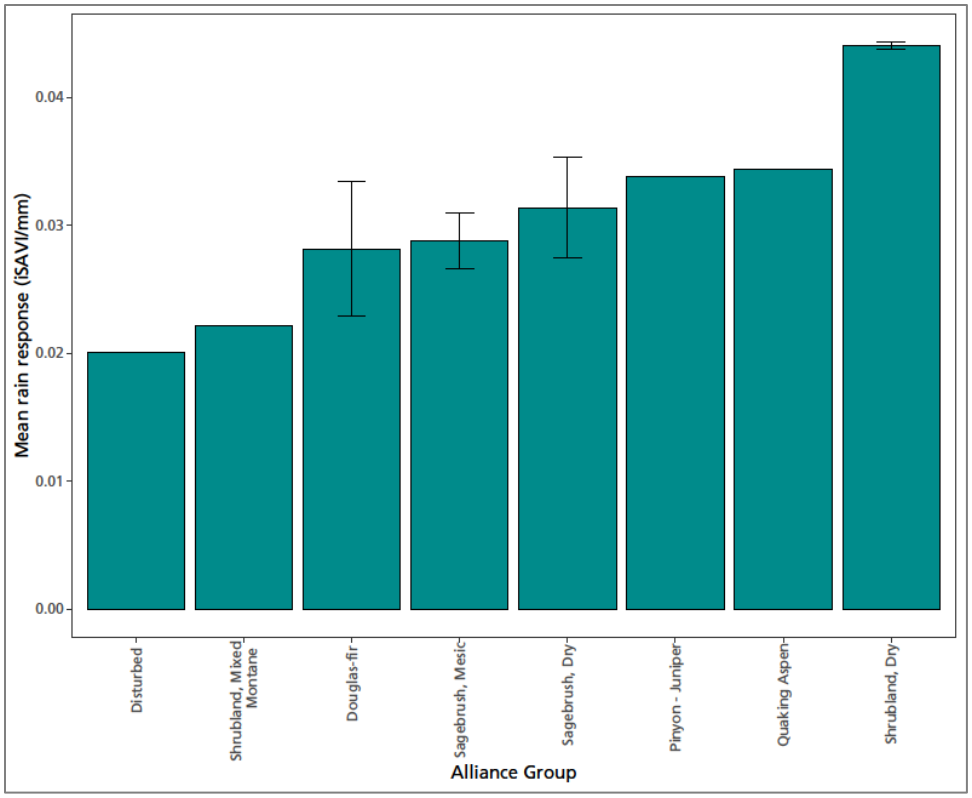

Figure 60. Sensitivity of growing season vegetation production to rain in polygons at Curecanti NRA where the relationship was significant (p-value < 0.05). Climate data summarized by water year. NPS / DAVID THOMA

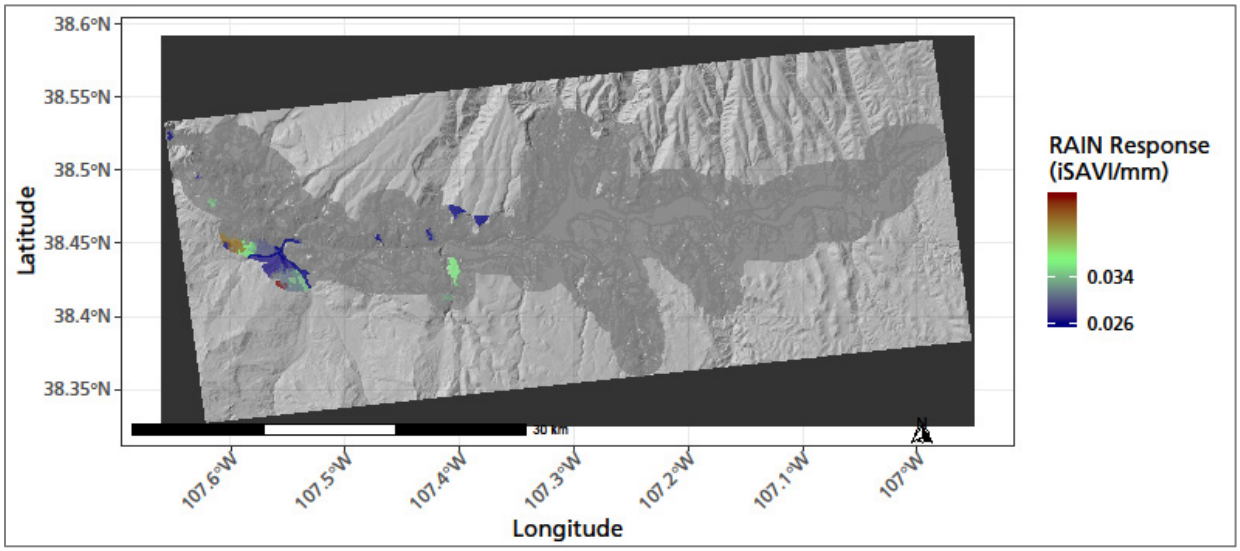

Figure 61. A map of Curecanti NRA showing the sensitivity of growing season vegetation production to rain in polygons where the relationship was significant (p-value < 0.05). Climate data summarized by water year. NPS / DAVID THOMA

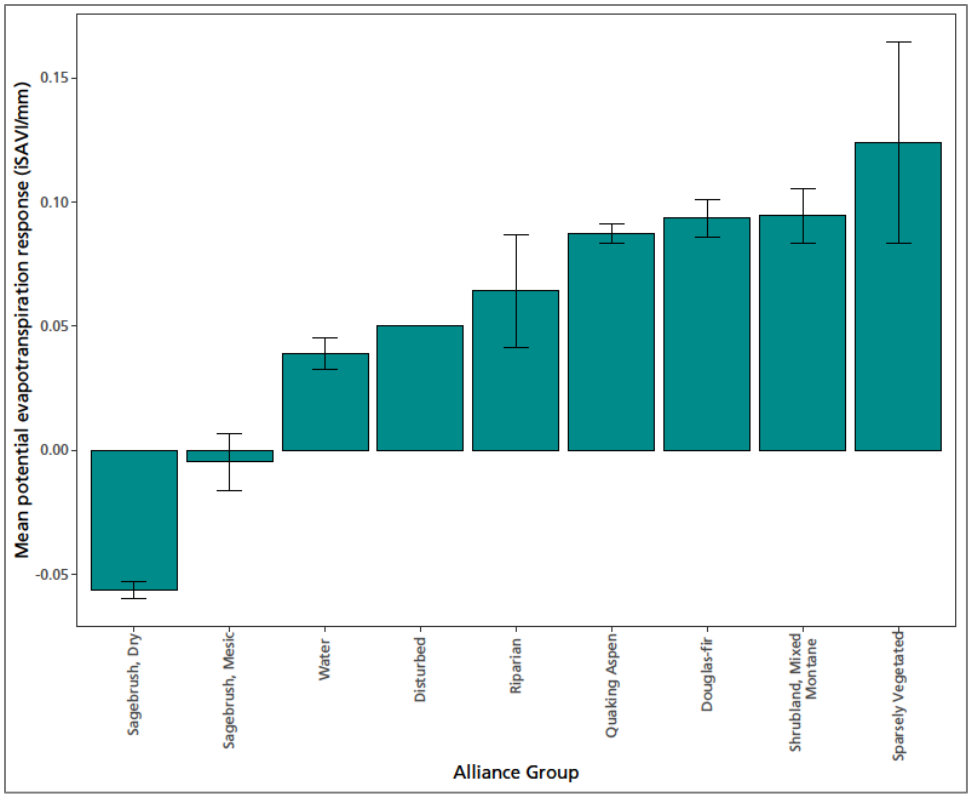

Figure 62. Sensitivity of growing season vegetation production to potential evapotranspiration in polygons at Curecanti NRA where the relationship was significant (p-value < 0.05). Climate data summarized by water year. NPS / DAVID THOMA

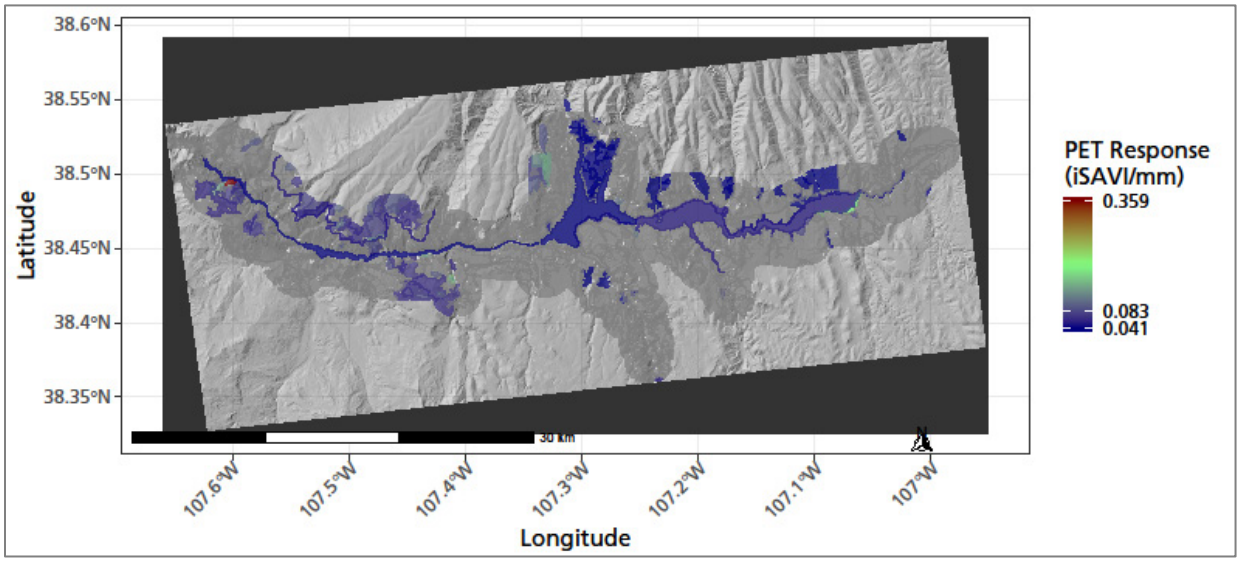

Figure 63. A map of Curecanti NRA showing the sensitivity of growing season vegetation production to potential evapotranspiration in polygons where the relationship was significant (p-value < 0.05). Climate data summarized by water year. NPS / DAVID THOMA

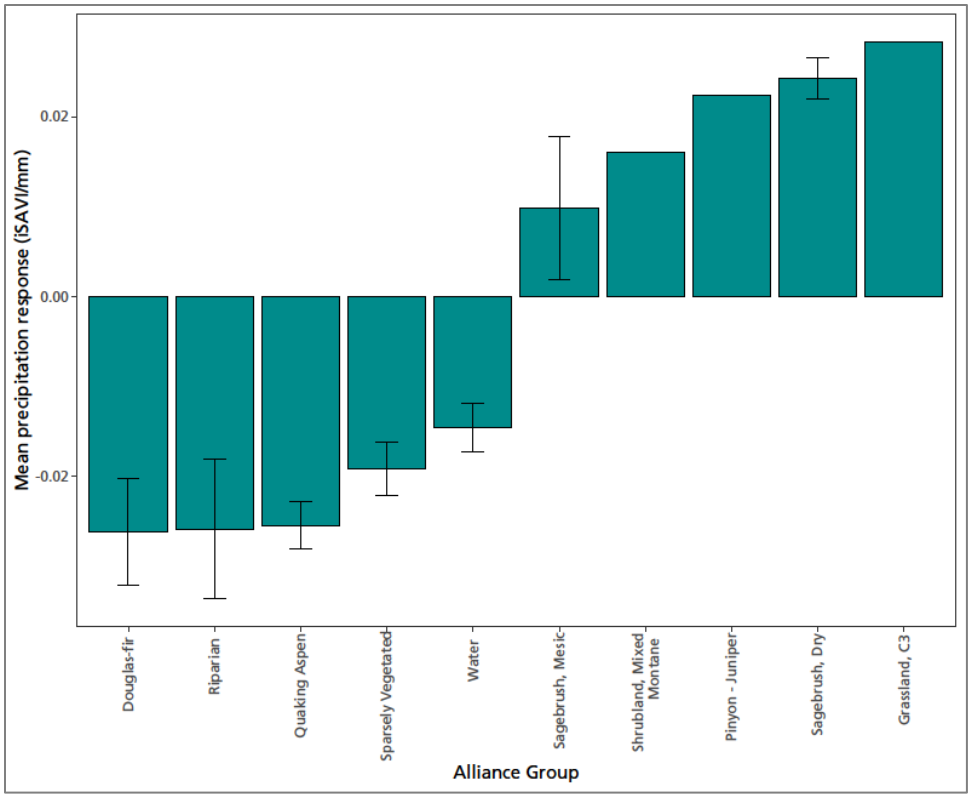

Figure 64. Sensitivity of growing season vegetation production to precipitation in polygons at Curecanti NRA where the relationship was significant (p-value < 0.05). Climate data summarized by water year. NPS / DAVID THOMA

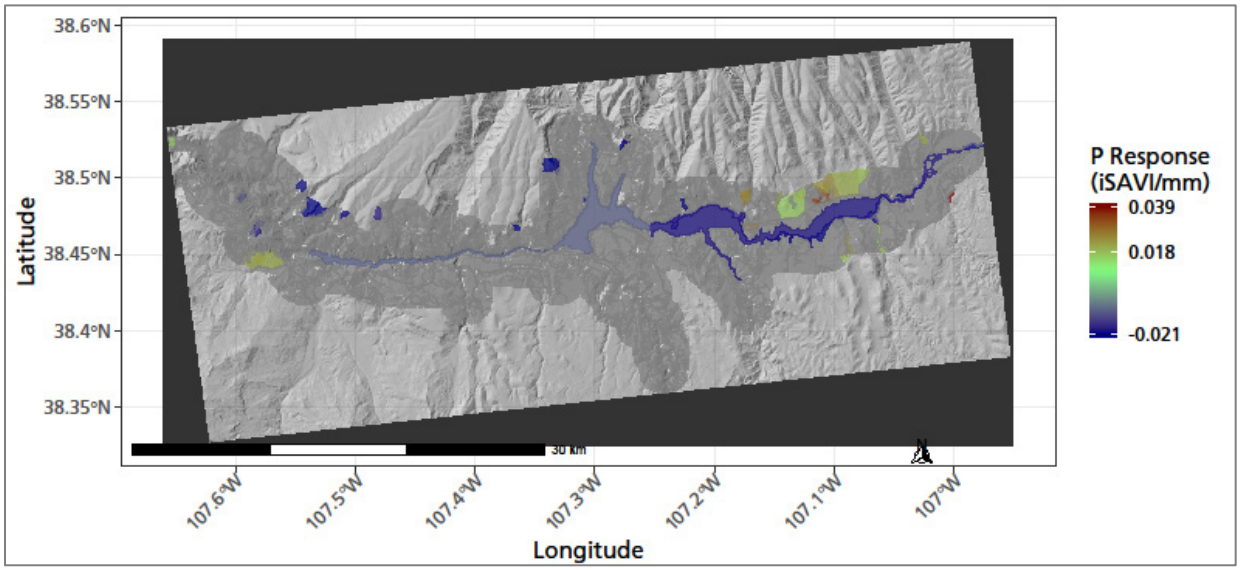

Figure 65. A map of Curecanti NRA showing the sensitivity of growing season vegetation production to precipitation in polygons where the relationship was significant (p-value < 0.05). Climate data summarized by water year. NPS / DAVID THOMA

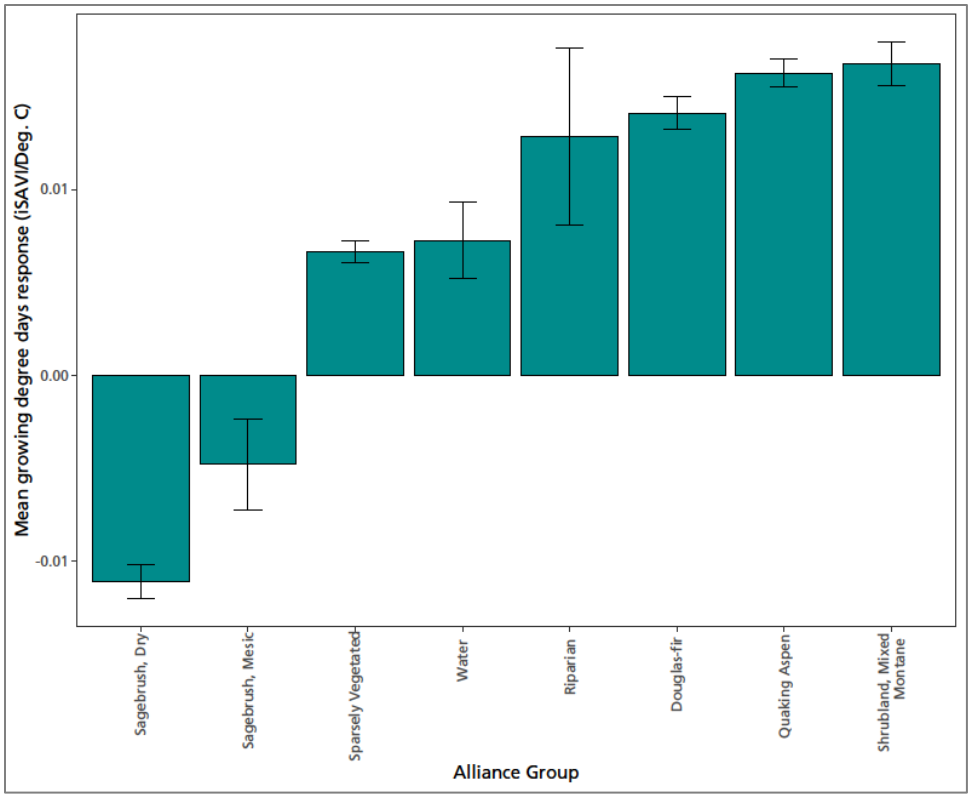

Figure 66. Sensitivity of growing season vegetation production to growing degree days in polygons at Curecanti NRA where the relationship was significant (p-value < 0.05). Climate data summarized by water year. NPS / DAVID THOMA

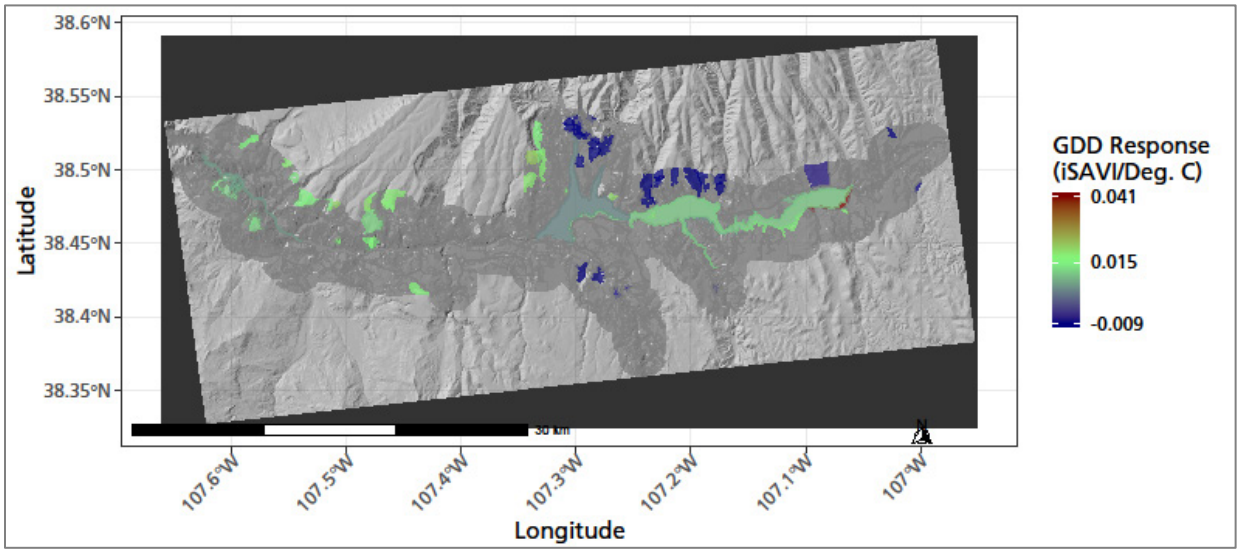

Figure 67. A map of Curecanti NRA showing the sensitivity of growing season vegetation production to growing degree days in polygons where the relationship was significant (p-value < 0.05). Climate data summarized by water year. NPS / DAVID THOMA

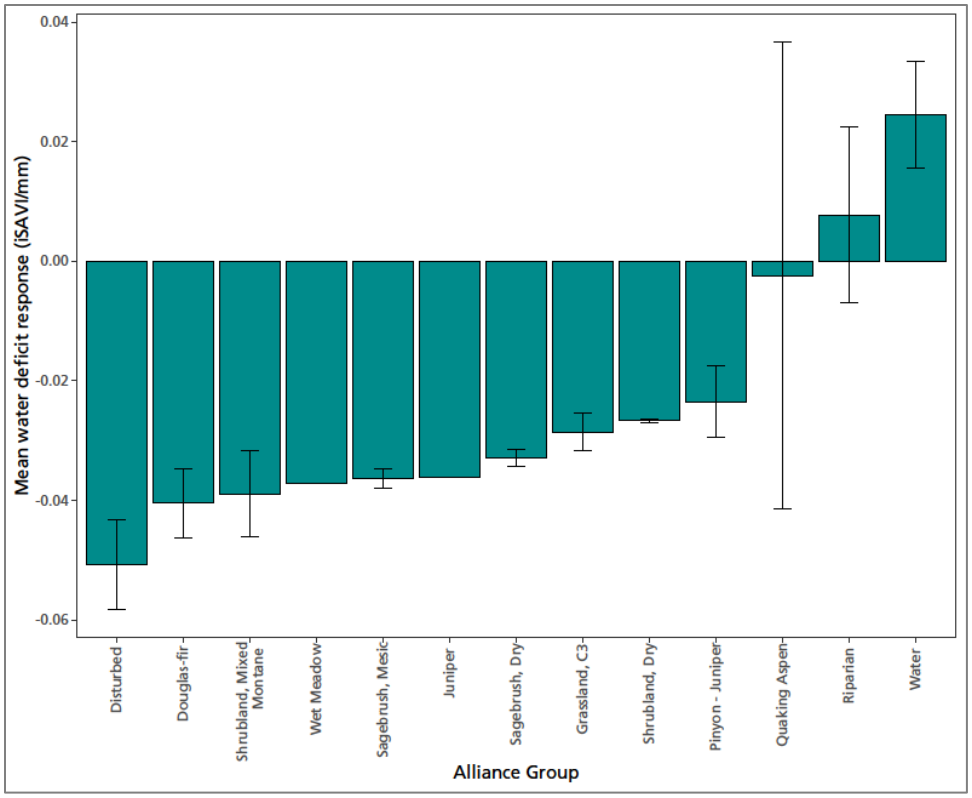

Figure 68. Sensitivity of growing season vegetation production to water deficit in polygons at Curecanti NRA where the relationship was significant (p-value < 0.05). Climate data summarized by water year. NPS / DAVID THOMA

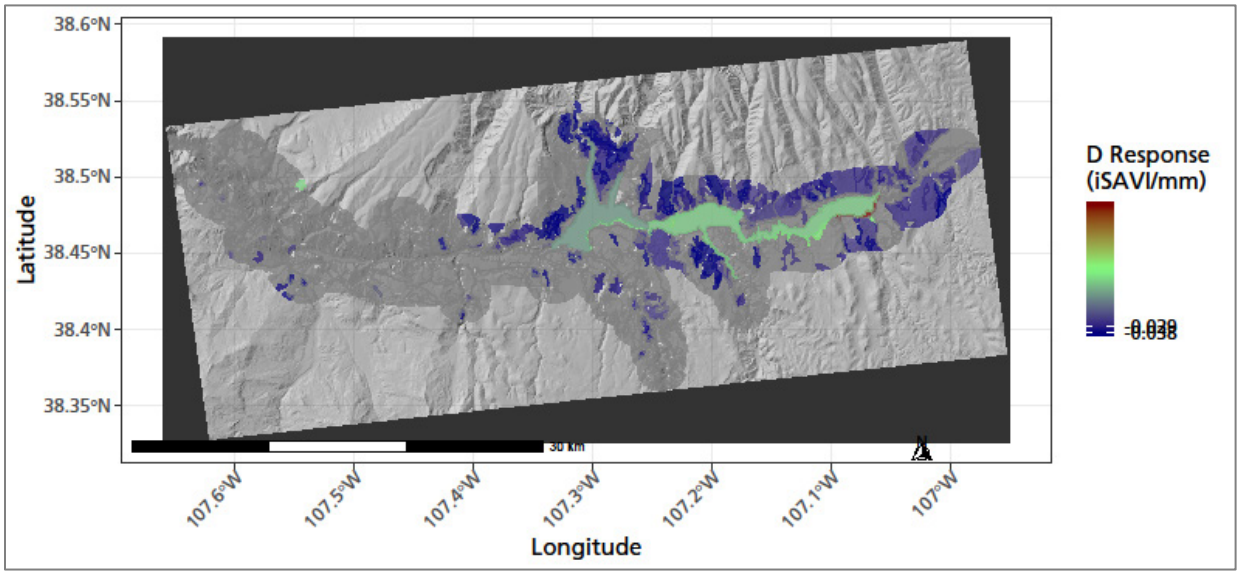

Figure 69. A map of Curecanti NRA showing the sensitivity of growing season vegetation production to water deficit in polygons where the relationship was significant (p-value < 0.05). Climate data summarized by water year. NPS / DAVID THOMA

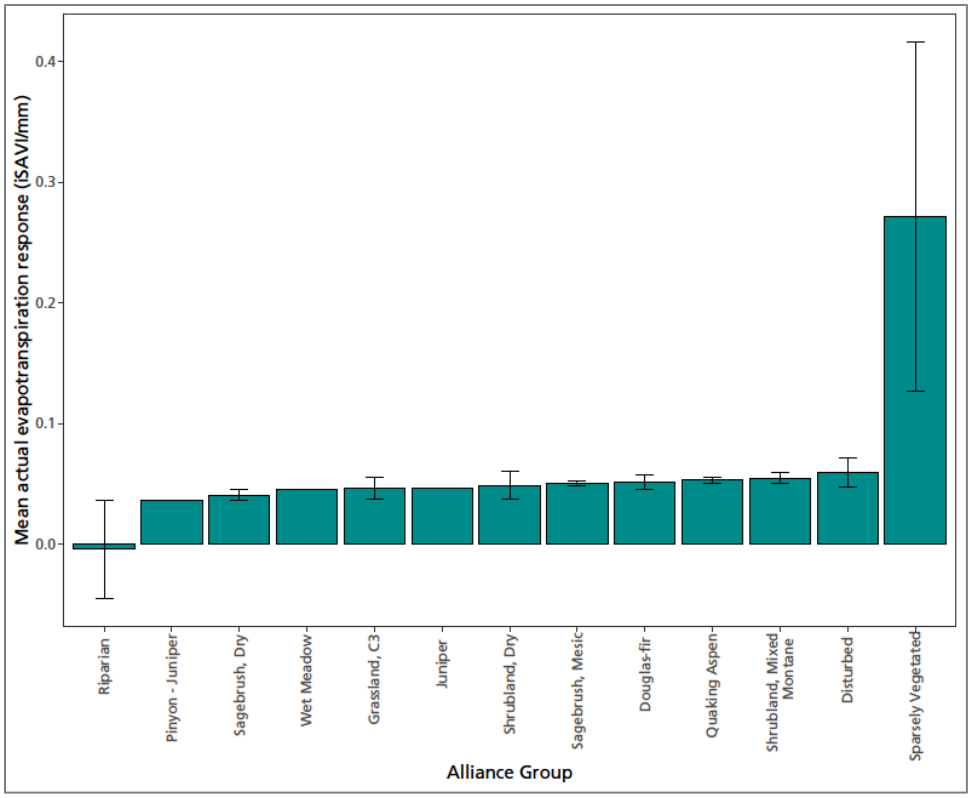

Figure 70. Sensitivity of growing season vegetation production to actual evapotranspiration in polygons at Curecanti NRA where the relationship was significant (p-value < 0.05). Climate data summarized by water year. NPS / DAVID THOMA

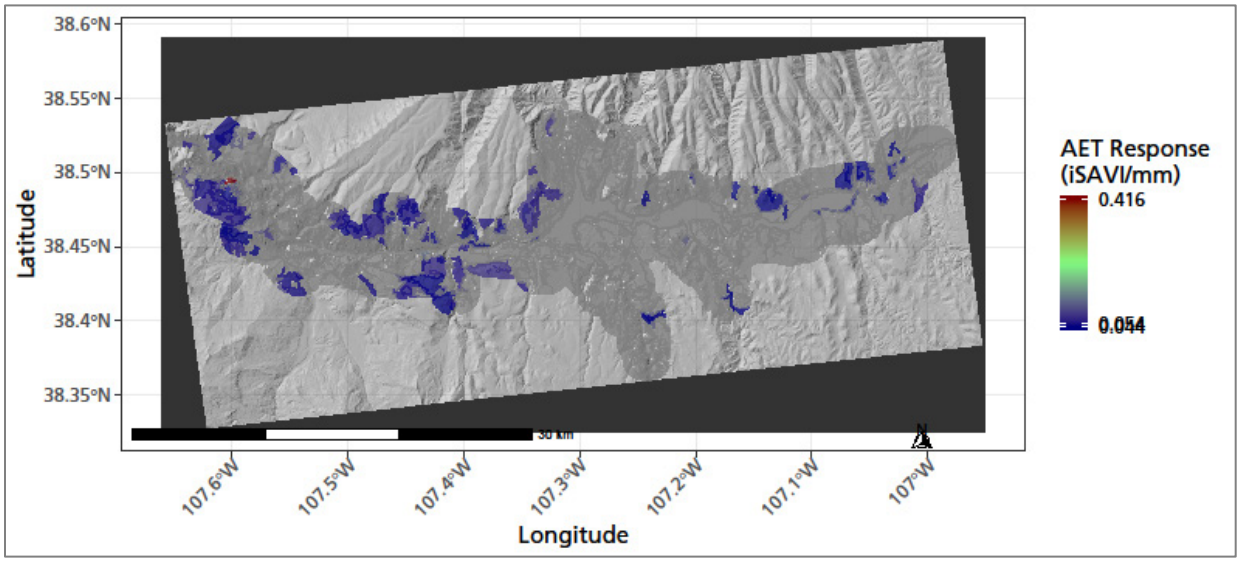

Figure 71. A map of Curecanti NRA showing the sensitivity of growing season vegetation production to actual evapotranspiration in polygons where the relationship was significant (p-value < 0.05). Climate data summarized by water year. NPS / DAVID THOMA

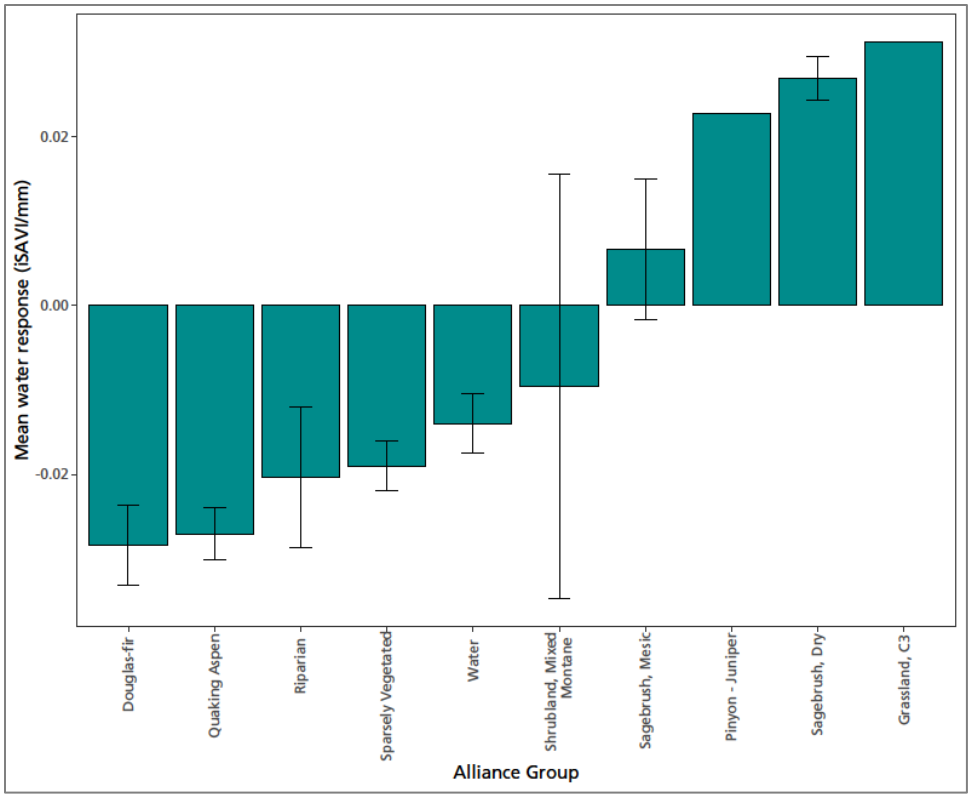

Figure 72. Sensitivity of growing season vegetation production to water in polygons at Curecanti NRA where the relationship was significant (p-value < 0.05). Climate data summarized by water year. NPS / DAVID THOMA

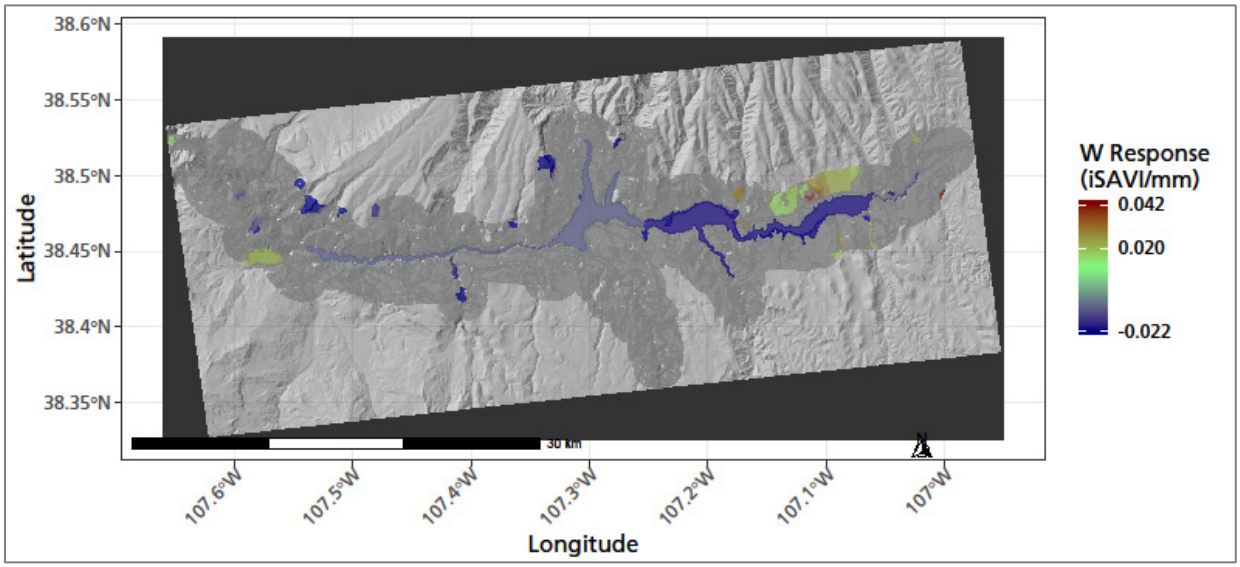

Figure 73. A map of Curecanti NRA showing the sensitivity of growing season vegetation production to water in polygons where the relationship was significant (p-value < 0.05). Climate data summarized by water year. NPS / DAVID THOMA

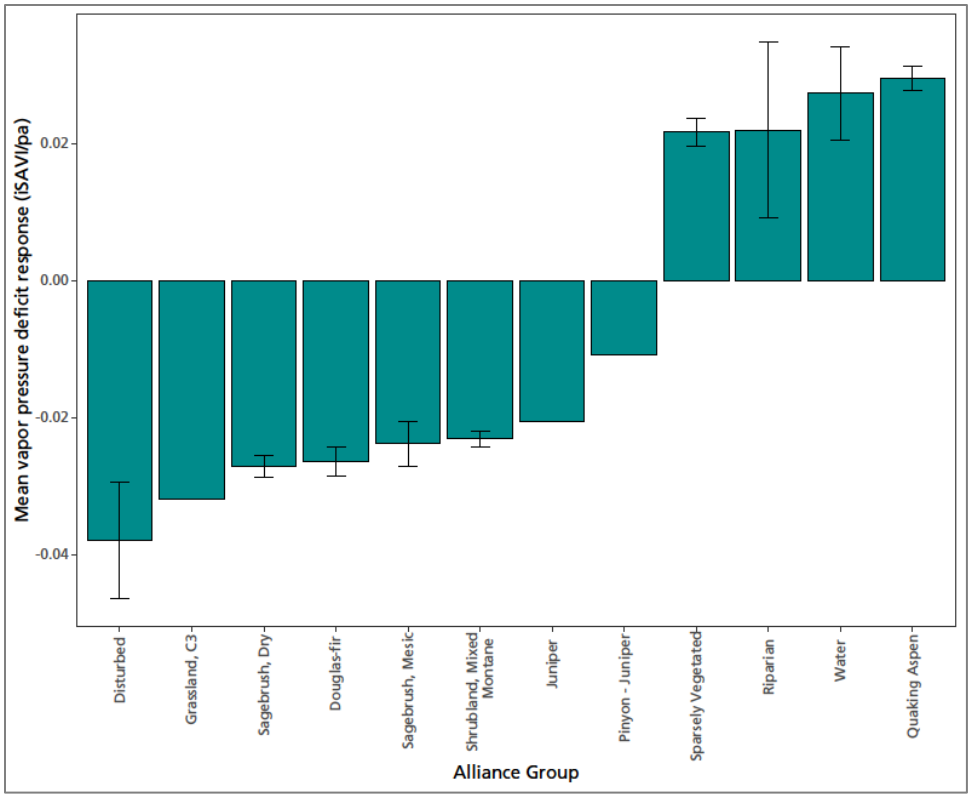

Figure 74. Sensitivity of growing season vegetation production to vapor pressure deficit in polygons at Curecanti NRA where the relationship was significant (p-value < 0.05). Climate data summarized by water year. NPS / DAVID THOMA

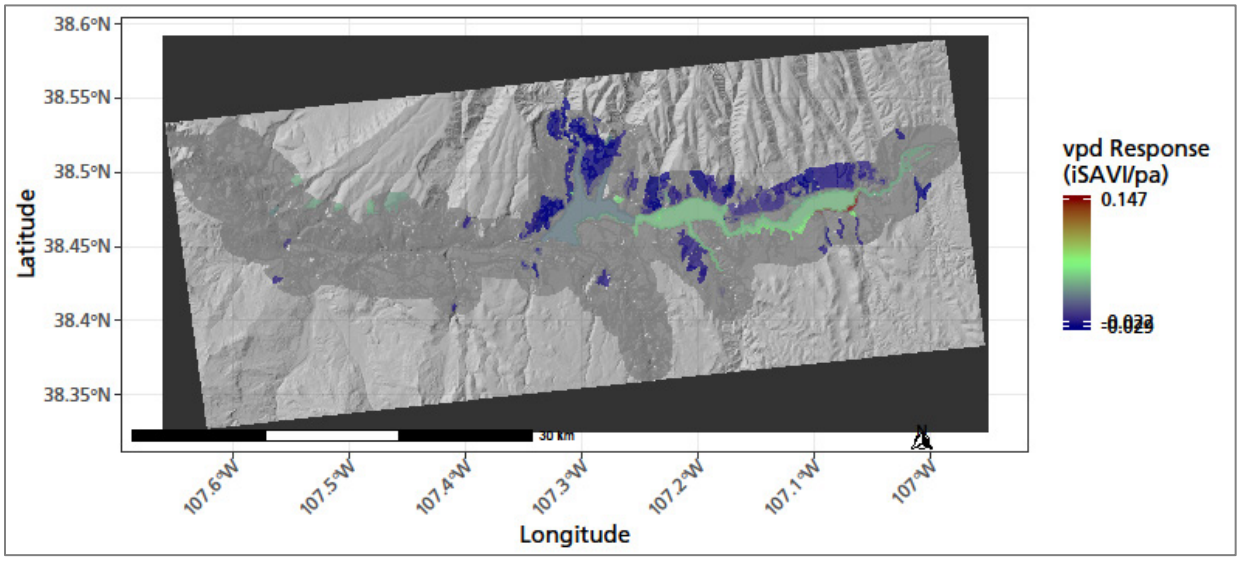

Figure 75. A map of Curecanti NRA showing the sensitivity of growing season vegetation production to vapor pressure deficit in polygons where the relationship was significant (p-value < 0.05). Climate data summarized by water year. NPS / DAVID THOMA

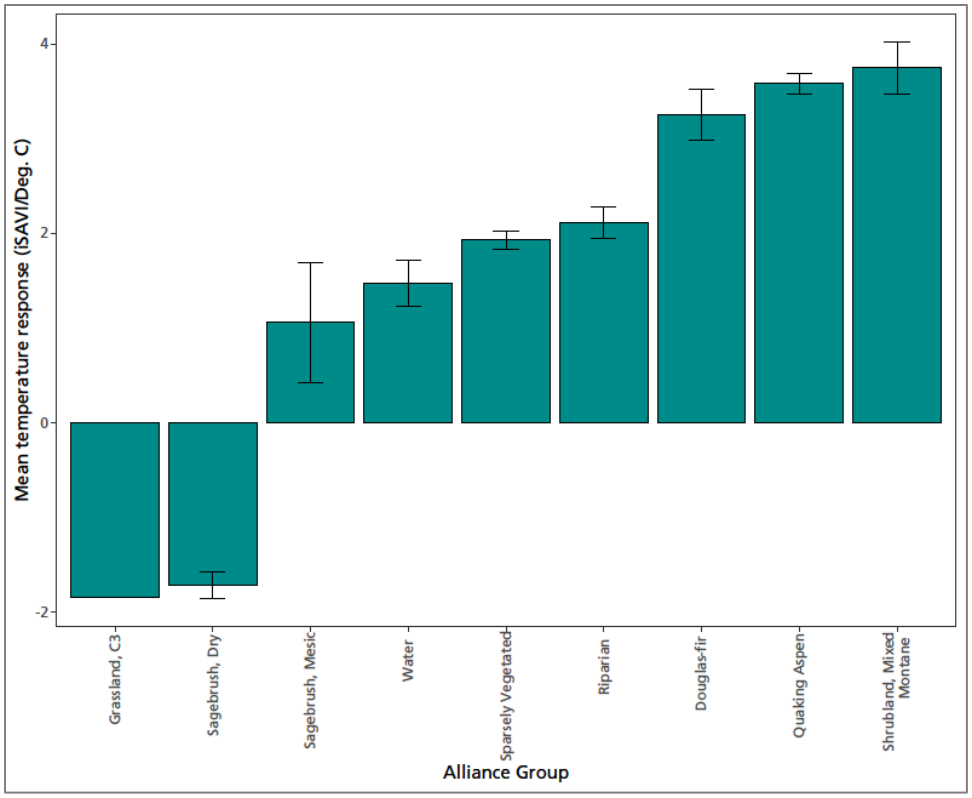

Figure 76. Sensitivity of growing season vegetation production to temperature in polygons at Curecanti NRA where the relationship was significant (p-value < 0.05). Climate data summarized by water year. NPS / DAVID THOMA

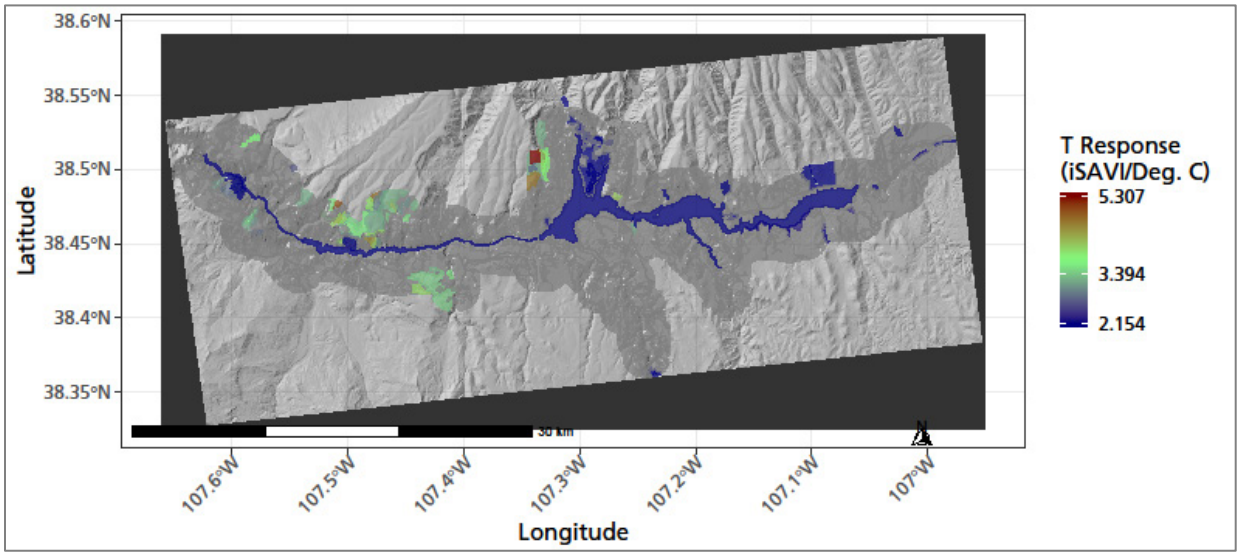

Figure 77. A map of Curecanti NRA showing the sensitivity of growing season vegetation production to temperature in polygons where the relationship was significant (p-value < 0.05). Climate data summarized by water year. NPS / DAVID THOMA

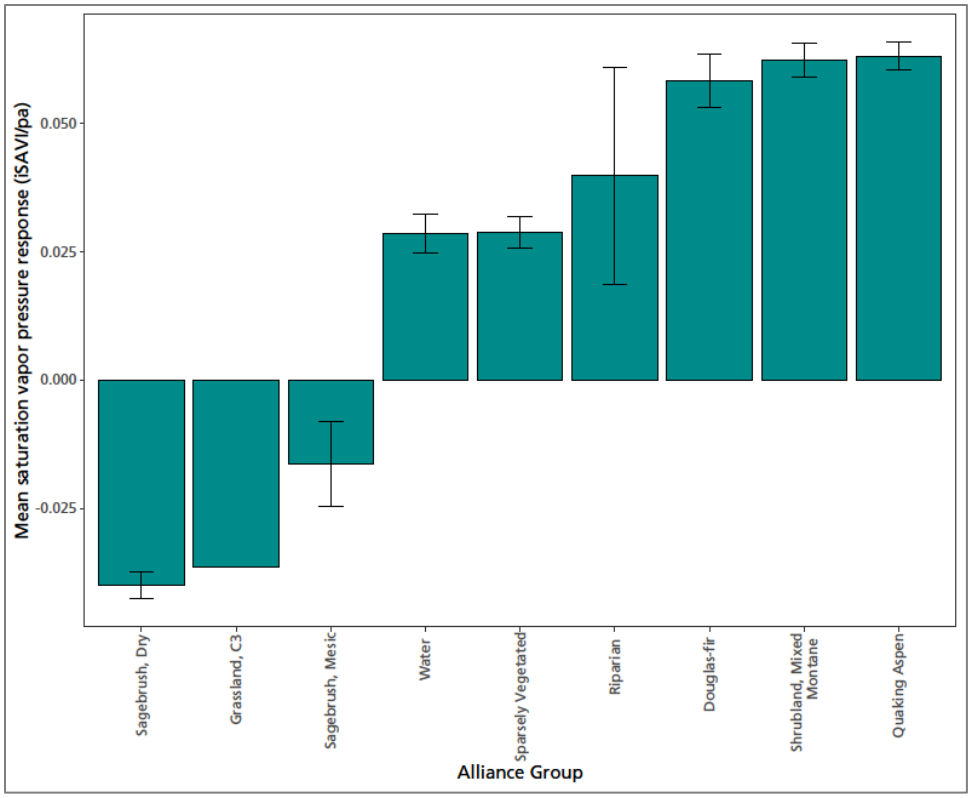

Figure 78. Sensitivity of growing season vegetation production to saturation vapor pressure in polygons at Curecanti NRA where the relationship was significant (p-value < 0.05). Climate data summarized by water year. NPS / DAVID THOMA

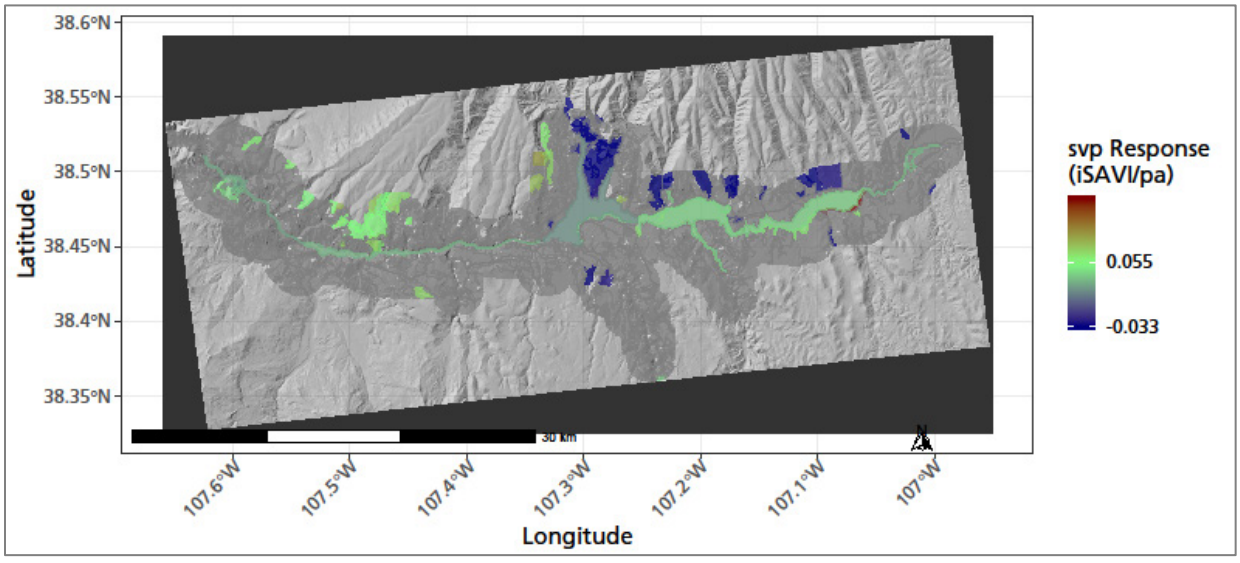

Figure 79. A map of Curecanti NRA showing the sensitivity of growing season vegetation production to saturation vapor pressure in polygons where the relationship was significant (p-value < 0.05). Climate data summarized by water year. NPS / DAVID THOMA

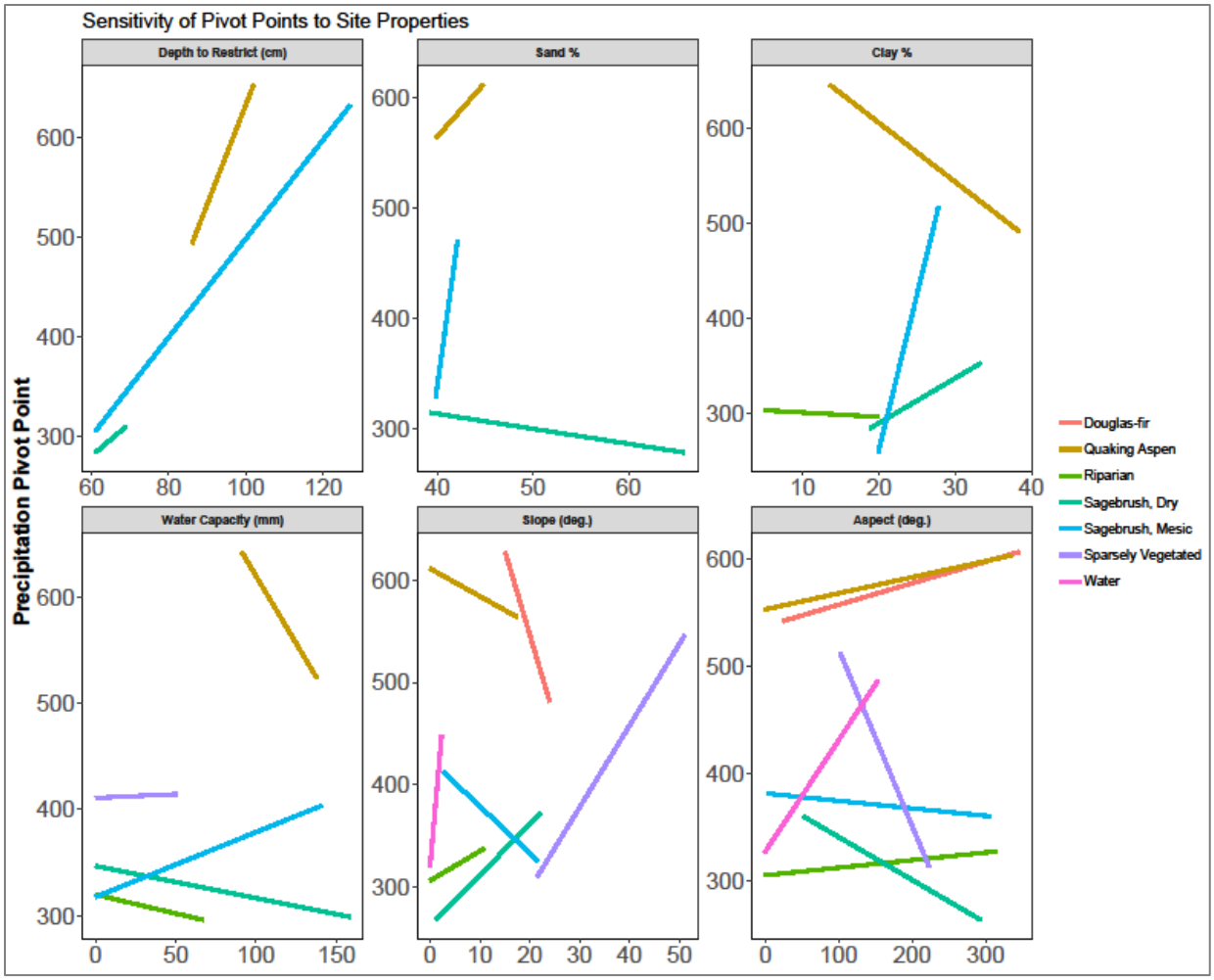

Figure 80. Variation in precipitation pivot points as related to soil and site characteristics. Steeper slopes indicate greater sensitivity of pivot points to site properties. These site properties are important modifiers of climate because they control water retention and distribution in the soil profile and, in the case of site slope and aspect, because they affect the heat load on vegetation. NPS / DAVID THOMA

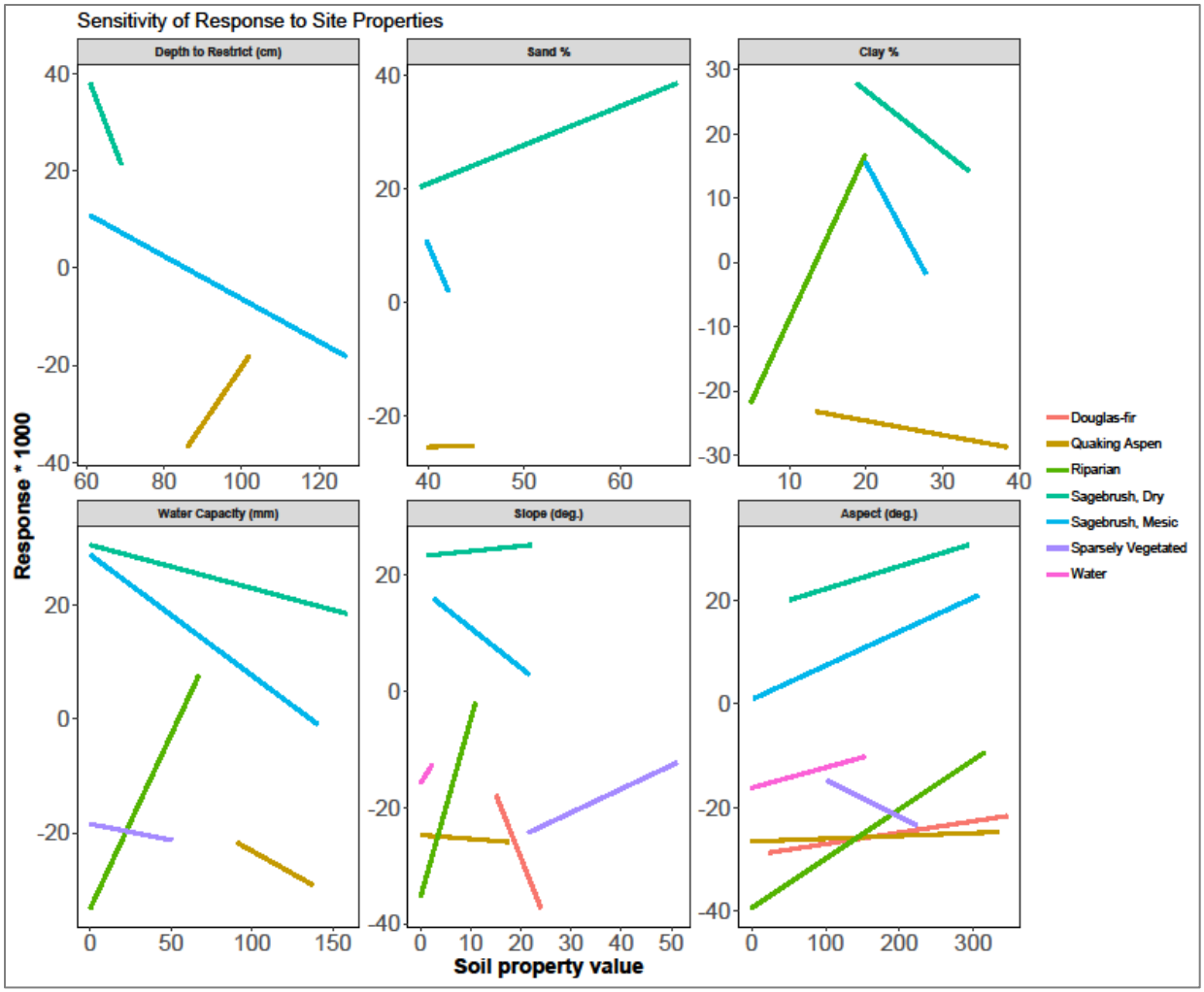

Figure 81. Variation in responses to precipitation as related to soil and site characteristics. Steeper slopes indicate greater sensitivity of responses to site properties. These site properties are important modifiers of climate because they control water retention and distribution in the soil profile and, in the case of site slope and aspect, because they affect the heat load on vegetation. NPS / DAVID THOMA

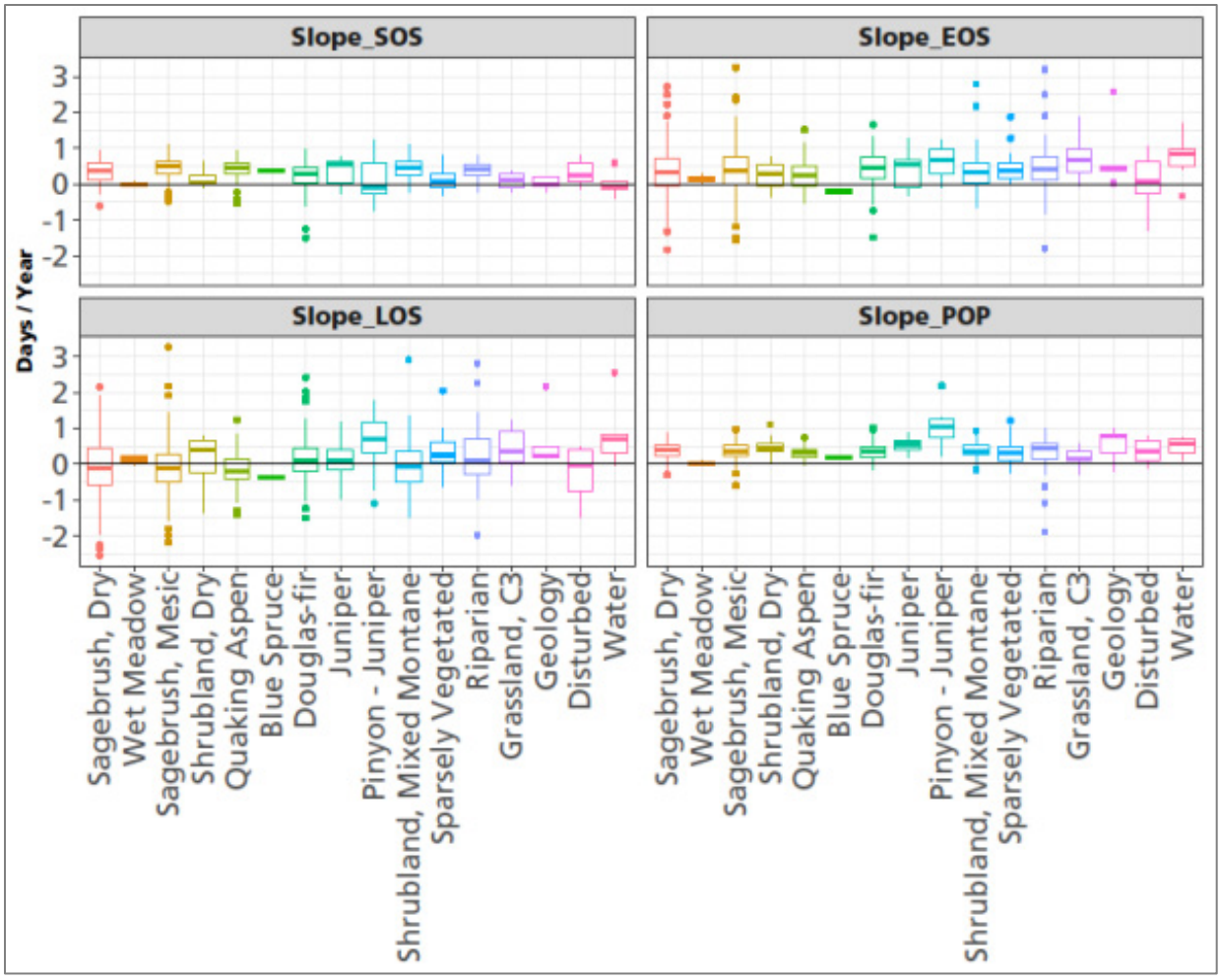

Figure 82. Direction and magnitude of change rate in land surface phenology metrics determined as ± days per year for the start of season date (Slope SOS), end of season date (Slope EOS), length of season (Slope LOS) and timing of peak SAVI (Slope POP). Slope refers to the slope of linear regression of phenology metric versus year for the period 2000–2019. NPS / DAVID THOMA

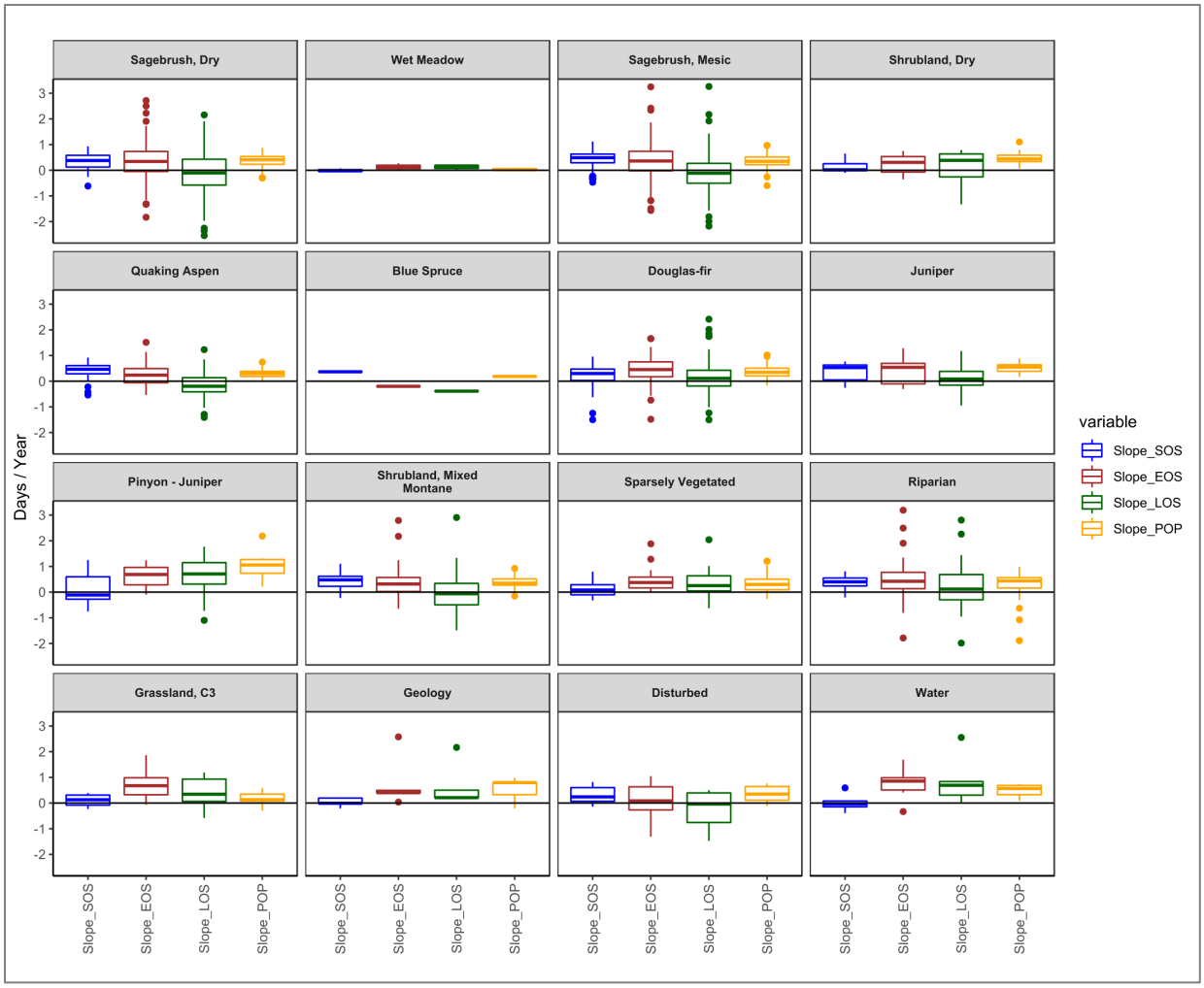

Figure 83. Direction and magnitude of change rate in land surface phenology metrics by alliance group, determined as ± days per year for start of season date (Slope SOS), end of season date (Slope EOS), length of season (Slope LOS) and timing of peak SAVI (Slope POP). Slope refers to the slope of linear regression of phenology metric versus year for the period 2000–2019. NPS / DAVID THOMA

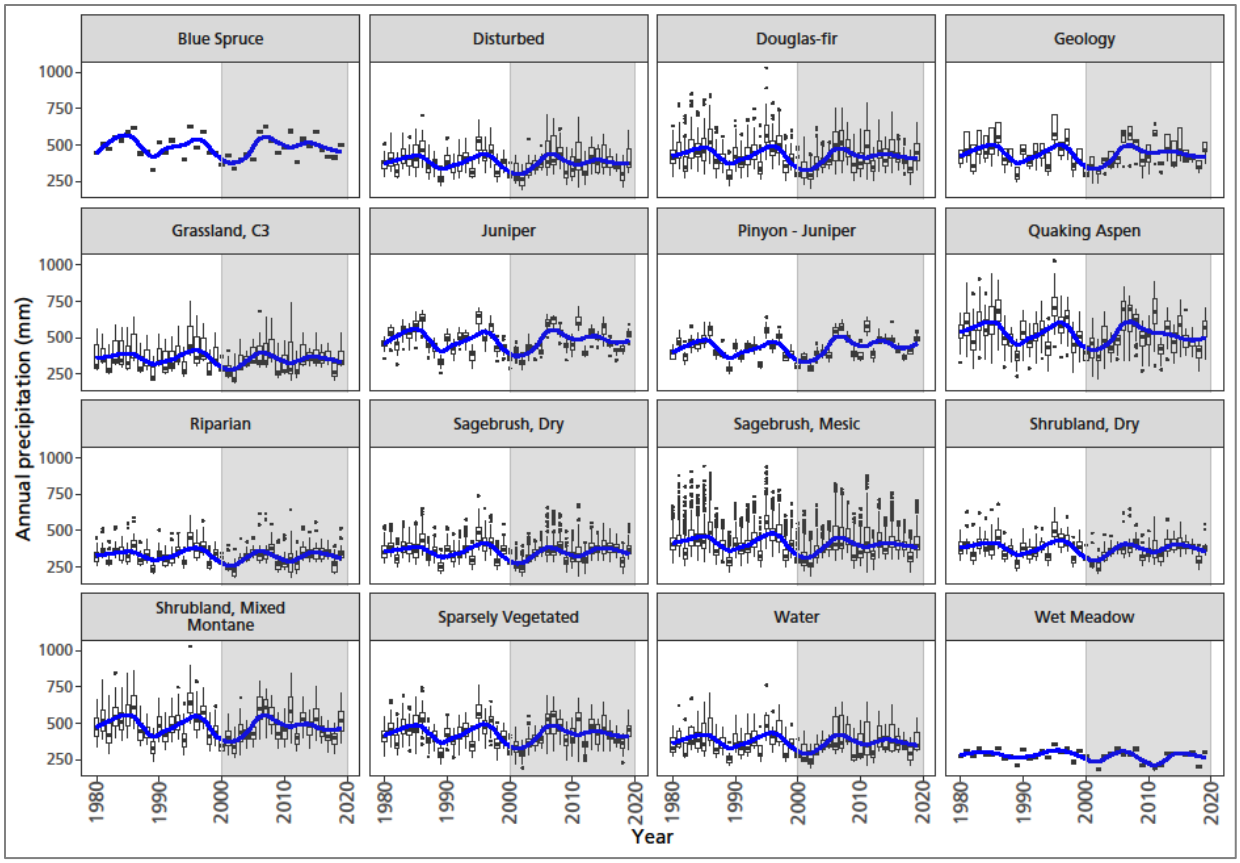

Figure 84. Cumulative annual precipitation over time (1980 to 2019) in vegetation alliance groups. Box plots demonstrate the range of variation within alliance groups by year. The blue line is a loess smooth with a 25 percent span to illustrate multi-year patterns. Gray shaded area includes the period investigated for relationships between production and climate when satellite imagery and climate data were both available. NPS / DAVID THOMA

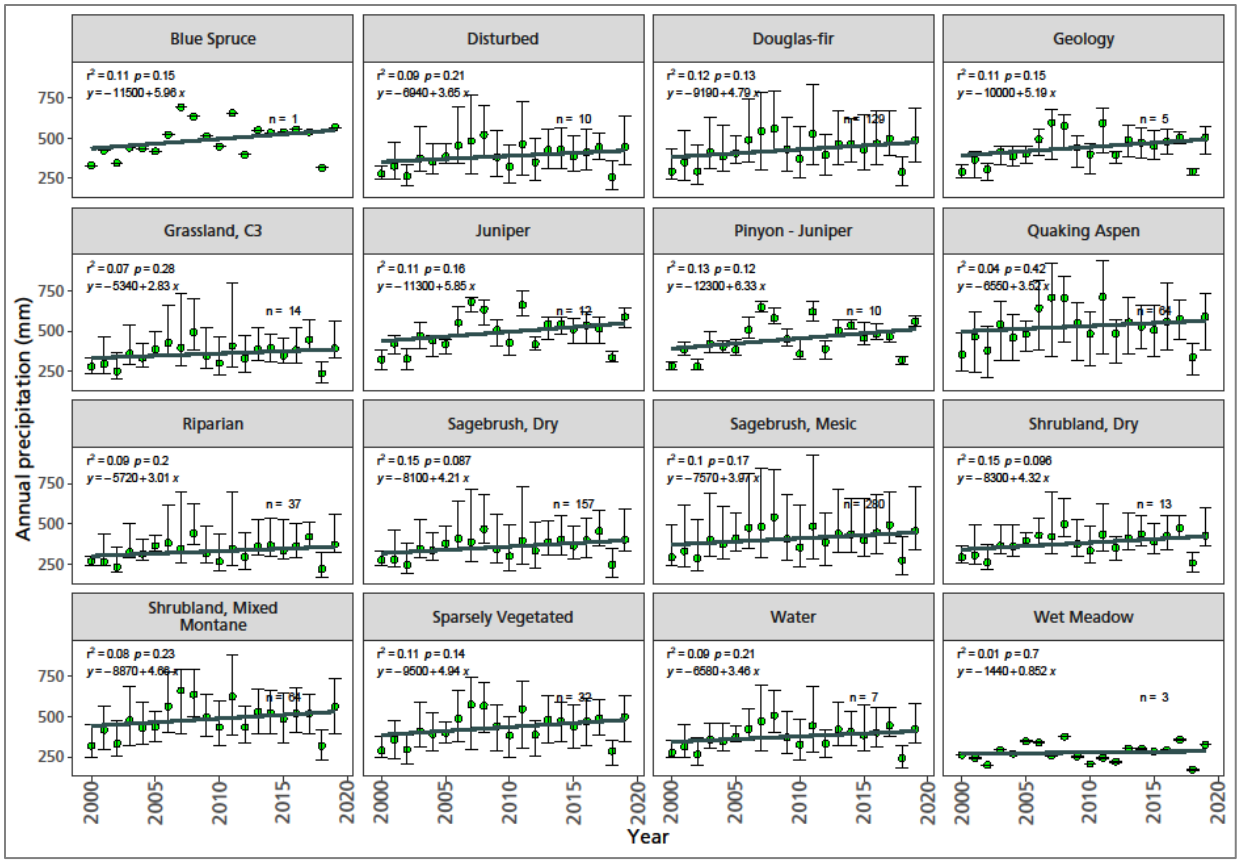

Figure 85. Cumulative annual precipitation over time (2000 to 2019) in vegetation alliance groups. The trend over time is shown for the period in gray in the previous figure. Bars are standard error. NPS / DAVID THOMA

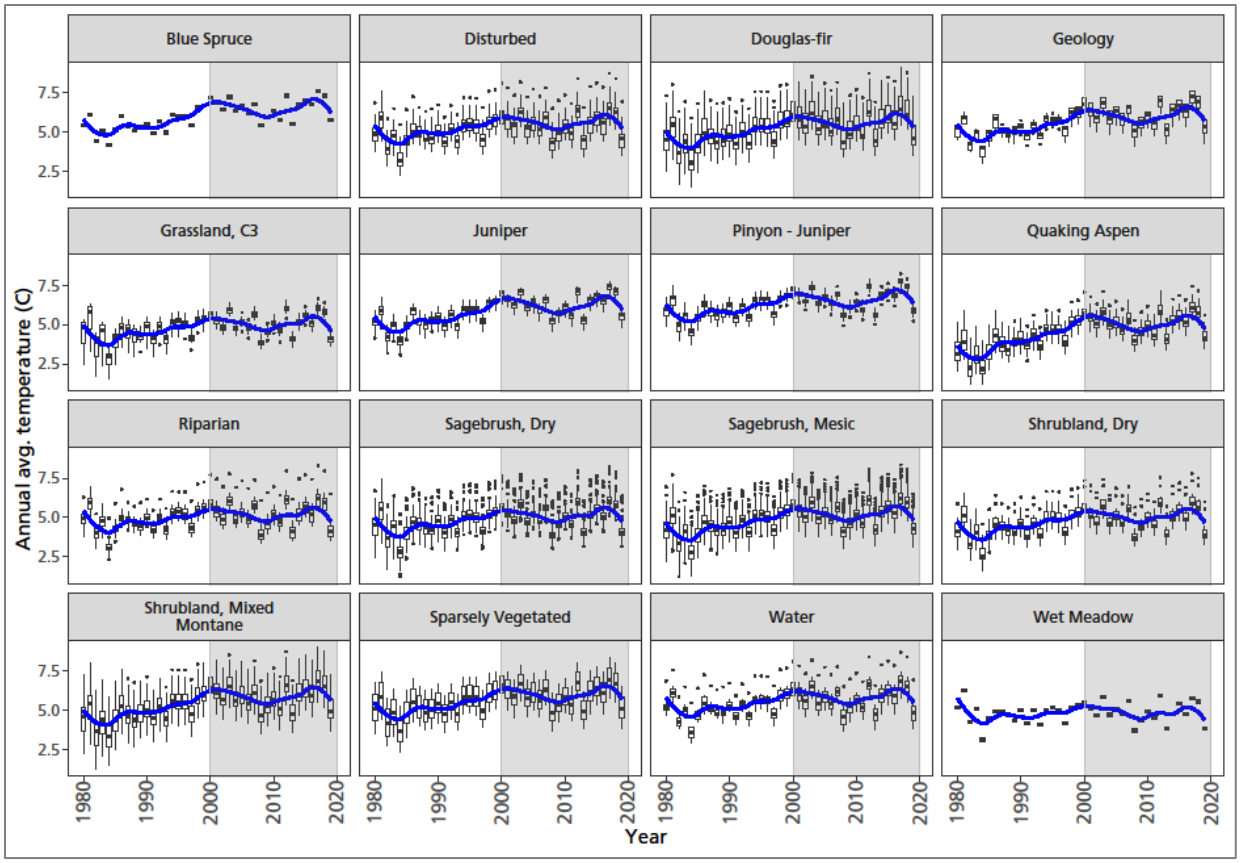

Figure 86. Annual average temperature over time (1980 to 2019) in vegetation alliance groups. Box plots demonstrate the range of variation within alliance groups by year. The blue line is a loess smooth with a 25 percent span to illustrate multi-year patterns. Gray shaded area includes the period investigated for relationships between production and climate when satellite imagery and climate data were both available. NPS / DAVID THOMA

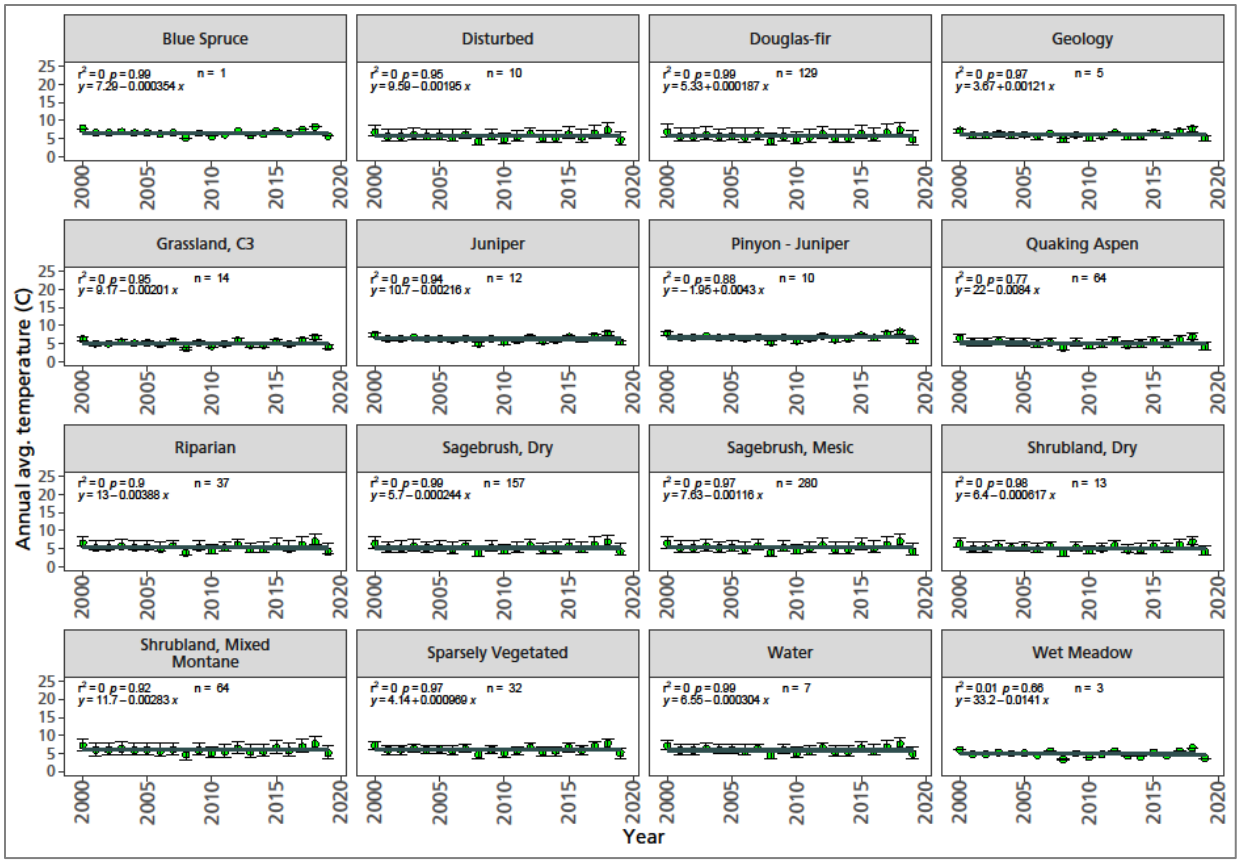

Figure 87. Annual average temperature over time (2000 to 2019) in vegetation alliance groups. The trend over time is shown for the period in gray in the previous figure. Bars are standard error. NPS / DAVID THOMA

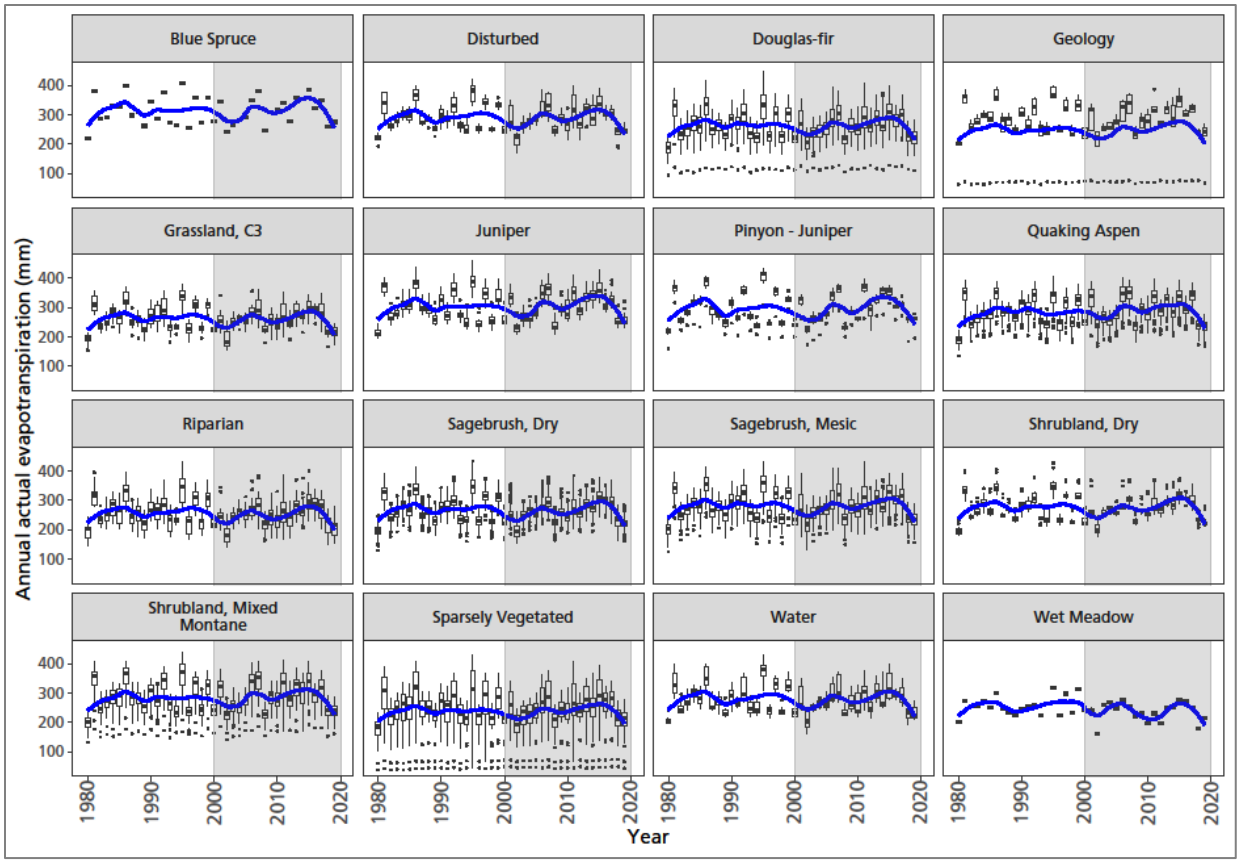

Figure 88. Cumulative annual actual evapotranspiration over time (1980 to 2019) in vegetation alliance groups. Box plots demonstrate the range of variation within alliance groups by year. The blue line is a loess smooth with a 25 percent span to illustrate multi-year patterns. Gray shaded area includes the period investigated for relationships between production and climate when satellite imagery and climate data were both available. NPS / DAVID THOMA

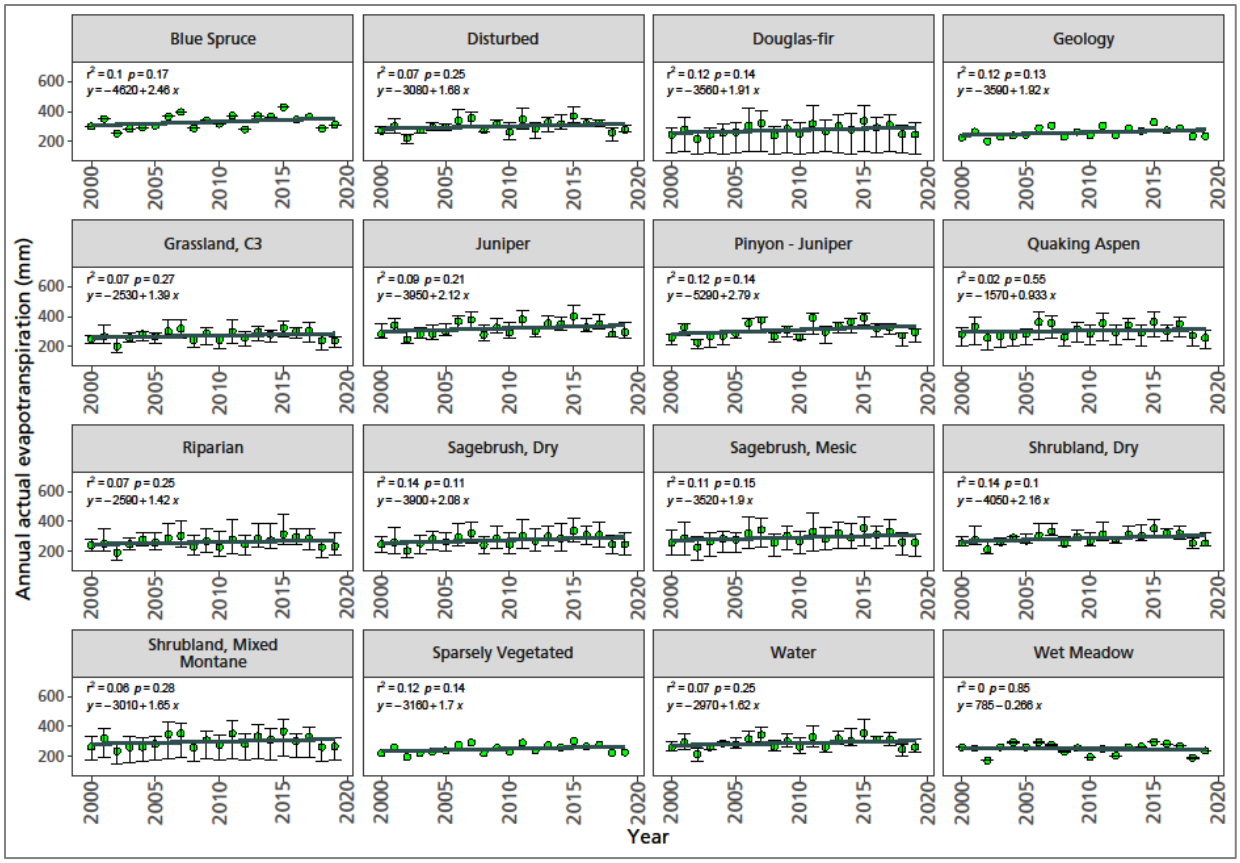

Figure 89. Cumulative annual actual evapotranspiration over time (2000 to 2019) in vegetation alliance groups. The trend over time is shown for the period in gray in the previous figure. Bars are standard error. NPS / DAVID THOMA

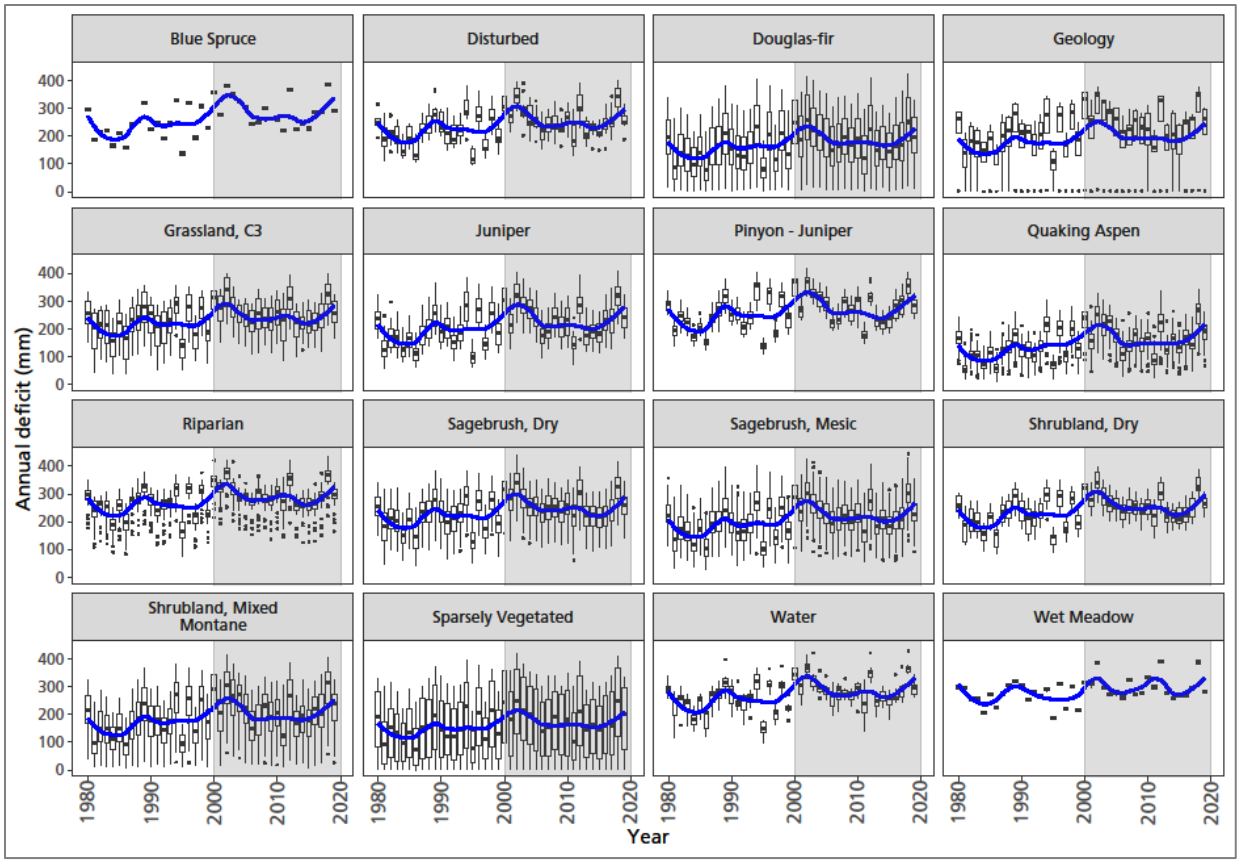

Figure 90. Cumulative annual water deficit over time (1980 to 2019) in vegetation alliance groups. Box plots demonstrate the range of variation within alliance groups by year. The blue line is a loess smooth with a 25 percent span to illustrate multi-year patterns. Gray shaded area includes the period investigated for relationships between production and climate when satellite imagery and climate data were both available. NPS / DAVID THOMA

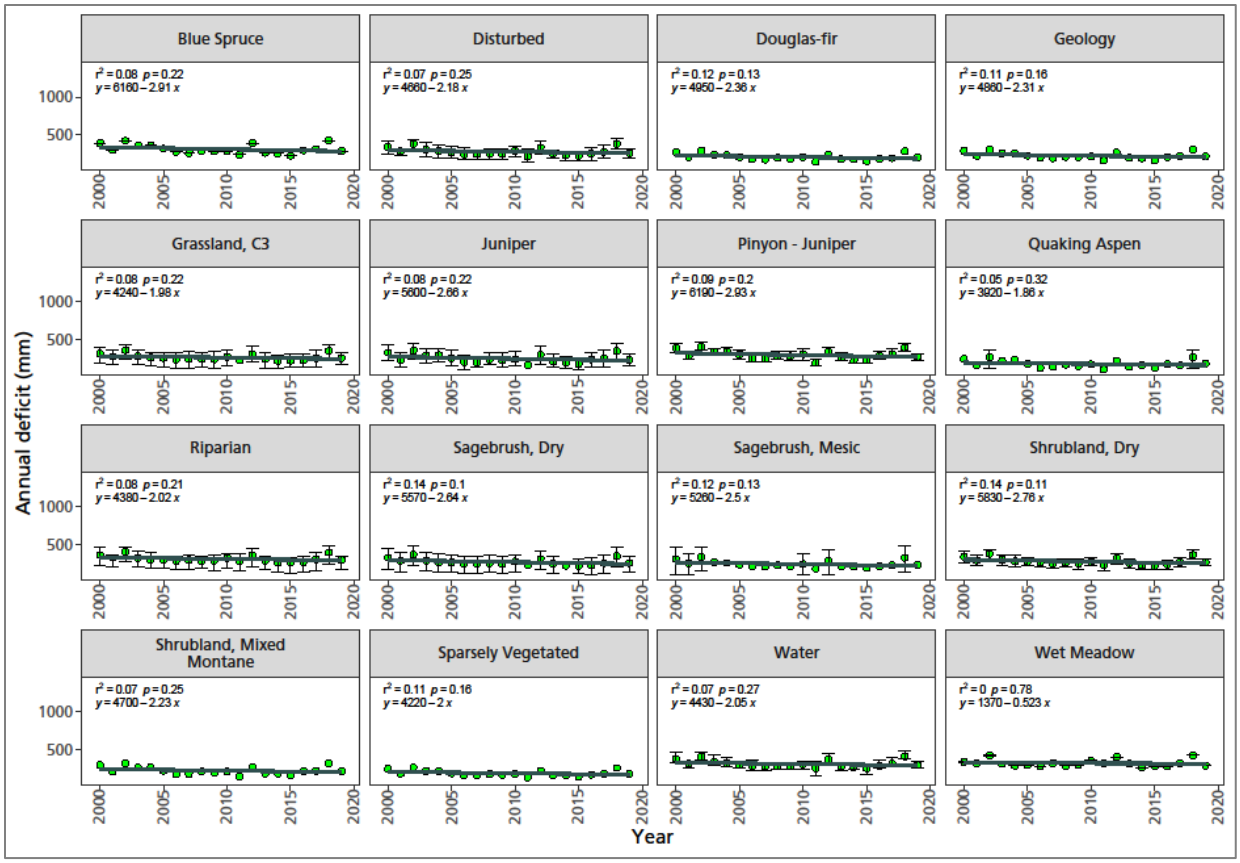

Figure 91. Cumulative annual water deficit over time (2000 to 2019) in vegetation alliance groups. The trend over time is shown for the period in gray in the previous figure. Bars are standard error. NPS / DAVID THOMA

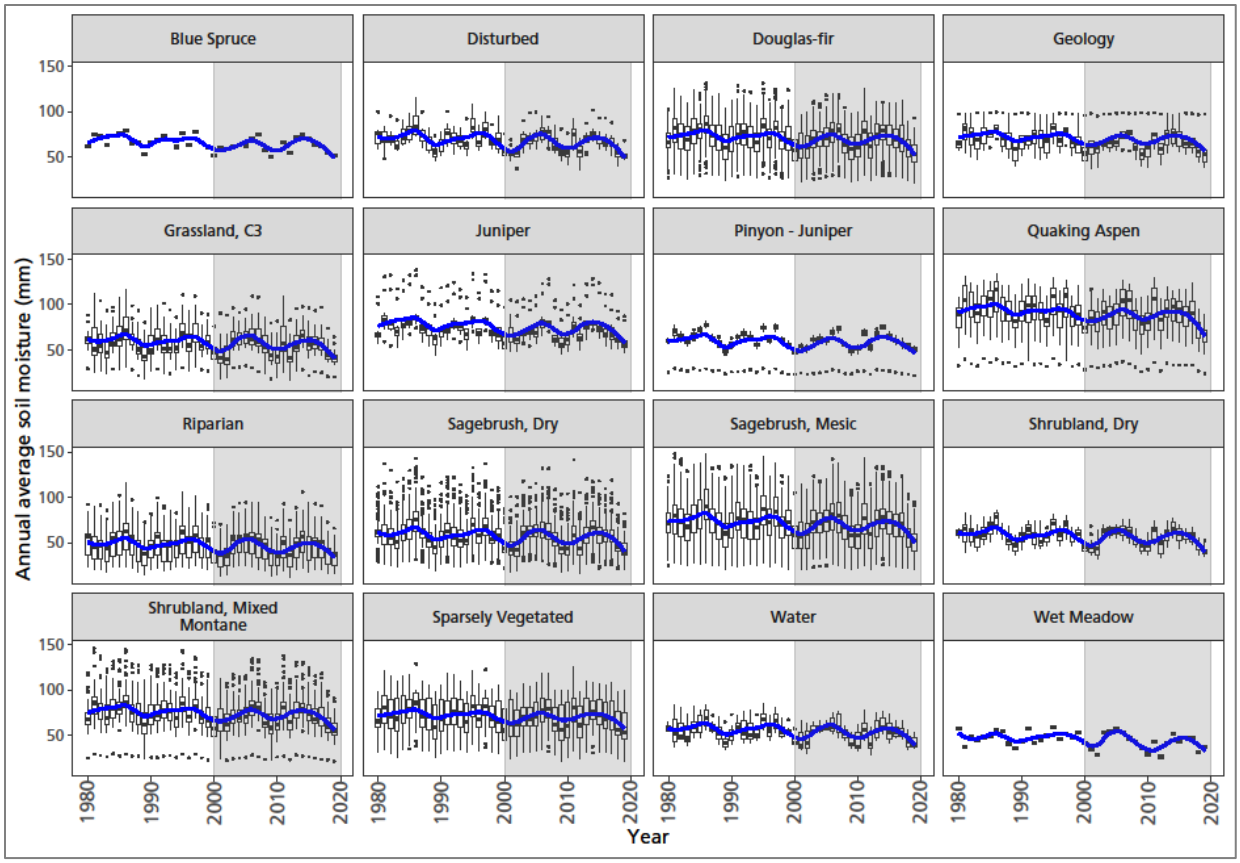

Figure 92. Annual average soil moisture over time (1980 to 2019) in vegetation alliance groups. Box plots demonstrate the range of variation within alliance groups by year. The blue line is a loess smooth with a 25 percent span to illustrate multi-year patterns. Gray shaded area includes the period investigated for relationships between production and climate when satellite imagery and climate data were both available. NPS / DAVID THOMA

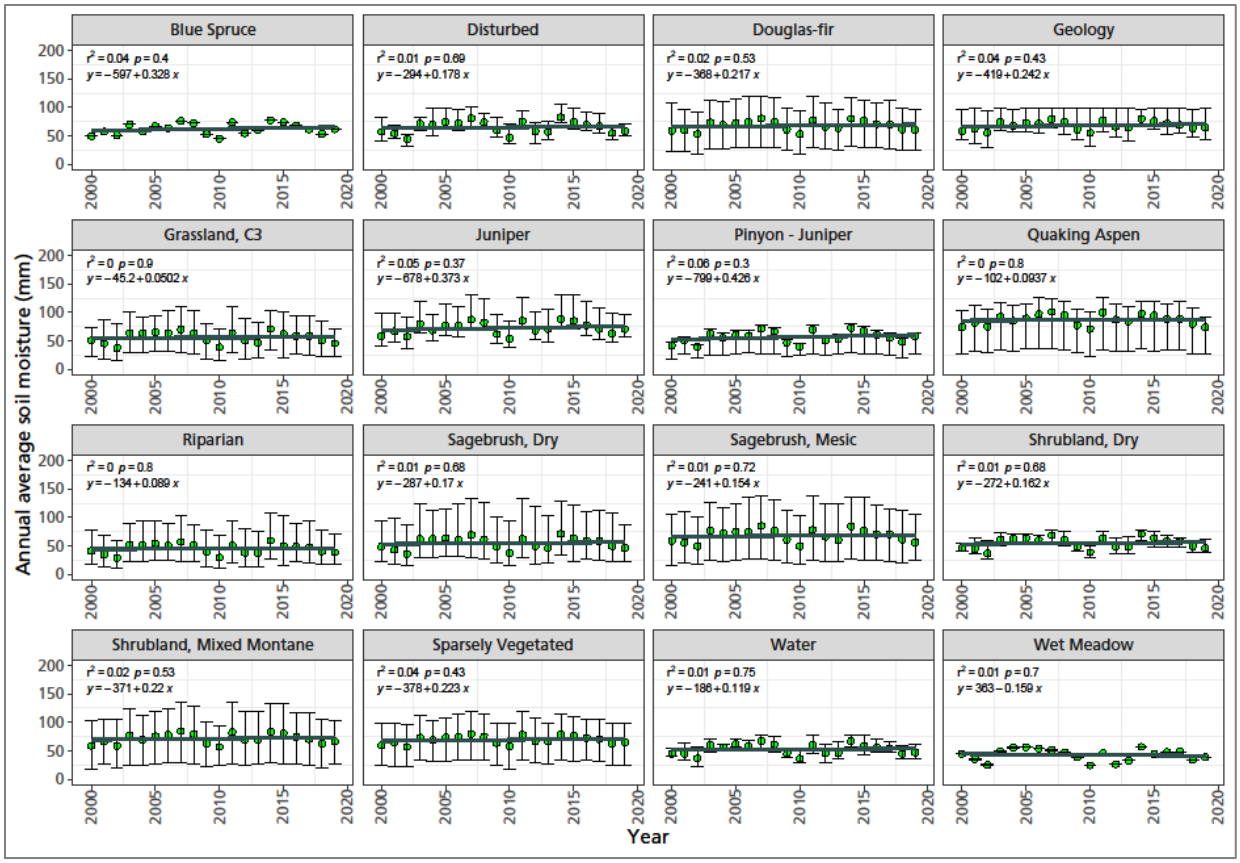

Figure 93. Annual average soil moisture over time (2000 to 2019) in vegetation alliance groups. The trend over time is shown for the period in gray in the previous figure. Bars are standard error. NPS / DAVID THOMA

National Park Service
U.S. Department of the Interior

Science Report NPS/SR—2025/219
https://doi.org/10.36967/2307122

Natural Resource Stewardship and Science
1201 Oakridge Drive, Suite 150
Fort Collins, CO 80525

NPS 616/195564, January 2025